THESIS FOR THE DEGREE OF DOCTOR OF PHILOSOPHY

Voltage Sags:
Single event characterisation, system performance and source location

by

ROBERTO CHOUHY LEBORGNE

Division of Electric Power Engineering
Department of Energy and Environment
Chalmers University of Technology
Göteborg, Sweden 2007

Voltage Sags:
Single event characterisation, system performance and source location

ROBERTO CHOUHY LEBORGNE

ISBN 978-91-7291-916-7

Doktorsavhandlingar vid Chalmers tekniska högskola
Ny serie nr 2597
ISSN 0346-718X

Division of Electric Power Engineering
Department of Energy and Environment
Chalmers University of Technology
SE - 412 96 Göteborg, Sweden
Telephone: +46 (0) 31 – 772 1000
Fax: +46 (0) 31 – 772 1633

Chalmers Bibliotek, Reproservice
Göteborg, Sweden 2007

To my family

Voltage Sags:
Single event characterisation, system performance and source location
ROBERTO CHOUHY LEBORGNE
Division of Electric Power Engineering
Department of Energy and Environment
Chalmers University of Technology

Abstract

This thesis deals with one of the most important disturbances that affect the quality of the electrical supply. Voltage sags cause industrial processes malfunction, producing an enormous economical impact. A voltage sag is defined as a short duration reduction of the rms voltage. A voltage disturbance is in general considered as a sag when the rms voltage remains below 90 % of nominal voltage for a period not exceeding 3 minutes, however, there is not full agreement about these limits. A comprehensive literature review on power quality and voltage sags is included in this thesis.

A voltage sag characterisation method based on instantaneous voltages and phasor analysis is introduced. Through the analysis of the voltage phasor the sag magnitude, the phase-angle jump and the event duration are obtained. A new method for the sag classification of unbalanced sags into ABC categories using instantaneous voltages is proposed.

The presentation of the voltage sag characteristics is also important for the understanding of the event. Several methods for the presentation of sag characteristics are described. Besides the usual rms voltage vs. time and phase angle vs. time representation, a new method based on the phasor locus, extreme phasors, and a set of phasor snapshots is proposed.

The system performance is assessed through sag indices such as voltage sag frequency. The indices are obtained from measurements and a deterministic method combined with two simulation tools: a time-domain simulation program and a short-circuit calculation program. Both approaches are very suitable to simulate voltage sags. The choice for one of the approaches should be based on the goals of the study and the availability of system data.

The system performance is also assessed by stochastic simulation using the method of fault positions. The performance of some selected buses is estimated and compared to the actual one obtained from a voltage sag survey. The strengths and shortcomings of the method of fault positions are discussed. The sensitivity of the method is analysed in terms of variations of the fault rate, fault type distribution, and fault position.

The location of the source of voltage sags is estimated considering two network regions: upstream and downstream to a certain monitored bus. Several methods

using voltage and current information are investigated and their performances are compared. A new method using only sag magnitude is introduced. The method is successfully applied in a simulated case study and verified by data obtained during a sag survey. The method shows its strength when applied in a sag survey where only voltage information is available.

Keywords: Power quality, voltage sags (dips), characterisation, indices, source location.

List of Publications

This thesis is based on the work contained in the following papers:

I. **Chouhy Leborgne, R.,** and Chen, P., 2006. Using PQ-monitor and PMU for voltage sag extended-characterization. *In Proc. IEEE PES Transmission and distribution Conference and Exposition Latin America, Aug.2006, Caracas*.

II. **Leborgne, R.C.**, Olguin, G., and Bollen, M.H.J., 2004. The influence of PQ-monitor connection on voltage dip measurements. *In Proc. IEE MedPower, Nov.2004, Cyprus.*

III. **Leborgne, R.C.**, and Karlsson, D., 2005. Phasor Based Voltage Sag Monitoring and Characterisation. *In Proc. CIRED International Conference on Electricity Distribution, Jun.2005, Turin*.

IV. **Chouhy Leborgne, R.**, Karlsson, D., and Olguin, G., 2005. Analysis of Voltage Sag Phasor Dynamics. *In Proc. IEEE-PES Power Tech, Jun.2005, St Petersburg*.

V. **Chouhy Leborgne, R.**, Carvalho Filho, J.M., Novaes, E.G.C., and Abreu, J.P.G., 2006. Voltage sag propagation: Case study based on measurements. *In Proc. IEEE 12th International Conference on Harmonics and Quality of Power, Oct.2006, Cascais, Portugal.*

VI. Carvalho Filho, J.M., **Chouhy Leborgne, R.**, Silveira, P.M., and Bollen, M.H.J., 2007. Voltage sag index calculation: Comparison between time-domain simulation and short-circuit calculation. *Electric Power System Research, in print.*

VII. Carvalho Filho, J.M., **Chouhy Leborgne, R.**, Abreu, J.P.G., Novaes, E.G.C., and Bollen, M.H.J., 2007. Validation of voltage sag simulation tools: ATP and short-circuit calculation vs. field measurements. Submitted to *IEEE Trans. Power Delivery, TPWRD-00032-2007.*

VIII. **Chouhy Leborgne, R.**, Olguin, G., and Bollen, M.H.J., 2004. Sensitivity Analysis of Stochastic Assessment of Voltage Dips. *In Proc. IEEE PowerCon, Nov.2004, Singapore.*

IX. **Chouhy Leborgne, R.**, Olguin, G., Carvalho Filho, J.M., and Bollen, M.H.J., 2006. Effect of PQ-monitor connection on voltage dip indices: PN vs PP voltages. *Electric Power Quality and Utilisation Magazine*, 2(1), 19-26.

X. **Chouhy Leborgne, R.**, Olguin, G., Carvalho Filho, J.M., and Bollen, M.H.J., 2007. Differences in voltage dip exposure depending upon phase-to-phase and phase-to-neutral monitoring connections. *IEEE Trans. Power Delivery,* 22 (2), 1153-59.

XI. **Chouhy Leborgne, R.**, Karlsson, D., and Daalder, J., 2006. Voltage sag source location methods performance under symmetrical and asymmetrical fault conditions. *In Proc. IEEE PES Transmission and distribution Conference and Exposition Latin America, Aug.2006, Caracas*.

XII. **Chouhy Leborgne, R.**, Karlsson, D., 2007. Voltage sag source location based on voltage measurements only. Submitted to *IEEE Trans. Power Delivery, TPWRD-00715-2006.*

The author has also contributed to the following publications:

Olguin, G., **Leborgne, R.C.**, and Coelho, J., 2004. Ensuring Electromagnetic Compatibility by Analytic Study of Voltage Dips Caused by Faults. *In Proc. IEEE–IAS VI Induscon, Out.2004, Joinville, Brazil.*

Olguin, G., **Leborgne, R.C.**, and Karlsson, D., 2005. Stochastic Assessment of Voltage Dips; the Method of Fault Positions versus a Monte Carlo Simulation Approach. *In Proc. IEEE-PES Power Tech, Jun.2005, St Petersburg*.

Oliveira, T.C., Carvalho Filho, J.M., Abreu, J.P.G., and **Chouhy Leborgne, R.**, 2006. Voltage Sags: Statistical Evaluation of Monitoring Results based on Predicted Stochastic Simulation. *In Proc. IEEE 12th International Conference on Harmonics and Quality of Power, Oct.2006, Cascais, Portugal.*

Chouhy Leborgne, R., Karlsson, D., and Daalder, J., 2006. Voltage sag source location: a new method based on voltage information. *In Proc. IEEE 12th International Conference on Harmonics and Quality of Power, Oct.2006, Cascais, Portugal.*

Chouhy Leborgne, R., and Makaliki, R., 2007. Voltage sag source location at grid interconnections: a case study in the Zambian system. *In Proc. IEEE PES Power Tech, July2007, Lausanne.*

Acknowledgments

This research is fully funded by the Ministerio da Educação do Brasil through its agency "Coordenação de Aperfeiçoamento de Pessoal de Nível Superior (CAPES)". The financial support is gratefully acknowledged.

For their support, guidance and inspiration I am deeply grateful to: Prof. Math Bollen, Prof. Jaap Daalder, Dr. Daniel Karlsson, and Prof. Gustaf Olsson.

I would like to thank Dr. Gabriel Olguin and Dr. Jose Maria Carvalho Filho for the fruitful discussions that motivated many of the papers presented in this thesis. The Power Quality Study Group of the Itajuba Federal University, Brazil, is gratefully acknowledged for sharing sag measurements.

I am grateful to Eng. Carlos Campinho, Eng. Marcio Accioly, Dr. Delmo Correia and Eng. Dalton Brasil from the Brazilian System Operator (ONS) for supplying the transmission system data and sag measurements.

For their friendship, cooperation and advice I am most grateful to Marcia Martins, Cuiqing Du and Massimo Bongiorno. I acknowledge the dedication and hard work of the master students I had the pleasure to supervise: Peiyuan Chen and Readlay Makaliki.

Also I would like to express my gratefulness to my colleagues at *Elteknik*; for their friendship and for the good times we spent together at coffee-breaks and parties. Above that I want to show my thankfulness to the technical and administrative personnel at *Elteknik*. They are essential for the success of the Department.

I am grateful to my relatives and friends that continuously encourage and support me.

My warmest embrace to my wife Christiane and our son Giosuè.

Roberto Chouhy Leborgne
Göteborg, Sweden
May 2007

Table of Contents

1 Introduction

This first chapter starts with a story for a general reader that describes the concept of power quality and how it affects our daily life. The motivation to develop this project and the aim of this thesis are explained. Finally the main scientific contributions of this research are presented.

1.1 Power quality for poets

Dr Sven Jonsson is a professor at Chalmers University. A certain day he woke up and suddenly realised that something wrong was going on... It was a wonderful bright morning, but since it was a winter morning he did not expect to see any sunlight that early. He felt he was missing something when he realised that the alarm clock had not gone on. Too late. He jumped from the bed and watched the clock, its numbers were flashing and asking to be set. He wondered why the clock failed during the night.

His PC, which is connected to a no-break that can supply reliable energy for one minute in case of an energy shortage, had managed to download a movie during the night. Considering this fact, Sven concluded that no major blackout had taken place that night, besides, the microwave clock was working well. Sven had a great dilemma to answer! Otherwise he would get into trouble with his boss explaining the reason to be so late this morning.

On his way to Chalmers he heard on the radio that there had been a major storm in southern Sweden the night before. He understood that the storm could be the main cause of his clock problems. Lightning during storms may cause faults in the power lines. These faults cause a voltage reduction in most of the busbars of the system, including the one that supplies electricity to Sven's house, or the one that supplies your home. This power quality event is called a **voltage sag**, and it lasts until the protection of the line trips, disconnecting the faulted line. When this line is the only electrical supply, the loads fed by this line undergo a complete electrical outage until the line is successfully reconnected.

Sven found out the origin of his time problems. But now he was concerned about how to solve it. "Is there any reliable energy source?" There is no fully reliable supply. The more reliable the supply the more expensive it is. Therefore we are talking about a cost/benefit compromise. The clock needs to improve its tolerance to voltage sags. As the clock power demand is low, a battery supply is enough to keep it working during these power quality events.

Despite the fact that these power quality events have been occurring in the power grid since it was built one hundred years ago, the interest of the

technical community in this issue has risen during the last two decades. Power quality events began to be disruptive ever since the extended use of sensitive electronic loads such as personal computers, home electronic devices, adjustable speed drives, and industrial automation. The focus of research has been characterisation of power quality disturbances, analysis of equipment electro-magnetic compatibility, and improvement of the equipment's tolerance.

Sven went back to his house, a nice cottage in the beautiful countryside 40 km away from town. It was dark outside because daylight in November is a rarity in the Nordic countries. Therefore, people are dependent on electric lighting the whole day.

He rested on the sofa and picked up the book he was reading. After 10 minutes, he started to feel very upset because the light was blinking. Somebody must be playing with the light switch, he thought. But as Sven lives by himself there was nobody who could be switching the lamp near the sofa. The annoying problem was a power quality disturbance called **flicker**, which is noticed as a variation in light intensity. It has been statistically proven that the level of annoyance follows a normal distribution reaching the maximum value when the variation happens 9 times per second.

What really bothered Sven was why his incandescent lamp was flickering. Sven was facing a power quality problem for the second time that day. As in the morning, he wanted to know the cause of the flicker and how to mitigate the effects of the disturbance.

He remembered that near his home there is a factory with several arc furnaces for steel production. These arc furnaces demand a huge amount of current that varies considerably during the melting process. The current variation produces a voltage variation that is proportional to the network impedance. The network impedance is related to the strength of the network. In other words, networks with a very large power generation and power transmission capacity have a low impedance. A strong network handles high demand variation very well with a minimum voltage variation.

Sven's cottage is away from town and electric energy is supplied by long power lines. These long lines have high impedance. As a consequence of the network weakness and the high variation of the neighbour's energy demand, Sven was facing voltage fluctuations. These fluctuations provoke the light variation called flicker. This problem doesn't happen often in cities, because the distribution networks are stronger and capable to handle high demand variations.

Flicker analysis is not a simple issue and the first researches were conducted in the 1960s. As incandescent lamps have been used since the origin of

electric systems, customers endured flicker disturbance for decades. Many utilities, concerned about this power quality disturbance, are working to satisfy customer demands. The solutions are not cheap: increase the power generation capacity, install new transmission lines, or relocate industrial customers.

Sven was concerned about his domestic problem and did not want to wait for years for a solution by the utility. He thought that probably the voltage variation was not simultaneous in all the three phases of the distribution system. Considering that his house has a three-phase supply, he connected the lamps to different phases, after making some little changes in the electrical wiring of the house. As a result, the variation of luminescence of each lamp was compensated by the others. Sven felt very proud of solving his flicker problem with a minimum of cost.

Sven was reading a letter from a friend who owns a small factory. His friend was concerned with a problem he was facing in many production lines in his factory. He noticed that many motors used in the paper mill were suffering overheating, which reduces the lifetime of motors dramatically. The expected lifetime of the motors is 20 years. However, he reported that after 5 years he started to replace the motors because of the degradation caused by that overheating. Therefore he wondered what was wrong with the motor specification.

Sven answered his friend why the motors were failing so early. Due to the increase of voltage **harmonics** in the network most of the motors are experiencing this fast ageing, and failing before completing half of their lifetime. He also explained that these voltage harmonics are a common disturbance in industrial electric networks where there are many power electronic loads. These power electronic loads are the main source of harmonics in electric networks.

Then, Sven described this power quality disturbance and wrote: “Harmonic distortion is characterised by the harmonic spectrum, where all frequencies are represented by the magnitude of the signal. There are filters that mitigate the harmonic distortion. The filters are tuned to eliminate a specific harmonic. We need to evaluate the harmonic spectrum in your factory to design the suitable filters to reduce the harmonic distortion to extend the lifetime of your motors. This solution will be possible if the cost of the filters is lower than the cost of motor replacement”.

This thesis presents an investigation about several aspects of voltage sags: characterisation of single events, power system performance and sag source location. Voltage sags, the power quality disturbance that caused the malfunction of Sven’s alarm clock, every year cause losses of billions of euros to manufacturing industries around the world.

1.2 Motivation for the project

Until the 1960s the main concern of consumers of electricity was the continuity of the supply, in other words the reliability of the supply. Nowadays consumers not only require reliability, but also power quality. For example, a consumer may face unexpected voltage reductions (voltage sags) every time there is a fault at some part of the system, affecting its sensitive loads. Depending on the sensitivity of the consumer's loads, this voltage sag may lead to a failure or disconnection of the loads or of the entire plant. Although the supply is not interrupted the consumer experiences a disturbance that causes an outage of the plant. Examples of very sensitive end users are hospitals, manufacturing industries, air traffic control towers, and financial institutions; all of them requiring reliable and high quality electrical supply.

In earlier studies, techniques have been developed for the analysis of voltage sags as experienced by three-phase equipment. These studies point out that three-phase sag characterisation must be superior over existing methods in order to appropriately describe this kind of events. These extended characterisation methods should be considered for the stochastic and statistical assessment of voltage sags, for the analysis of voltage sag propagation, and for the estimation of equipment sensitivity.

The location of the source of the disturbance plays a fundamental role to decide about responsibilities and financial penalties. This information is extremely important considering the new power system management in de-regulated environments, where many transmission and distribution companies exchange electric energy and also power quality disturbances.

1.3 Aim and thesis outline

The objective of this research is to investigate the most harmful power quality disturbance. Most of the voltage sag aspects, such as: characterisation, propagation, simulation methods, and source location have been addressed.

Chapter 1 offers an explanation for the general reader about power quality. The motivation for this research, the aim and thesis outline, and the main scientific contributions are also included in this chapter.

Chapter 2 presents a literature review about power quality and voltage sags. The power quality review is divided in sections in order to show some of the issues that drove the research of this topic.

Chapter 3 describes the methods for the characterisation of voltage sags. Unbalanced voltage sags are highlighted since they are the most common

type of sags in power systems. Some of the results presented in the Papers I, II, III, IV and V are highlighted in this chapter.

The proposed methods for the extended characterisation of sags are tested on measurements obtained from a scaled model of a power system. Two measurement devices are used: a PQ-monitor and a PMU - phasor measurement unit.

A novel method to obtain the sag type using the theoretical relation between phase-to-phase and phase-to-neutral sag magnitudes is proposed and implemented in a set of simulated events. Voltage sags are also characterised using the voltage phasors.

Voltage sag propagation is addressed in detail. The analysis is based on measured sags and includes: the effect of fault characteristics, the generation dispatch, and the vertical and horizontal propagation.

Chapter 4 introduces the indices to describe the system performance regarding voltage sags. The need for voltage sag simulation is explained. Some of the results presented in the Papers VI, VII, VIII, IX and X are particularly addressed. Two types of programs for voltage sag magnitude estimation are compared. One is an electromagnetic transient program and the other is a short-circuit calculation program. The results are also confronted with actual measurements. The system performance obtained deterministically by the simulation of a set of recorded faults is also compared with the measured sag performance.

The system performance regarding voltage sags is also estimated by stochastic simulation (method of fault positions). The results are compared with actual measurements and the strengths and shortcomings of this simulation approach are addressed. The sensitivity of the method of fault positions regarding the main fault uncertainties (fault rate, fault type, and fault location) is analysed. Finally, voltage sag indices obtained from phase-to-phase and phase-to-neutral voltages are compared.

Chapter 5 presents several methods to locate the source of voltage sags. Several methods that use voltage and current information are implemented on a set of simulated voltage sags. The performance of the methods is analysed. A novel method that uses only voltage information is proposed. The method is applied on simulated sags showing a good performance. The method is then applied on measured sags presenting an outstanding performance. The main results presented in this chapter are extracted from Papers XI and XII.

In Chapter 6 the conclusions of this work are presented and ideas for future research are proposed.

1.4 Scientific contribution of this thesis

The main contributions of this research are related to three aspects of voltage sags: the single-event characterisation, the system performance estimation, and the sag source location. Therefore one chapter has been devoted to each one of these aspects.

From the characterisation viewpoint, this thesis introduces a method based on the instantaneous voltages and the voltage phasors. Through the analysis of these quantities the retained voltage, the phase-angle jump, and the event duration are obtained, and three-phase unbalanced sags are classified in the ABC voltage sag types (Bollen, 2000). A new method using phase-to-neutral instantaneous voltages for the sag classification is introduced. The method is based on the theoretical relations between phase-to-phase and phase-to-neutral sag magnitudes.

Several methods for the presentation of the sag characteristics are described. Additionally, a new method based on a combined representation in terms of the phasor locus, the extreme phasors, and a set of snapshots is developed. The use of a new measurement device, the PMU, is tested for voltage sag characterisation.

The programs used for the sag magnitude calculation are addressed. An extensive investigation including measurement results for comparison is provided. A sensitivity analysis of the method of fault positions is performed. An evaluation of the strengths and weaknesses of the method for the stochastic estimation of sags is done. The limitation of the method to estimate the short term performance is discussed.

The methods for the location of the sag source are investigated and their performance is evaluated. A new method using only voltage information is proposed. The method is evaluated by simulated and measured sags. The performance under diverse load conditions is discussed.

2 Literature Review

A literature review about power quality is explored in this chapter, including general aspects but highlighting voltage sags.

2.1 Power quality

The subject of power quality has been present in the technical literature since the 1960s; however the number of publications has increased significantly in the last decade, as shown in Figure 1 and Figure 2. The survey at the IET-INSPEC database was made with the following entries:

- (power AND quality) within abstract
- (voltage sag OR voltage dip) within abstract

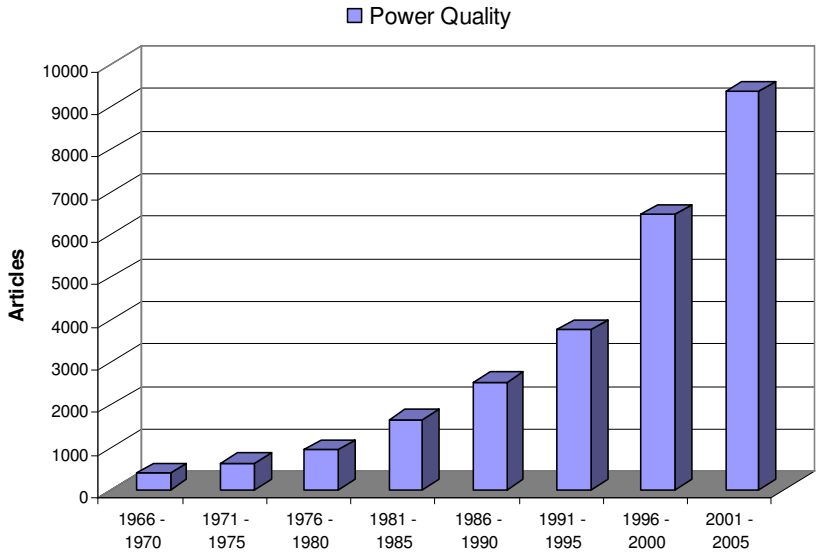

Figure 1 - Power quality publications

Several reasons have been given to explain the current interest in power quality (Bollen, 2000):

Electronic and power electronic loads have become much more sensitive than previous electric equipment. Industrial customers are much more aware of the economical losses that power quality problems may cause in their processes.

Often the same equipment that is sensitive to the quality of the voltage will itself cause voltage disturbances. This is the case with several power converters, whose input current is non-sinusoidal, containing a high level of harmonic distortion. The distortion of the demanded current leads to harmonic components in the supply voltage.

There is an increasing need for performance criteria to assess the quality of the power supplied. This is especially important for the monopolistic part of the chain formed by generation, transmission, and distribution of electricity. The natural monopoly that transmission and distribution companies possess requires a quality framework where compulsory quality levels are given. Regulator bodies will have to create such a quality framework in terms of power quality indices and objectives.

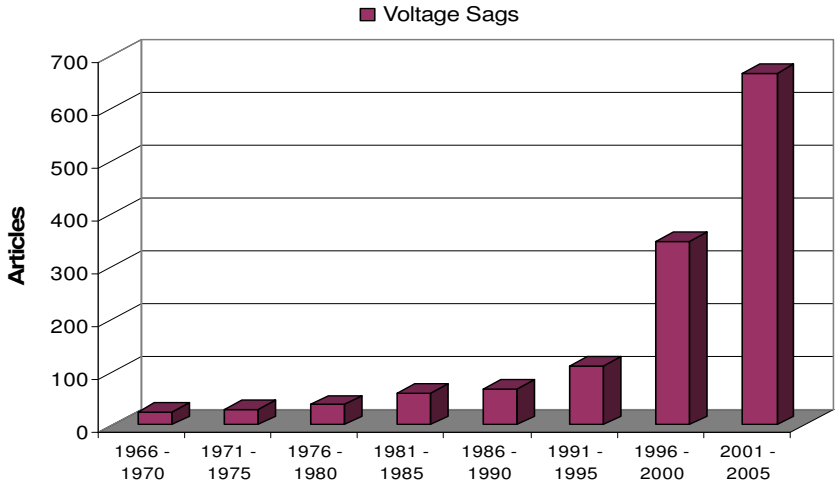

Figure 2 - Voltage sag publications

Despite the well-known blackouts of 2003 and 2006 (FERC, 2003), (ERGEG, 2006), the power supply has become so reliable that in most developed countries long interruptions and blackouts have become atypical phenomena. As a result, an increasing attention is given to second order problems such as short interruptions, voltage sags, harmonic distortion, etc.

The availability of power quality monitors means that voltage and current quality can actually be monitored on a large scale.

2.1.1 Power quality definitions

Back in the 1970s the definition of the power quality included limits applied to the fluctuations of frequency and voltage, voltage unbalance, voltage transients, voltage harmonics, and interruptions. Moreover, the purposes of quality control were to reduce consumer complaints and increase the use of electric power as well as to obtain data for better control and planning of power supply systems (Hilger, 1972).

Meynaud (1983) claimed that the quality of the electricity could be characterised by two factors: one for the continuity of supply, and a second for the quality of the voltage. He listed the causes and effects of the voltage distortion and discussed the nature, parameters and consequences of rapid

voltage variations, voltage sags, harmonics, voltage asymmetry, and transient overvoltages.

Today there is not a general agreement about the meaning of "power quality". For example, the Institute of Electrical and Electronic Engineers in its standard IEEE std. 1100 defines power quality as "the concept of powering and grounding sensitive equipment in a matter that is suitable to the operation of that equipment". Despite this definition the term power quality is used in a more general way within IEEE (Bollen, 2000). IEC-International Electrotechnical Commission has adopted, instead of power quality, the concept of electromagnetic compatibility defined as "the ability of an equipment or system to function satisfactorily in its electromagnetic environment without introducing intolerable electromagnetic disturbances to anything in that environment" (IEC 61000, 1990).

2.1.2 Effects on loads

Special installations such as army, aircraft, and navy facilities motivated the research in this field, looking for more reliable and secure installations and focusing on reducing malfunction of critical electric devices due to electromagnetic incompatibility. The need for a sine-wave voltage with constant frequency and amplitude was pointed out (Kajihara, 1968), (Frichtel and Dougherty, 1970), (Hucker, 1970), (Giorgi, 1975).

Research efforts concerning industrial plant planning and operation regarding the performance of sensitive electric loads under poor power quality conditions are found in the literature since the 1970s (McFadden, 1969, 1970), (Plette, 1969).

Manufacturers and users of electric devices used to take electric power practically for granted because circuits were operating with adequate unused capacity. Unfortunately, two simultaneous trends in manufacturing technology made this simple approach increasingly risky.

The first phenomenon related to power quality was the tremendous growth in the use of electric power in industries. The power systems started to be operated at or even beyond their design capacities, with generally adverse consequences to their performance. The changes were qualitative as well as quantitative. In many plants, an increasing part of the electric load is composed of electric arc furnaces, rectifiers, thyristor converters, and other equipment that are sources of power quality disturbances.

The second tendency was towards sensitive loads that demand high power quality. For these reasons, many engineers started to find that power quality evaluation was needed when planning a new industrial installation (McGranaghan, 1995).

Total reliance on sensitive electronic systems for such important functions as data processing, communications, and process control has been taken for granted in commercial, industrial, and governmental activities. These new applications required higher power quality levels. Intermittent power disturbances, capable of disrupting electronic equipment were inherent to both commercial and industrial power systems. Any power-related disruption causing downtime and financial loss was likely to precipitate a study to determine appropriate corrective actions (Key, 1979).

Transmission and distribution utilities are facing an increasing pressure to fully utilise their existing systems because of the rise of capital, fuel, and environmental costs. Simultaneously, standards for quality of supply were under review. To mitigate problems related to poor power quality, customer participation in quality control was proposed to achieve the cheapest overall cost of system operation (Outhred and Schweppe, 1980).

The problems reported in industrial processes due to power quality disturbances have also been studied from an economical point of view, and the losses have been quantified. Reason (1988) analysed that manufacturers of electronic equipment redefined the meaning of power quality. The quality of the power delivered by utilities had steadily improved over the years, but sensitive electronic equipment needed a higher level of power quality. The author argues that in too many cases, manufacturers tried to focus on the utility as the party solely responsible for power quality. He showed that in fact, the causes of power quality problems were usually found in incorrect wiring within the customer's premises.

2.1.3 Power quality standardisation

The standardisation of power quality is also a long and never-ending story. Deloux (1974) claimed that international standardisation had done little towards drawing up detailed requirements to ensure the electromagnetic compatibility between the supply and the loads, in the event of disturbed voltage. From this point of view the situation was changing considerably, as he reported at the CENELEC - European Committee for Electrotechnical Standardisation. It was necessary to define quality criteria, develop suitable means of measuring quality and ratify recommendations and standards. A large-scale international standardising work primarily concerned with voltage quality, has been running since then (Lonngren, 1974).

Heikkila (1976) also claimed that the lack of international standards implied the need for national recommendations and regulations concerning devices causing harmonics. The increasing occurrence of harmonics in electricity networks deteriorates the quality of supply, provokes telephone interferences, and increases losses in networks and consumer devices.

Furthermore, the criteria for harmonic evaluation were defined by using spectral methods, determining the length and frequency of measurements (Konstantinov *et al*., 1978).

The UNIPEDE - International Union of Producers and Distributors of Electrical Energy issued one of the first standards on power quality. This report outlines the quality of the electricity supply in terms of noise spikes, variation of voltage levels and audio and radio frequency contents (Colding, 1982).

McEachern (1993) claimed the need of standards regarding power quality in order to determine the power quality status of distribution systems. It was concluded that there were no standards, at least not in 1993. Many different groups were working towards this goal, including IEEE, IEC, ANSI - American National Standards Institute, CBEMA - Computer and Business Equipment Manufacturers Association, and EPRI - Electric Power Research Institute.

A historical review on the standards related to power quality within IEEE is given below:

- ANSI/IEEE Std 519-1981 "IEEE guide for harmonic control and reactive compensation of static power converters"
- IEEE Std C57.18-10-1998 "IEEE standard practices and requirements for semiconductor power rectifier transformers"
- IEEE Std C62.48-1995 "IEEE guide on interactions between power system disturbances and surge-protective devices"
- IEEE Std 493-1997 "Recommended Practice for the Design of Reliable Industrial and Commercial Power Systems", Appendix N
- IEEE Std 493-1997 "IEEE recommended practice for the design of reliable industrial and commercial power systems", Chapter 9
- IEEE Std 519-1992 "IEEE recommended practices and requirements for harmonic control in electrical power systems"
- IEEE Std 1100-1999 "IEEE recommended practice for powering and grounding electronic equipment"
- IEEE Std 1124-2003 "IEEE guide for the analysis and definition of DC-side harmonic performance of HVDC transmission systems"
- IEEE Std 1159-1995 "IEEE recommended practice for monitoring electric power quality"
- IEEE Std 1159.3-2003 "IEEE recommended practice for the transfer of power quality data"

- IEEE Std 1250-1995 "IEEE guide for service to equipment sensitive to momentary voltage disturbances"
- IEEE Std 1346-1998 "IEEE recommended practice for evaluating electric power system compatibility with electronic process equipment"
- IEEE Std 1531-2003 "IEEE Guide for Application and Specification of Harmonic Filters"
- IEEE Std 1564 draft 6 "Recommended Practice for the Establishment of Voltage Sags Indices"

IEC has presented a standard on electromagnetic compatibility (IEC 61000, 1990), which covers most of the power quality issues. This document consists of 6 parts, named: General, Environment, Limits, Testing and measurements techniques, Installation and mitigation guidelines, and Generic standards. Electromagnetic disturbances are classified by IEC in several categories as listed in Table 1.

Table 1 - Classification of electromagnetic phenomena according to IEC

Conducted low-frequency	Harmonics and inter-harmonics
	Signal systems (power line carrier)
	Voltage fluctuations
	Voltage sags and interruptions
	Voltage imbalance
	Power-frequency variations
	Induced low-frequency voltages
	DC in AC networks
Radiated low-frequency	Magnetic fields
	Electric fields
Conducted high-frequency	Induced continuous wave voltages or currents
	Unidirectional transients
	Oscillatory transients
Radiated high-frequency	Magnetic fields
	Electric fields
	Electromagnetic fields
	Continuous waves
	Transients

2.2 Voltage sags

As mentioned, voltage sags and voltage dips are considered synonyms in this thesis. This assumption is based on the similarity of the definitions found in the standards commented here. According to the IEEE Std 1346-1998 a voltage sag is "a decrease in rms voltage or current at the power frequency for duration of 0.5 cycle to 1 minute". IEC has the following definition for a dip (IEC 61000-2-1, 1990) "A voltage dip is a sudden reduction of the voltage at a point in the electrical system, followed by a voltage recovery after a short period of time, from half a cycle to a few seconds". From the previous definitions it is evident that both voltage sag and voltage dip refer to the same disturbance. Moreover, IEC states that "voltage sag is an alternative name for the phenomenon voltage dip" (IEC 61000-2-8, 2002) regarding voltage dips and short interruption on public electric power systems.

The interest in voltage sags is new in the power quality area. The main concern about voltage sags is their effect on sensitive electrical devices, such as personal computers, adjustable speed drives, programmable logic controllers, and other power electronic equipment. Mestres (1972) described the arrangements made by *Electricité de France* for facilitating the qualitative analysis of the service in the field of short interruptions. Another early research project investigated the possibilities of calculating the effects of voltage sags on industrial consumers using digital simulation (Poeata *et al*., 1978).

Wagner *et al*. (1990) presented a case study involving monitoring power quality disturbances at a representative plant and identifying the disturbances that disrupt production. The sensitivity of electronic control equipment was measured to form a plant disturbance threshold chart. Voltage sags were the only disturbance to directly cause production losses and were the most common disturbance. The most sensitive components failed when the voltage dropped to 80-86 % of rated voltage. On the other hand, the least sensitive loads failed when the voltage dropped to 30 % of the rated voltage. From the test results, the calculated sag threshold to affect production at the utility PCC - point of common coupling was 87 % of the nominal voltage for more than 8.3 ms.

McGranaghan (1995) analysed the effects of voltage sags in process industry applications. The author described the causes of voltage sags that affected industrial processes, their impacts on equipment operation, and the possible solutions. The definition proposed focuses on system faults as the major cause of voltage sags. The sensitivity of different type of loads, including adjustable speed drives, programmable logic controllers, and

motor contactors was analysed. The author also described the available methods of power conditioning for these sensitive equipment.

Heine *et al*. (2002) developed a method for estimating the frequency and cost of voltage sags. The annual number and cost of voltage sags were determined for five Finnish distribution companies. The method of fault positions was applied for the calculation of voltage sag frequency. The economic consequences were assessed by multiplying the sag frequency and cost by the number of customers. The cost of a single voltage sag was determined from a survey that had been carried out in three Nordic countries in the mid 1990s. In addition, they estimated the total annual sag-related cost for each of the companies considered in this study and for each customer category. Finally they concluded that the total cost per company appeared to be much higher than had generally been assumed.

Leborgne *et al*. (2003) investigated an alternative method for the characterisation of industrial process sensitivity to voltage sags using a power quality monitoring system. Several methods used for voltage sag characterisation were analysed. The load behaviour was classified for the measured sags. As a result, a method based on the sag magnitude for the characterisation of load sensitivity was presented. It was concluded that the loads were sensitive to sag magnitudes below 0.70 pu.

Stockman *et al*. (2004) described the vulnerability of adjustable speed drives to voltage sags. Then, three embedded mitigation methods were addressed to protect textile processes against voltage sags. Practical measurements with a sag generator were shown. The use of embedded solutions such as kinetic buffering and boost converter increased the voltage sag immunity of the process.

Djokic *et al*. (2005) discussed the sensitivity of adjustable speed drives to voltage sags and short interruptions on the basis of extensive test results. Existing standards and previously published papers were critically reviewed and a description of test procedures needed for appropriate assessment of adjustable speed drives sensitivity was presented. The results demonstrated that although the behaviour of this equipment has a rather complex pattern, a simple representation of adjustable speed drives sensitivity to various types of voltage sags and short interruption can be established.

Research about mitigation methods for voltage sags are also found in the literature. Johns and Morgan (1994) proposed that the voltage sag impact on industrial processes can be mitigated using ride-through coordination. The utility predicted for the new plant site: the depth, duration and number of expected sags, and the expected malfunctions. The predictions were provided so that they could be included in the new machinery quotations. Because the ride-through predictions for the machinery at the new plant site

were known up front and site specific, mitigating the effects of voltage sags could be built into the machinery and did not necessarily require UPS type equipment. Management weighed additional purchase cost with long term downtime cost based on the machine vs. utility specifications and selected the best economic alternative.

Gomez and Campetelli (2000) proposed voltage sag mitigation by using current-limiting fuses. The authors analysed the coordination of the voltage sag equipment susceptibility curves and the specific energy of the current-limiting fuses. There are several fuse types, which allow the best selection to be made for the reduction of the voltage sag duration, using the fuse energy control characteristic.

Tosato and Quaia (2000) also presented a mitigation solution by reduction of the fault-clearing time. The reduction of the clearing time may lead to a substantial power quality improvement because the majority of sensitive industrial processes (including computer systems, power electronics and variable speed drives) are capable of riding through a sag of very limited duration (typically below half a period). This possibility exists with modern technologies. Later, Tosato (2001) presented the fault current limitation as a way to limit the expected voltage sag amplitude. Since the depth of the voltage sag is proportional to the fault current, limiting the fault current by means of a device connected at the beginning of the most exposed radial feeders was proposed.

Sannino and Svensson (2000) proposed the mitigation of voltage sags based on the application of power electronic devices. A series-connected voltage source converter using vector control and a filter compensation algorithm was presented. The fast control logic is based on the decomposition of the unbalanced supply voltages into instantaneous positive and negative sequence components in a rotating coordinate system. Furthermore, the voltage source converter performance was improved through the implementation of an algorithm to compensate for the steady-state voltage drop on the converter output filter.

Woodley and Sezi (2000) presented another solution for sag mitigation using power electronic devices. The authors described a multi-module dynamic voltage regulator that demonstrated its benefits in protecting large sensitive customer loads from supply system disturbances providing a practical means to minimise down-time in large industrial facilities.

Sang-Yun *et al.* (2000) introduced a voltage sag mitigation method by using feeder transfer in power distribution systems. The authors proposed a method using the switching for sectionalizing points of distribution networks. Customers connected to a bus affected by a voltage sag are switched to another bus supplied by another source.

Macken *et al*. (2004) analysed the incidence of distributed generation for voltage sags mitigation. Two solutions are presented to prevent sensitive equipment from disruptive operation. The emphasis of this paper is on the transient response of the solutions for balanced and unbalanced voltage sags.

Degeneff *et al*. (2000) stated that the cost associated with power quality events depends upon many factors but generally varies from 50 to 400 US$/kVA per year (end user power). The authors analysed the numerous mitigation methods proposed, e.g., uninterruptible power supply, ferroresonant transformers, static transfer switches, transformers with electronic tap-changers, and static voltage compensators. Finally, they presented a comparison of the total owning cost of various equipment options. The total owning cost is found by combining the investment cost of the equipment, with the present value of the operating cost, and the addition cost incurred due to limitations of the device.

Dettloff (2000) analysed another way to reduce the cost of voltage sags to end users. The author describes the contracts between the energy provider and its customers taking into account the power quality performance. In 1995, Detroit Edison entered into long-term pricing and service quality agreements with Chrysler Corporation, Ford Motor Company, and General Motors. The terms are specified in an agreement known as the Special Manufacturing Contract. The service agreement covers voltage interruptions and voltage sags. Detroit Edison became liable for interruptions and voltage sags that exceeded performance targets.

The utility interest to assess their performance regarding voltage sags is also found in the literature. One of the first references in this field was authored by Ermakov and Cherepov (1983), where the authors proposed a statistical analysis of voltage sags in the Soviet Union network. The quality of the voltage was assessed with the aid of a statistical analyser, which measured the amplitude distribution of sags in relation to a nominal level.

Marquet (1993) introduced a software package for the determination of magnitude, duration and number of voltage sags in medium voltage networks at *Electricité de France*. These results enabled customers to know the voltage sag indices at any location in the network, indicating the minimum ride-through needed by the loads to be unaffected by voltage sags.

Sabin *et al*. (1999) presented the performance of a distribution grid based on a monitoring survey. This work describes the methods for collecting, characterising, and analysing rms voltage variation measurements. The measurements were collected at the primary distribution systems of 24 utilities in different geographic regions of the United States.

Brazil also runs a project to evaluate the sag performance of Brazilian network busbars. The Brazilian electric energy market can be characterised as a functionally unbundled model, which implies that generation, transmission, distribution, and commercialisation activities are segregated. The Brazilian ONS - Independent System Operator has been working to bring into force all the previous concerns with respect to the question of power quality. Therefore, a measurement survey has been initiated. This project has as its prime motivation the assessment of the quality of power at the end consumer and has striven to achieve the immediate objectives of identifying the main causes and mechanisms of sag propagation in the system, as well as to define and characterise the phenomenon and its indices (Macedo Correia and Oliveira Campones do Brasil, 2003).

Thallam and Heydt (2000) introduced a set of indices to evaluate the grid performance for three-phase voltage sags. The electric power acceptability curves are an empirical set of curves that represent the intensity and duration of bus voltage disturbances. Alternative indices for the assessment of voltage sags, such as voltage sag energy, were proposed.

The complex issues involving voltage sags are the consequence of the different requirements on equipment manufacturers, distribution utilities and end users. In the environment of a more competitive energy market, equipment manufacturers and distribution utilities have made efforts towards achieving the satisfaction of their customers. The contribution of power quality standards is very important, although the definitions and criteria for the power quality analysis are not yet well defined (Ribeiro, 1999).

3 Single Event Characterisation

This chapter presents an overview of the characterisation of voltage sags. Unbalanced voltage sags are highlighted since they are the most common type of sags in transmission and distribution networks. Laboratory experiments to characterise voltage sags using a PQ-monitor and a phasor measurement unit - PMU are reported. A new method to obtain the voltage sag type from phase-to-ground and phase-to-phase voltages is introduced. Several methods for voltage sag representation based on phasor analysis are proposed. The propagation of voltage sags in power systems is analysed using actual measurements taken from a power grid.

3.1 Magnitude, duration, and phase-angle jump

Magnitude and duration are the two most important sag characteristics. Sag magnitude is defined as the minimum rms voltage. Alternatively, sag magnitude may be defined as the amplitude of the voltage drop, leading to an opposite meaning, as shown in Figure 3. Therefore it is necessary to specify if magnitude refers to the retained voltage or to the drop of the voltage. The expressions "sag magnitude", "retained voltage", "remaining voltage" are considered synonyms in this thesis. The term "residual voltage" can be also found in the literature and is normally used to express the "retained voltage". The voltage sag duration is the period of time when the voltage is lower than a stated limit, as shown in Figure 3.

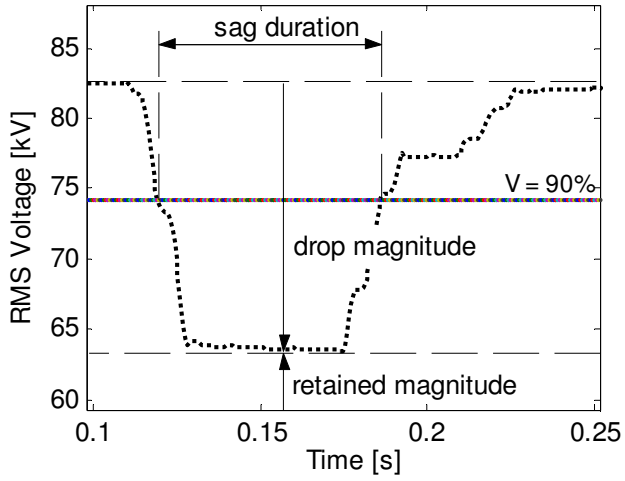

Figure 3 - Voltage sag magnitude and duration

According to IEEE Std. 1159 (1995), sag magnitudes range from 0.10 pu to 0.90 pu of nominal voltage and sag durations from a half-cycle to one

minute. Furthermore, sags may be classified according to their duration in instantaneous, momentary, and temporary as shown in Table 2.

Table 2 - Classification of voltage sags according IEEE 1159

Type of Sag	Duration	Magnitude
Instantaneous	0.5 - 30 cycles	0.10 - 0.90 pu
Momentary	30 cycles - 3 s	0.10 - 0.90 pu
Temporary	3 s – 1 min	0.10 - 0.90 pu

The power system voltage is described by a sine wave. A voltage sag can be seen as a reduction of the amplitude of the waveform. Figure 4 shows the voltage waveform during a voltage sag. The amplitude of the instantaneous voltage can also be used to characterise the sag magnitude.

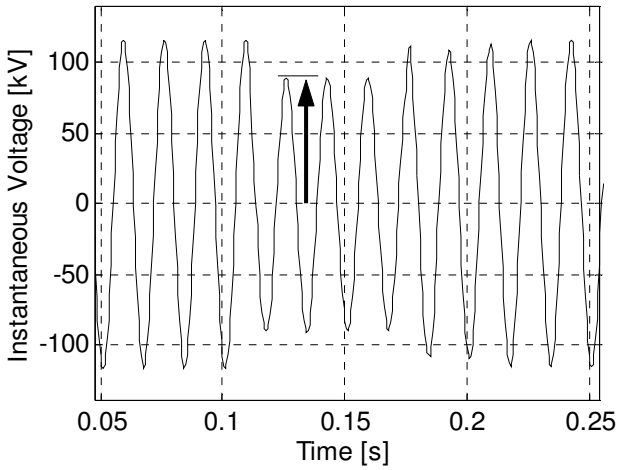

Figure 4 - Voltage waveform during voltage sag

Considering that a voltage sag is defined as a reduction of the rms voltage, it is natural to use the rms voltage to define the voltage sag magnitude. The rms voltage is calculated by

$$V_{rms}(k) = \sqrt{\frac{1}{N}\sum_{i=k-N+1}^{k} v_i^2} \tag{3.1}$$

where N is the number of samples per cycle, v_i is the instantaneous sampled voltage and k is the instant when the rms voltage is estimated. Here the rms voltage is estimated *á posteriori*; the rms voltage is calculated with the previous N instantaneous voltage samples. This algorithm is called "one-cycle window", meaning that the rms values are estimated based on one cycle of instantaneous values.

Alternatively it is possible to estimate the rms value using only half a cycle of instantaneous values. This algorithm is called a "half-cycle window"

$$V_{rms\,(1/2)}(k) = \sqrt{\frac{2}{N}\sum_{i=k-(N/2)+1}^{k} v_i^2} \tag{3.2}$$

The half cycle algorithm is more sensitive to changes in the voltage and has a faster response to detect an event. However, the half-cycle algorithm shows oscillations when there is a second harmonic component in the voltage signal. Figure 5 shows the rms voltage estimation using one-cycle and half-cycle algorithms. The figure shows that the half-cycle algorithm is faster to detect the starting and ending of the events. Nevertheless, the estimation of event duration is not much different and do not affect the sag indices estimation (Kagan *et al.*, 2000).

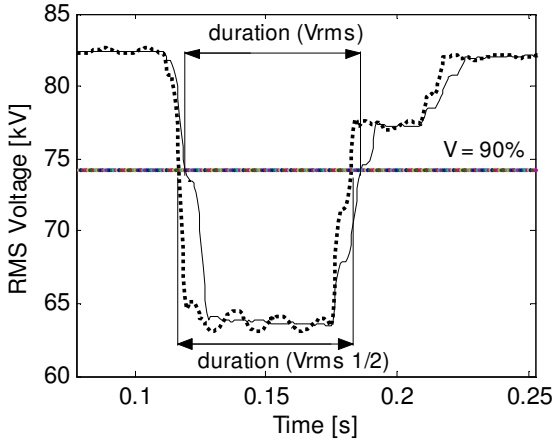

Figure 5 - Rms voltage estimated using a half-cycle algorithm (dotted line) and a one-cycle algorithm (solid line)

The rms voltage is not a constant value during the event. In this thesis the voltage sag magnitude is characterised by the minimum rms value during the event, as shown in Figure 6. This is the usual approach for the system performance evaluation, where the single event characteristics are not so relevant.

It is also possible to consider the fundamental voltage to obtain the voltage sag characteristics. The fundamental voltage is a complex quantity obtained by the decomposition of the instantaneous voltage in its Fourier components, where the second component of the series corresponds to the fundamental frequency (50 or 60 Hz). The rms value of the fundamental voltage behaves similarly as the rms value of the complete voltage, as shown in Figure 7. This similarity is seen for normal conditions (acceptable harmonic levels). In addition, voltage sag magnitude and duration estimated

using fundamental voltages are sufficiently accurate for most sag analysis (Ohrstrom and Soder, 2003).

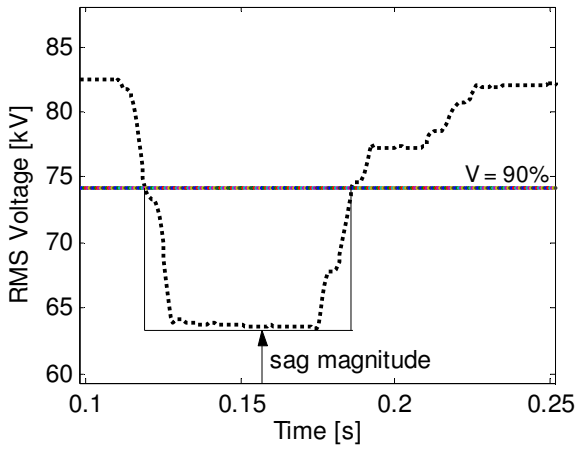

Figure 6 - Sag magnitude characterisation (solid line) and rms voltage (dotted line)

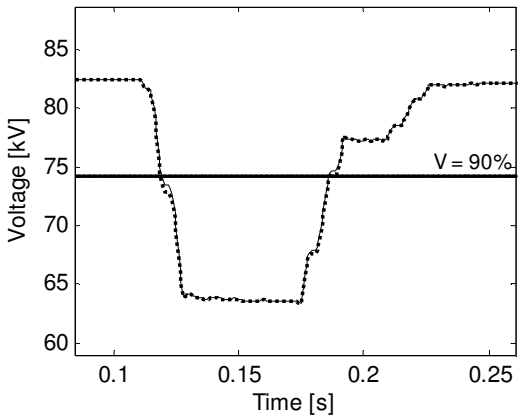

Figure 7 - Rms voltage (solid line) and rms of fundamental voltage (dotted line)

The fundamental voltage is obtained using the FFT - Fast Fourier Transform, where FFT is an efficient algorithm for computing the DFT - Discrete Fourier Transform. DFT is the appropriate Fourier analysis for a sampled vector, such as the instantaneous voltage.

The analysis of power systems in the frequency domain is based on the assumption that the frequency (f) remains constant and that all electrical entities have the same frequency. Under these conditions the voltages and currents are represented by complex entities known as phasors. These phasors have a constant magnitude and the angle varies constantly at a speed of $2\pi f$ [rad/s].

A fault in the power system affects not only the magnitude of the voltage phasors but also the angle of the phasors. The change of the phasor angle is called phase-angle jump associated with the voltage sag. The phase-angle jump is seen as a shift in the zero crossing of the instantaneous voltage and

it is a cause of failure of power electronic converters that use phase-angle information for their firing control (Bollen, 2000).

The phase-angle jump (Ψ) is the difference between the actual voltage-angle (arg[$V(t)$]) and the reference voltage-angle ($\Phi_o(t)$), as shown in Figure 8. The reference angle ($\Phi_o(t)$) follows a straight line because it rotates with constant speed ($2\pi f_o$). The actual angle coincides with the reference angle until the starting of the event. Then the actual angle diverges from the reference angle causing the phase-angle jump. After the event the actual angle may not coincide with the reference one. The actual angle may keep a constant shift if the post-event frequency is the same as the pre-event frequency; otherwise the actual angle diverges constantly with respect to the reference angle.

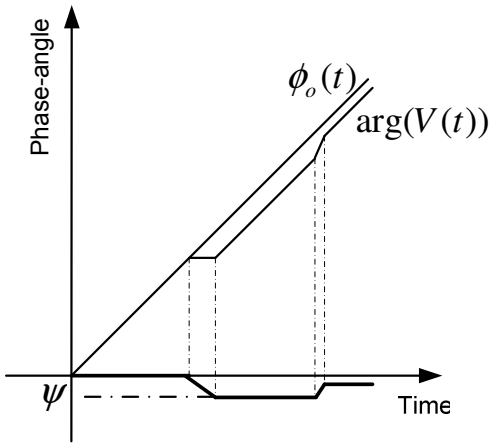

Figure 8 - Phase-angle jump schematic representation

The phase-angle jump can be obtained from measured instantaneous voltages and from simulated sags, using time domain tools such as electro-magnetic transient programs. In these cases, when the instantaneous voltage is available, the complex voltages are obtained using the Discrete Fourier Transform. Once the complex voltages are known the voltage angle is estimated as the argument of the complex value.

The algorithm presented above has been applied to the voltage sag shown in Figure 4. The estimated phase-angle jump is shown in Figure 9. The starting and ending sag transition periods must be neglected to estimate the maximum absolute deviation of the phase-angle because they are a consequence of the Fourier Transform algorithm applied to a non-periodic signal and do not represent the physical reality.

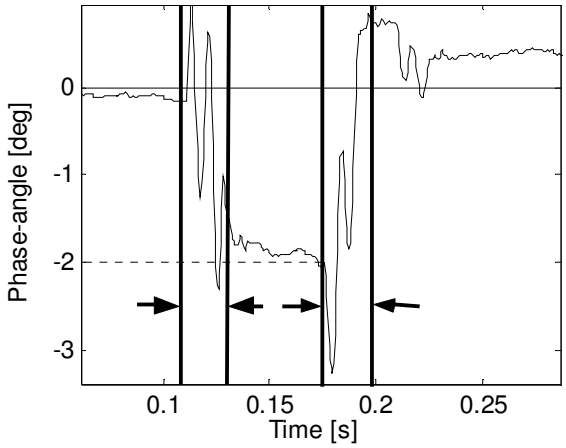

Figure 9 - The starting and ending transient periods, indicated by the arrows, should be neglected to estimate the phase-angle jump (-2 deg)

3.2 Three-phase events

The voltage sags observed in transmission and distribution networks generally affect more than one of the phases. Moreover, each one of the three phases may perceive different voltage sag characteristics. Figure 10 shows an unbalanced voltage sag, where two phases are affected. In addition, the voltage sag has different magnitude and duration in each phase, indicated as V_a, t_a, V_b, and t_b in Figure 10.

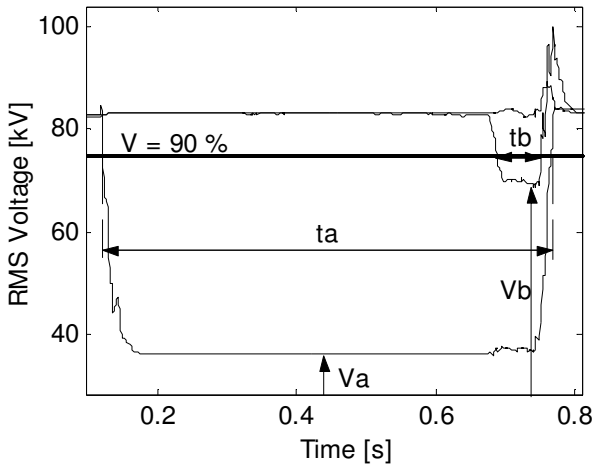

Figure 10 - Unbalanced voltage sag, phases V_a and V_b

Two different approaches to characterise three-phase voltage sags can be found in the literature. One approach is to consider each phase individually and treat the three-phase event as three single phase events; estimating magnitude, phase-angle jump and duration for each single event (Martinez and Arnedo, 2004).

A more common approach is to consider the three-phase sag as one combined event. Single event-characteristics are obtained as a result of the phase aggregation. The lowest voltage and the longest duration may be chosen to characterise the three-phase sag (Bollen and Zhang, 2003).

Bollen and Zhang (2003) developed two methods to obtain a three-phase voltage sag characterisation called "ABC classification" and "symmetrical components classification". Due to its simplicity the ABC classification is more used than the symmetrical components classification.

In the ABC classification seven types of voltage sags are distinguished. The complex voltages and the phasor diagram of each type of sag are shown in Table 3.

Table 3 - Three-phase voltage sags according the ABC classification

Type A $\overline{V}_a = V$ $\overline{V}_b = -\frac{1}{2}V - j\frac{\sqrt{3}}{2}V$ $\overline{V}_c = -\frac{1}{2}V + j\frac{\sqrt{3}}{2}V$ 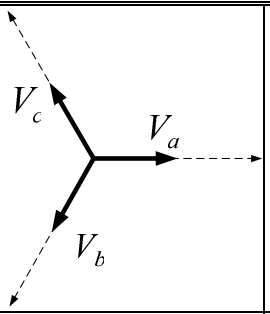	**Type B** $\overline{V}_a = V + V_0$ $\overline{V}_b = -\frac{1}{2}E_1 - j\frac{\sqrt{3}}{2}\overline{E}_1$ $\overline{V}_c = -\frac{1}{2}E_1 + j\frac{\sqrt{3}}{2}\overline{E}_1$ 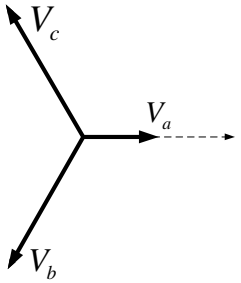
Type C $\overline{V}_a = E_1$ $\overline{V}_b = -\frac{1}{2}E_1 - j\frac{\sqrt{3}}{2}V$ $\overline{V}_c = -\frac{1}{2}E_1 + j\frac{\sqrt{3}}{2}V$ 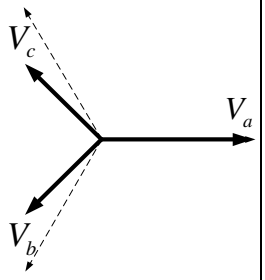	**Type D** $\overline{V}_a = V$ $\overline{V}_b = -\frac{1}{2}V - j\frac{\sqrt{3}}{2}E_1$ $\overline{V}_c = -\frac{1}{2}V + j\frac{\sqrt{3}}{2}E_1$ 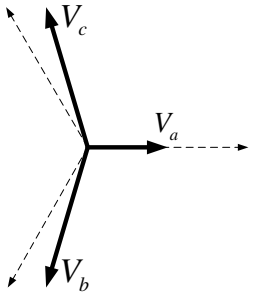
Type E $\overline{V}_a = E_1$ $\overline{V}_b = -\frac{1}{2}V - j\frac{\sqrt{3}}{2}V$ $\overline{V}_c = -\frac{1}{2}V + j\frac{\sqrt{3}}{2}V$ 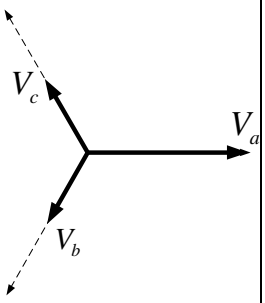	**Type F** $\overline{V}_a = V$ $\overline{V}_b = -\frac{1}{2}V - j(\frac{\sqrt{3}}{6}V + \frac{\sqrt{3}}{3}E_1)$ $\overline{V}_c = -\frac{1}{2}V + j(\frac{\sqrt{3}}{6}V + \frac{\sqrt{3}}{3}E_1)$ 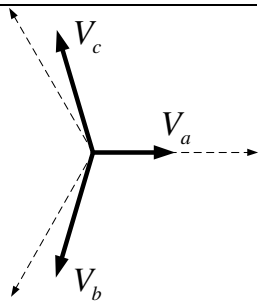
Type G $\overline{V}_a = \frac{2}{3}E_1 + \frac{1}{3}V$ $\overline{V}_b = -\frac{1}{3}E_1 - \frac{1}{6}V - j\frac{\sqrt{3}}{2}V$ $\overline{V}_c = -\frac{1}{3}E_1 - \frac{1}{6}V + j\frac{\sqrt{3}}{2}V$ 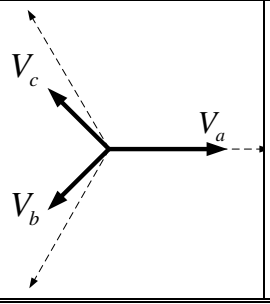	

The pre-event voltage in phase A is denoted as E_1, recalling to the equivalence between phase A voltage and positive sequence voltage in a balanced system. The voltage in the phase that experienced the sag or between the two phases that experienced the sag is called characteristic voltage and it is noted as V. The only exception is the sag type B, where the faulted phase voltage is not equal to the characteristic voltage because the characteristic voltage does not have any zero sequence component, as shown in Table 4.

Table 4 - Characteristic voltage

Fault type	**Characteristic voltage – V_{ch}**
LLLG	$V_{ch} = V_1 = V_a$
SLG	$V_{ch} = V_1 + V_2$
LL and LLG	$V_{ch} = V_1 - V_2$

The characteristic voltage is a complex value that can be obtained analytically from the positive and negative sequence voltages as shown in Table 4. The absolute value of the characteristic voltage is proposed to represent the three-phase sag magnitude. The advantage of this index is that it does not change when a voltage sag propagates through a delta/wye transformer.

The sag types shown in Table 3 are described considering phase A as the reference phase. It means that another set of equivalent equations can be derived if phase B or C are set as the reference phase.

The ABC classification was developed, among other reasons, to analyse the propagation of a voltage sag from transmission to distributions levels, when the disturbance propagates through a transformer. The generation and propagation of the different types of voltage sags are indicated in Table 5.

For instance, when there is a LLG fault at the location I, a sag type E is seen at this location. However, at location II below a delta/wye transformer the same event is seen as a sag type F and at location III below another delta/wye connected transformer the sag is observed as type G. An extensive investigation on voltage sag propagation based on system measurements is reported in Section 3.6.

Table 5 - Voltage sag types propagation through a delta/wye transformer

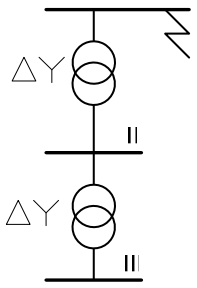

	Location / Voltage sag type			
Fault type	**I**	**II**	**III**
LLLG	A	A	A
SLG	B	C	D
LL	C	D	C
LLG	E	F	G

3.3 Extended characterisation through measurements

This section is included in Paper I.

In order to measure and characterise voltage sags an analogue network model is used. The analogue network is a three-phase scaled model of a 400 kV transmission system that includes: a generation plant, transmission lines, two transformers with on-load tap changers, and passive and dynamic loads. The scaled model operates at 400 V.

The line model consists of six identical π-sections, each corresponding to a 150 km 400 kV line. The sections can be connected arbitrarily in series or parallel. The scaled values of each transmission line resistance, inductance and capacitances are:

Transmission line: $R = 50.0\ m\Omega,\ L = 2.05\ mH,\ C = 46.0\ \mu F$.

The generic system configuration investigated is shown in Figure 11. It represents a transmission grid where a group of loads are supplied through two transmission lines. The loads include pure resistive loads and an IM - induction machine. The load characteristics are:

Induction machine: $U_N = 380\ V,\ I_N = 62\ A,\ PF = 0.81,\ n_N = 1450\ rpm$

Three-phase resistive loads: $U_N = 400\ V,\ P_N = 9\ kW$

Two measurement devices were used during the tests. A PQ-monitor recorded instantaneous voltages sampled at a fix frequency of 7.2 kHz. A PMU recorded the positive sequence complex voltage every cycle (20 ms).

The measurements obtained by the PQ-monitor and the post-processing work done with MatLab are summarised in Table 6 and Table 7. The estimated sag characteristics are: the voltage phasors, the minimum phase

voltage, the maximum phase-angle jump, the absolute value of the characteristic voltage, the angle of the characteristic voltage, and the sag type.

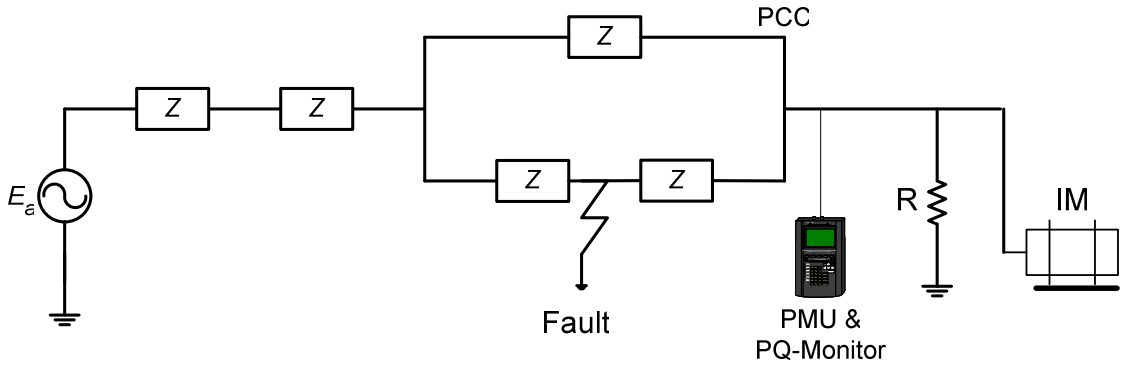

Figure 11 - Generic system configuration investigated

The sag magnitudes obtained by the minimum phase value and the characteristic voltage are compared. The average difference is 12 %. For SLG and LL faults a larger difference is obtained. This is explained by the definition of the characteristic voltage during a SLG and a LL fault. During the SLG faults, the characteristic voltage is obtained as the sum of positive and negative sequence voltages, whereas the minimum phase voltage includes the zero sequence component. During the LL faults, the difference between the two values is caused by the phase-angle jump of the two faulted phases.

The phase-angle jump of the characteristic voltage and the largest of the three phases' angle-jumps are now compared. For the LLLG faults, the phase-angle jump obtained by the phase voltage and the characteristic voltage are in accordance with each other. Because for symmetrical faults there are only positive sequence voltages in the system, the definition of the characteristic voltage is the voltage in phase A. Consequently, both phasors are the same and experience identical phase-angle jump during the sag.

For asymmetrical faults, however, the results obtained from the characteristic voltage and the phase values do not agree with each other.

The angle of the characteristic voltage will be equal to the symmetrical phase angle if the two healthy phases in a SLG fault (or the two faulted phases in a LL or LLG fault) are symmetrical with respect to the axis where the third phase (the symmetrical phase) lies on. The difference occurs because the phase-angle jump of the characteristic voltage deviates from the phase-angle jump of the symmetrical phase, due to the realistic asymmetry of the two healthy phases in the SLG fault (or two faulted phases in LLG fault). The difference that occurs under the load condition of induction machine has the same justification.

Table 6 - PQ-Monitor results resistive load

Fault type	Phasors	V_{ph} [V]	$\Delta\Phi$ (deg)	$\lvert V_{ch}\rvert$ [V]	$arg\ V_{ch}$ (deg)	Sag Type
LLLG	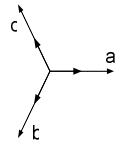	112	1.7	113	1.5	A
SLG	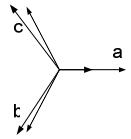	111	11	182	2.5	B
LL	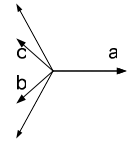	149	22.7	113	4.1	C
LLG	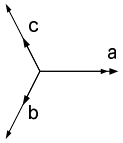	111	2.3	113	2.4	E

Note: V_{ph}: minimum phase retained voltage. $\Delta\Phi$: maximum phase-angle jump, V_{ch}: characteristic voltage.

Table 7 - PQ-Monitor results resistive load + induction machine

Fault type	Phasors	V_{ph} [V]	$\Delta\Phi$ (deg)	$\lvert V_{ch}\rvert$ [V]	$arg\ V_{ch}$ (deg)	Sag Type
LLLG	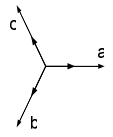	115	-4.1	115	-3.8	A
SLG	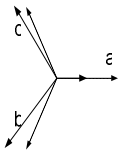	113	-13.8	184	-2.0	B
LL	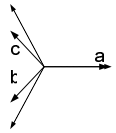	146	-13.4	130	1.1	C
LLG	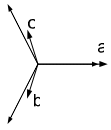	116	9.4	127	2.1	E

For a LL fault, the maximum phase-angle jump of the phase voltages will not necessarily occur in the symmetrical phase. Instead, the maximum

phase-angle jump of the phase voltages will appear in one of the faulted phases. As the phase-angle jump of the characteristic voltage is normally equal to the phase-angle jump of the symmetrical phase, which is the non-faulted phase, there is a large difference between the two definitions of phase-angle jump.

The sag type based on the ABC classification is determined by the voltage phasors. Although the obtained phasors do not comply exactly with the phasors presented in Table 3 it is possible to identify the actual phasor diagrams and classify them into the different sag types. The ABC classification method, although intuitive, can not be easily implemented in terms of a computational algorithm.

As shown in Table 6, the phase-angle jumps are all positive for a resistive load condition when calculated from the phase voltages or the characteristic voltage. On the other hand, as shown in Table 7, the phase-angle jumps are negative for the induction machine load under LLLG, SLG, and LL faults, based on the phase voltage calculations. Therefore, in general terms it can be stated that the phase-angle jump associated with a voltage sag is negative when there is a high penetration of induction machine loads and the phase-angle jump is positive when the load is mainly resistive.

The next aspect is to compare the different results of the voltage sag characterisation obtained by the PQ-monitor and the PMU. In order to be able to compare both types of measurements, the PQ-monitor data is processed using a MatLab routine to obtain the positive sequence voltage. Then the minimum value of the positive sequence voltage magnitude is used to characterise the sag magnitude.

The results are summarised in Table 8 for each type of fault and load condition. The positive sequence voltages obtained by the PMU recordings comply with those obtained by the PQ-monitor, and the relative errors are all within 5 %. Therefore, the PMU can produce relatively accurate results for the positive sequence voltage magnitude.

Now the phase-angle jumps obtained by the PQ-monitor and the PMU are compared. As shown in Table 9, the largest difference between the measurements is 5.7 degrees obtained during a LLLG fault. However, in most cases the difference is rather small and both devices show the same trend: positive phase-angle jumps for resistive loads and negative-phase angle jumps for an induction machine load. The exception is for the LLLG where the PMU measured a positive phase-angle jump for an induction machine load, making the large difference compared to the PQ-monitor measurement.

Table 8 - Positive sequence voltage obtained by the PQ-Monitor and the PMU

Positive sequence voltage [V]			
Fault type	**Measurement device**	**Resistive load**	**Resistive load + induction machine**
LLLG	PMU	110	113
	PQ-monitor	113	114
SLG	PMU	197	190
	PQ-monitor	207	198
LL	PMU	169	164
	PQ-monitor	173	164
LLG	PMU	160	156
	PQ-monitor	163	157

From the laboratory measurements it is possible to conclude that the classification of the sags into ABC types agreed very well for all the fault types and load conditions. The characteristic voltage can be used to estimate the sag magnitude and the phase-angle jump.

Table 9 - Phase-angle jump measured by the PQ-Monitor and the PMU

Phase-angle jump of positive sequence voltage (deg)			
Fault type	**Measurement device**	**Resistive load**	**Resistive load + induction machine**
LLLG	PMU	4.4	1.8
	PQ-monitor	1.5	-3.9
SLG	PMU	2.8	-0.3
	PQ-monitor	2.0	-2.7
LL	PMU	2.7	-1.4
	PQ-monitor	3.0	-1.8
LLG	PMU	1.7	-1.9
	PQ-monitor	1.7	-1.0

3.4 From instantaneous voltages to voltage sag type

This section is covered in Paper II.

Obtaining the voltage sag type from measured voltages is not straightforward. One of the main problems is that the method presented in Section 3.2 was developed for a simplified system model. When actual voltages are analysed the voltage sag classification is not so evident. In this section a new method to classify three-phase voltage sags is developed.

When the instantaneous PN - phase-to-neutral voltages are available the instantaneous PP - phase-to-phase voltages can be obtained as the difference of the instantaneous PN voltages. Then PN and PP complex voltages can be obtained using the Fast Fourier Transform. The relation between the minimum PN and the minimum PP voltages expressed in pu will be used to classify the three-phase unbalance sags into the ABC categories.

A theoretical relation between the minimum PN and the minimum PP voltage can be formulated for each type of sag using the equations shown in Table 3. The PP voltages have been normalised by the $\sqrt{3}$ factor. The equations that relate PN and PP sag magnitudes are shown in Table 10.

Table 10 - Theoretical relation between PP and PN sag magnitudes

Sag type	PP vs. PN
A	$V_{PP} = V_{PN}$
B	$V_{PP}^2 = \left(\frac{1}{2\sqrt{3}} + \frac{V_{PN}}{\sqrt{3}} \right)^2 + \frac{1}{4}$
C	$V_{PP}^2 = \frac{4}{3} V_{PN}^2 - \frac{1}{3}$
D	$V_{PP}^2 = \frac{1}{4} + \frac{3}{4} V_{PN}^2$
E	$V_{PP} = V_{PN}$
F	$3V_{PP}^2 = (2 + \frac{1}{3}) V_{PN}^2 + \frac{1}{3} V_{PN} + \frac{1}{3}$
G	$V_{PP} = -0.0707 + \frac{\sqrt{3.112 V_{PN}^2 - 0.327}}{1.556}$

These theoretical relations, that identify each type of voltage sag, are plotted and presented in Figure 12, where each curve is named with the letter that identifies the sag (A, B, C, D, E, F, and G) according to the ABC classification.

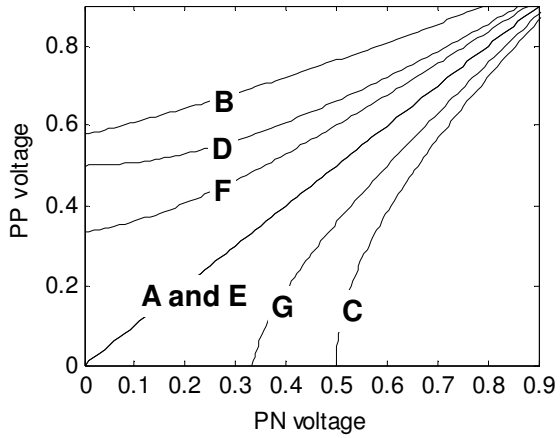

Figure 12 - Theoretical curves for each type of voltage sag

In order to test the applicability of this method, voltage sags are generated by the simulation of faults in a transmission grid. The results are presented in four plots, one for each type of fault (SLG, LL, LLG, and LLL), as shown in Figure 13. The obtained sags can be characterised by the proximity to the reference curves. The dispersion observed in the plotted sags can be explained as the effect of the sag propagation through transformers that change the sag type.

The type of fault that caused the voltage sag can be identified observing the region of the chart where the sag is plotted. Therefore, this method has two direct applications, characterisation of three-phase sags and classification of the sag source (type of fault).

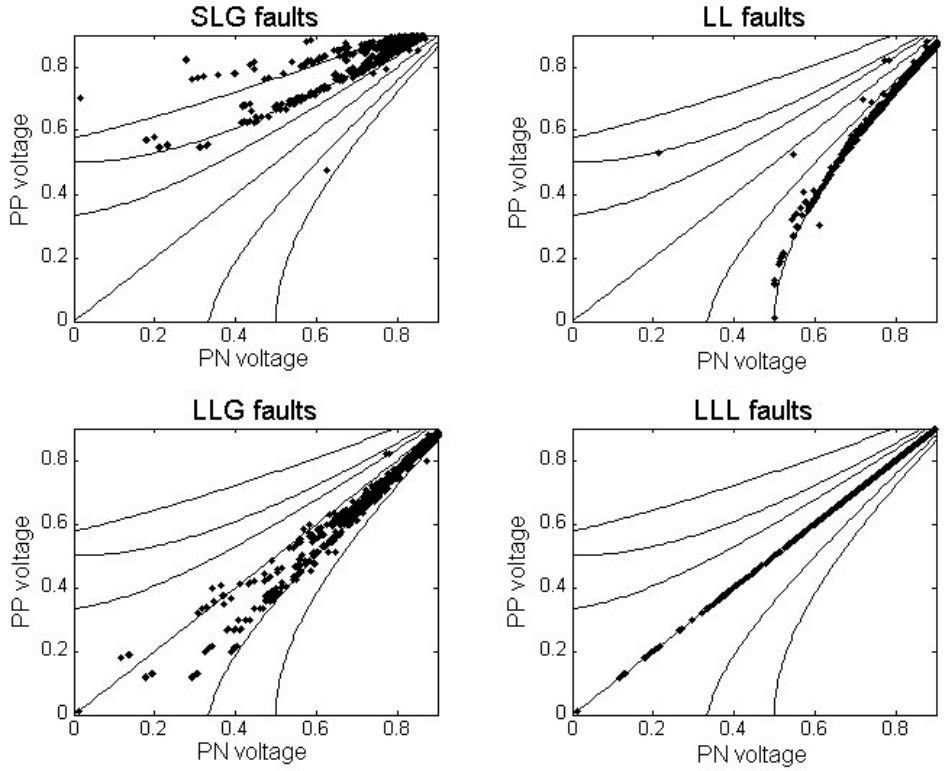

Figure 13 - PP vs. PN sag magnitudes for each type of fault

3.5 Characterisation based on phasors

This section is extracted from Papers III and IV.

During voltage sags the magnitude and angle of the voltage phasors are affected. Previous studies have focused on the magnitude variation, which was considered to be the most important parameter for sensitive loads. Recently, studies on voltage sags also started to include the phase-angle variation, which also causes malfunctions of electronic devices such as three-phase converters (Bollen, 2000).

During a sag the voltage phasors can be assessed through the independent analysis of magnitude and phase-angle versus time respectively, as shown in Figure 14. This event was recorded at a sample rate of 32 points per cycle. Voltage magnitude and phase-angle are obtained applying the Discrete Fourier Transform over a window of one cycle of the instantaneous voltage. The results are updated for each new voltage sample. Thus, the algorithm is applied 32 times every cycle obtaining a quasi-continuous estimation of magnitude and phase-angle jump.

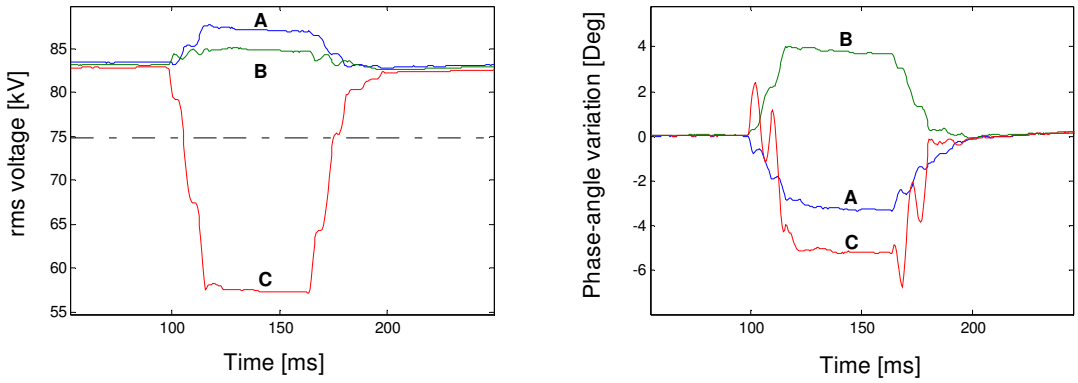

Figure 14 - Voltage sag represented by rms voltage vs. time and phase-angle variation vs. time

The phasors can also be analysed in a two-dimensional chart where the imaginary part is plotted versus the real part, as shown in Figure 15. This chart shows both the phasor locus and the extreme phasors. The phasor locus is the path that the phasor follows during the sag. The extreme phasors are a couple of phasors that represent the phasor with the minimum rms voltage and the phasor with the largest phase-angle variation. The pre-event phasors (dashed line), the pre-event phasor magnitude (external circle, solid line), and the sag threshold (internal circle, dashed line) are also represented.

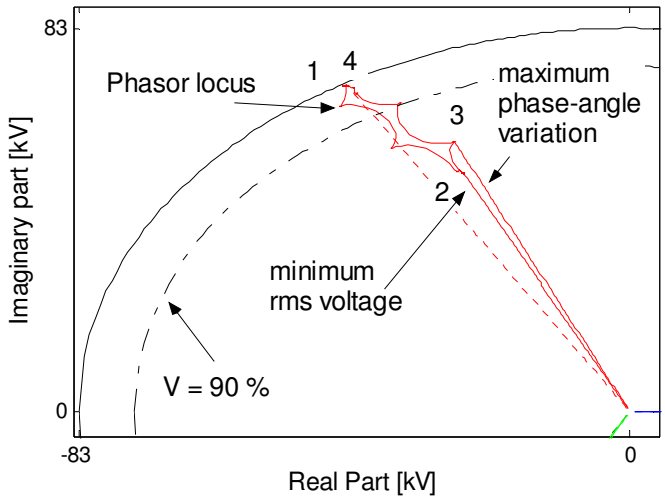

Figure 15 - Voltage sag phasor characterisation including: threshold V=90 %, maximum phase-angle variation, minimum rms voltage, and phasor locus (1-2-3-4)

In order to reintroduce the time reference while keeping the visual effect from the chart of the phasors, the during-event phasors can be seen in a sequence of snapshots, as shown in Figure 16. In this figure, it can be observed how the phasors "move" during the event. The first and last graphs show the precise time when one of the phasors intersects the sag threshold (V=90 %). These 6 snapshots are selected to show the phasors behaviour

during this voltage sag, nevertheless more than 100 snapshots are available to describe this sag-event.

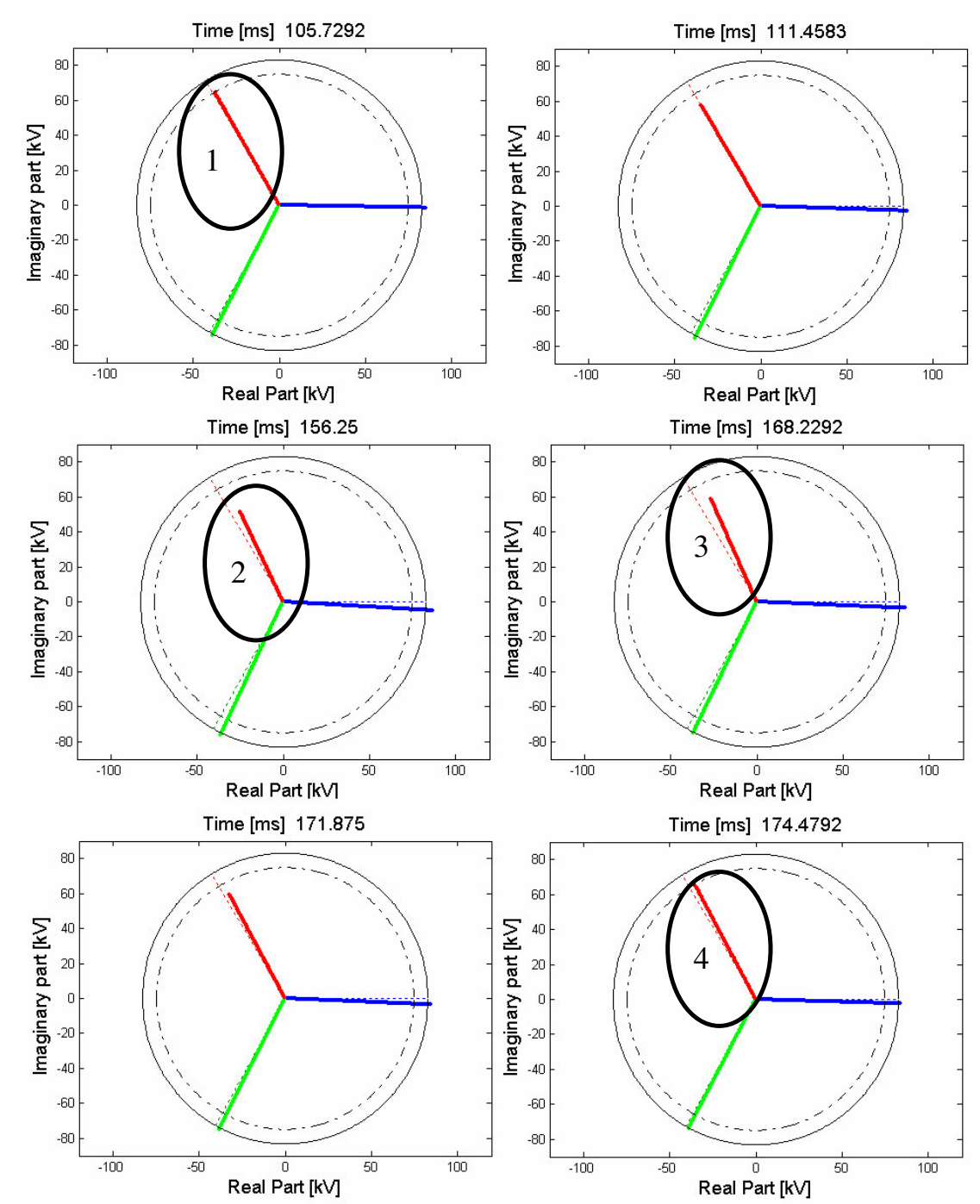

Figure 16 - Voltage sag shown by a sequence of phasor snapshots: voltage sag initiation (1), minimum rms voltage (2), maximum phase-angle variation (3), voltage sag ending (4)

This kind of visual representation is becoming more common in power system analysis as a consequence of the installation of PMU - phasor measurement units.

3.6 Analysis of voltage sag propagation

This section is covered by Paper V.

Most of the sensitive loads are connected at low and medium voltage levels. They are affected by voltage sags caused by faults in the nearby distribution system and by faults at the transmission level, sometimes far away from the load connection. Hence, it is relevant to analyse the propagation of the sags at the same voltage level (horizontal propagation) as well as the propagation between different voltage levels (vertical propagation).

In order to understand the vertical propagation of voltage sags it is necessary to analyse how the voltage sag type changes from the primary to the secondary side of a transformer. When a voltage sag propagates through a transformer, the relation between the phasors on the secondary side is normally not the same as the relation between the phasors on the primary side. For example, in a delta/wye transformer, a phasor at the secondary side is the subtraction of two phasors from the primary side. The consequences are that the zero sequence component is filtered and the positive and negative sequences are rotated by a multiple of +/-30 degrees respectively.

In a meshed transmission grid, the horizontal propagation of a voltage sag may be larger than its vertical propagation. However, from the fault location to the sensitive load location, a voltage sag travels through the network on a combined process of horizontal and vertical propagation. Therefore, both horizontal and vertical propagations have to be addressed.

The analysis of the horizontal propagation is more complex and requires computer simulations. It can be assumed that the voltage sag type is not changing. However, its magnitude and duration may be affected by the proximity of generation plants and large induction machines that behave like generators at the beginning of the sag. The topology of the network and the impedance of the lines also play an important role on the voltage sag propagation.

Few attempts have been made in order to quantify the propagation of the voltage sags. One of the proposals is the use of a SPI - sag propagation index (Gnativ and Milanovic, 2001)

$$SPI_{\%V} = \frac{N_{Bi}}{N_{Bt}} \tag{3.3}$$

where $\%\ V$ is a voltage threshold (50 %, 70 %, 90 %), N_{Bi} is the number of buses experiencing voltage sag with magnitude less than $\%\ V$, and N_{Bt} is the total number of buses.

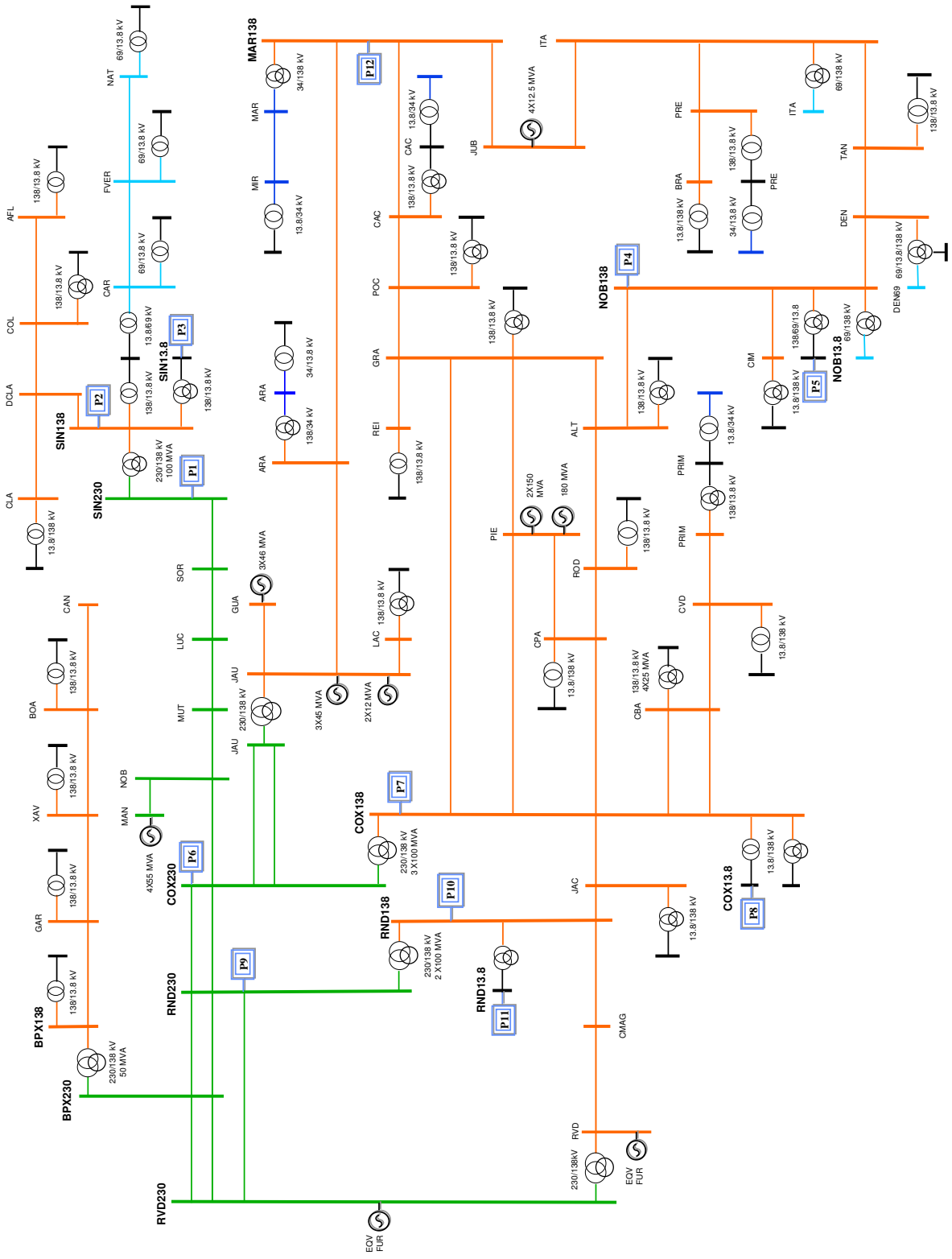

Figure 17 - Diagram of the monitored power system

The system used in the case study is shown in Figure 17. The network contains 67 transmission lines (138 and 230 kV) with a total length of 6619 km. The generation capacity is larger than the present demand and the

excess of generated power is exported to another regional grid through the RND substation.

A total of 12 buses (P1…P12) located at 5 substations were selected for voltage sag monitoring. The criteria for the bus choice included: network topology, load concentration, sensitive loads location, main generation plants, and transformer connections.

The monitoring system consists of 12 PQ-monitors that work with the same time-stamp due to GPS synchronisation. The communication between the PQ-monitors and the centralised server is established using the mobile telephone network. The measurements included: voltage phasors, rms voltage vs. time, and magnitude and duration at each phase. The selected sag threshold was 0.85 pu in order to neglect the most shallows sags and not to overload the communication system

After six months of measurements, 30 events were selected for the propagation analysis. The 30 fault-events generated a total of 89 voltage sags at the 12 monitored buses. The histogram and the cumulative distribution of the voltage sags magnitudes are presented in Figure 18. Although there is a high concentration of sags with magnitudes between 0.7 and 0.85 pu, half of the sags have a magnitude below 0.70 pu. These sags may cause the malfunction of industrial processes as observed in previous studies (Leborgne *et al*., 2003).

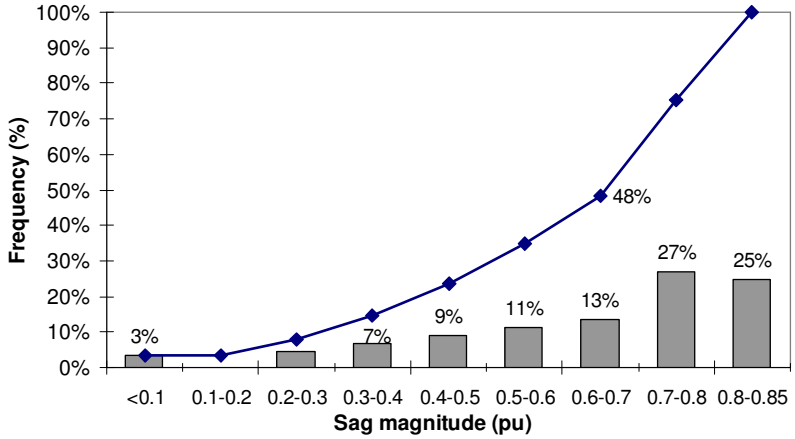

Figure 18 - Distribution of voltage sag magnitudes. The solid line denotes the accumulated frequencies of sag magnitude

The histogram of the voltage sag durations is shown in Figure 19. Approximately 50 % of the sags have a duration of less than 100 ms. These sag durations agree with the protection setting used by the utility, where the fault-clearing time for the first zone is about 100 ms.

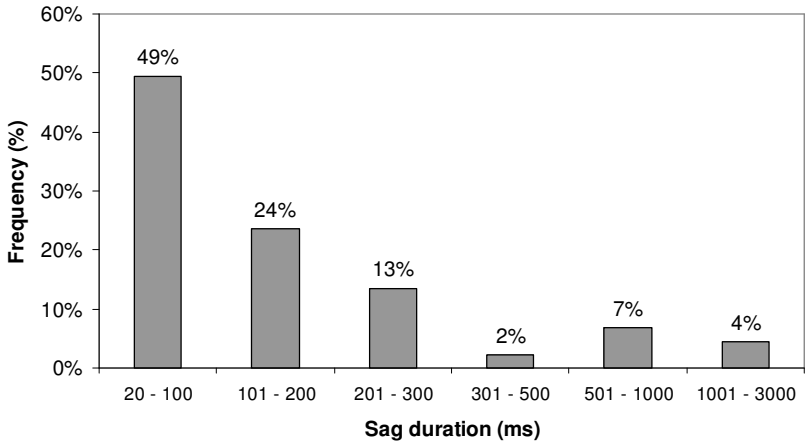

Figure 19 - Histogram of voltage sag durations

In order to characterise the severity of the events considering the propagation of the voltage sags the SPI was estimated. The SPI was calculated considering the number of PQ-monitors that triggered, normalised by the total number of installed PQ-monitors. The index for the 30 faults is shown in Figure 20.

It is important to mention that most of the faults do not affect a large part of the system. In average, each fault triggers 25 % of the monitors (the average SPI is 0.25). However, some of the faults were considerably more severe. For example, one of the events triggered 11 PQ-monitors (SPI=0.91).

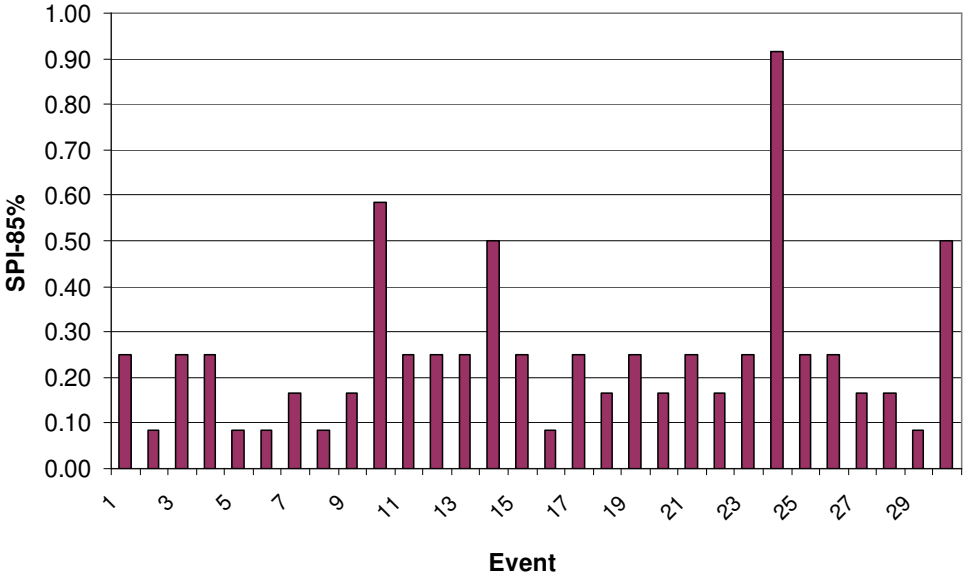

Figure 20 - SPI-85 % for the 30 events

3.6.1 Fault characteristics and generation dispatch

The analysis of the SPI permits the localisation of the fault positions that cause more damage to the system from the voltage sag point of view. For instance, it could be interesting to investigate the events 10, 14, 24, and 30 that produced voltage sags in at least half of the monitored buses, as shown in Table 11.

The four events with the largest SPI (E10, E14, E24, and E30) are marked in Figure 21. The faults located near generation units produced voltage sags at a large number of buses. Here, three of the four highlighted events are located along lines that are connected to the bus COX, one of the main generation buses.

Figure 21 shows the region of influence for the events E10 and E14. This is an illustrative way to visualise the propagation of the sags. We can clearly see that the region of influence of the event E10 is larger than the region of influence of the event E14. The regions of influence that are shown in Figure 21 are due to a sag threshold of 0.85 pu. A lower sag threshold would define smaller regions of influence.

Table 11 - Events with large propagation index

Event #	PQ-Monitors triggered	Fault Characteristics
E10	P4/P5/P6/P7/P8/P9/P10	LL radial line from COX 138 kV
E14	P6/P7/P8/P9/P10/P11	LLG RND-COX 138 kV
E24	P1/P2/P3/P4/P5/P6/P7/P8/P9/P10	LLL NOB-SIN 230 kV
E30	P1/P6/P7/P9/P10/P11	LL RND-COX 138 kV

It is also relevant to investigate the variation of the SPI for the different types of faults that happened during the monitoring period. Hence, the SPI is averaged for each type of fault. Table 12 shows the number of faults and the average SPI for each type of fault.

As expected, the voltage sags caused by LLL faults propagate in average more than voltage sags caused by other types of fault. The sags caused by SLG faults are the ones with the lowest SPI, approximately half of the SPI obtained for LLL faults.

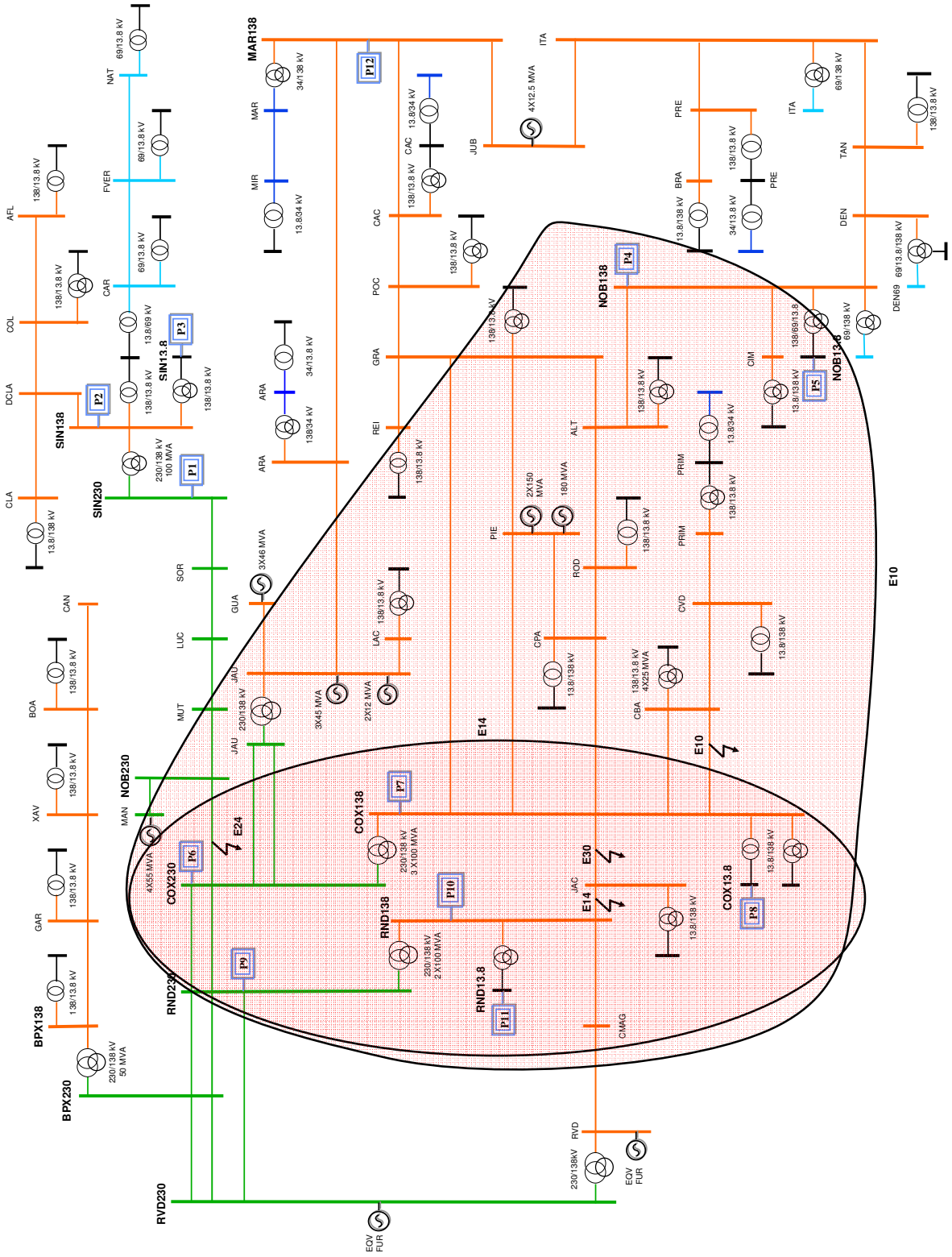

Figure 21 - Location of the events with large SPI. The region of influence for the events E10 and E14 is represented by the shadowed region

Table 12 - Average SPI calculated for each type of fault

	Type of fault			
	SLG	**LL**	**LLG**	**LLL**
# faults	13	8	3	6
SPI	0.17	0.28	0.28	0.35

It is interesting to see that there is an inverse relation between the SPI value and the number of faults. For example, the number of SLG faults is about double the number of LLL faults, whereas the SPI is about half. Therefore, for the monitored period the number of monitored buses affected by sags caused by SLG faults and LLL faults were similar.

The generation unit dispatch also influences the sag propagation. In the monitoring period the thermal-generation units were not dispatched when the events E20, E22, E23, E24, and E25 occurred. When the average SPI is estimated considering the generation dispatch a considerable difference is found, as shown in Table 13. In the analysed grid, the thermal generation reduces the propagation of the sags and improves the system performance.

Table 13 - Average SPI calculated for each generation state

Generation state	**Average SPI**
Thermal-generation ON	0.23
Thermal-generation OFF	0.35

It is interesting to analyse more in detail the event E24 because it caused sags at almost all monitored buses. The fault was located at the 230 kV system that supplies the 138 kV network when the thermal-generation is not dispatched. Therefore, a fault in the 230 kV system during these generation conditions was expected to cause voltage sags in most of the 138 kV buses, as confirmed by the event E24.

3.6.2 Vertical and horizontal propagation

Considering the meshed characteristic of the system, the horizontal propagation of sags is expected to be more relevant than the vertical one. Table 14 shows the average SPI considering the voltage level where the faults happen and the voltage level of the measured buses. The results agree with the predictions. The horizontal propagation of the faults at 230 kV reached a SPI of 0.50 whereas the vertical propagation to the 138 kV and 13.8 kV levels reached a SPI of 0.167. The reduction of the vertical propagation can be explained by the combined effects of the transformer winding connections, the rotational loads, and the distributed generation.

Table 14 - SPI calculated for vertical and horizontal propagation

	Average SPI at		
Faults at	**13.8 kV**	**138 kV**	**230 kV**
138 kV	0.198	0.325	0.194
230 kV	0.167	0.167	0.500

The vertical and horizontal propagation of voltage sags can also be studied through the detailed analysis of a single event, for example the event E14. This event was a LLG fault at the line RND-COX (138 kV). The magnitude and duration of the measured sags generated by the event E14 are shown in Table 15.

Table 15 - Voltage sag characteristics for the event E14

PQ-monitor	Magnitude (pu)	Duration (ms)
P6 – 230 kV - COX	0.85	72
P7 – 138 kV – COX	0.81	82
P8 – 13.8 kV – COX	0.80	83
P9 – 230 kV – RND	0.82	65
P10 – 138 kV - RND	0.74	79
P11 – 13.8 kV - RND	0.72	86

The analysis of the vertical propagation is intended to explain the changes on the magnitude, duration, and sag type at different voltage levels. The event E14 occurred at 138 kV. Therefore, the voltage sag magnitude at this level (P7 and P10) is lower than the sag magnitude at the bulk 230 kV system (P6 and P9).

The duration of the sags increases at lower voltage levels as a consequence of the post-fault voltage sag caused by the high currents due to induction motors re-starting. For example, the sag duration at P10 (RND 138 kV) is 79 ms whereas the sag duration at P11 (RND 13.8 kV) is 86 ms.

The sag type can be extracted from the phasor diagrams, shown in Table 16. The sags were generated by a LLG fault between phases A and C, hence the sag is type E with phase B being the symmetrical phase, at the buses were the faulted line is connected (P7 ad P10). The vertical propagation from 138 kV to 230 kV should not affect the sag type due to the winding connection of the 230/138 kV transformers. These transformers are wye/wye grounded at both sides. The phasor diagram at P6 and P9 shows the same type of sag as observed at P7 and P10.

On the other hand, the vertical propagation to 13.8 kV changes the sag type as a consequence of the transformer winding connections. The 138/13.8 kV transformers are delta/wye, therefore the sag type changes from type E at P7

and P10 to type F with phase C being the symmetrical phase at P8 and P11, respectively.

Additionally, the sag type changes during the propagation to the distribution level due to the pre-fault system unbalance. The voltage unbalance affects the sag classification because this characterisation method was proposed for a pre-fault balanced system.

For the horizontal propagation the sag magnitude at a certain voltage level is evaluated. For the analysed event the voltage sag magnitude at 138 kV is higher at COX than at RND. One of the explanations for this is the proximity of the generation units to the bus COX. This phenomenon is repeated at the 13.8 kV and 230 kV levels when the horizontal propagation is evaluated. The concentration of generation near COX keeps the voltage at this substation higher than at the RND substation.

Table 16 - Voltage phasors recorded for the event E14 (voltages in pu)

P6 – 230 kV – COX V_A=0.86 V_B=0.99 V_C=0.85 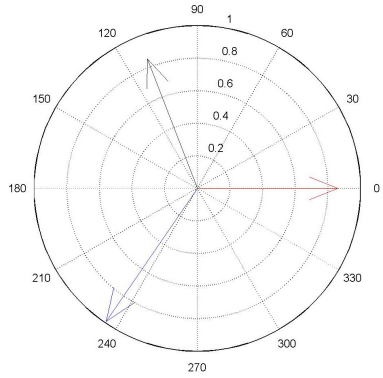	P9 – 230 kV – RND V_A=0.82 V_B=1.0 V_C=0.83 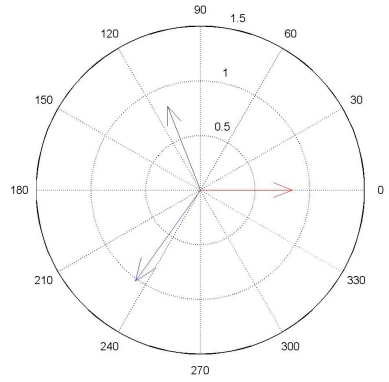
P7 – 138 kV – COX V_A=0.81 V_B=0.97 V_C=0.81 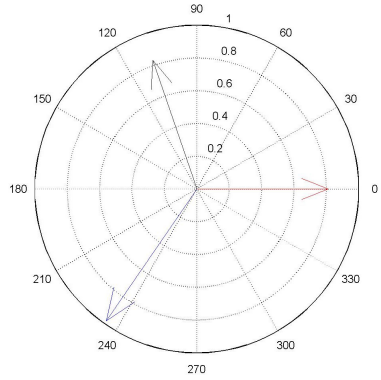	P10 – 138 kV – RND V_A=0.74 V_B=0.94 V_C=0.74 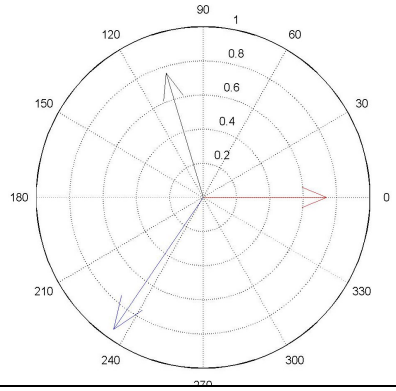
P8 – 13.8 kV – COX V_A=0.94 V_B=0.94 V_C=0.80 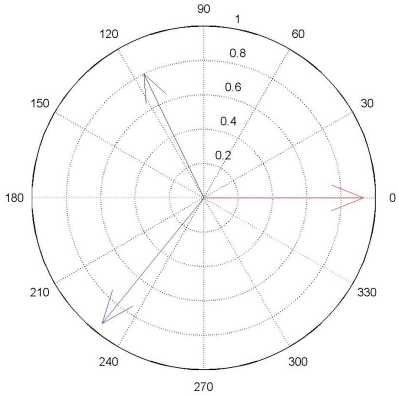	P11 – 13.8 kV – RND V_A=0.89 V_B=0.90 V_C=0.72 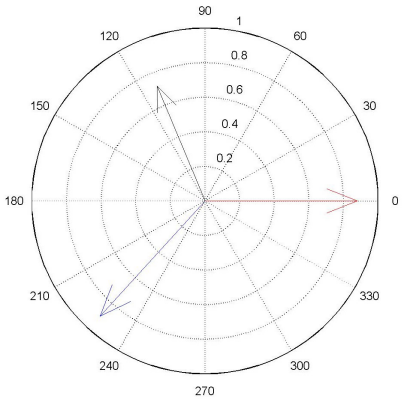

4 Power System Performance

This chapter describes the indices used to evaluate voltage sags from a single event to the system performance. The main tools available for the simulation and calculation of voltage sag magnitude are described and evaluated. The performance of the simulations are compared with actual measurements. The stochastic methods for voltage sag assessment are introduced. The sensitivity of the method of fault positions regarding the main fault uncertainties (fault rate, fault type, and fault location) is analysed. The sag indices obtained by stochastic assessment are compared with actual system measurements. Finally, voltage sag indices obtained from phase-to-neutral and phase-to-phase voltages are compared.

4.1 Sag indices

Voltage sags indices are the set of values used to describe the performance of a given site or system regarding voltage sags. In order to obtain this performance a five step method is recommended (IEEE Std. 1564 draft 6, 2004):

- Obtain instantaneous voltages;
- Calculate event characteristics as a function of time;
- Calculate event indices;
- Calculate site indices from the event indices;
- Calculate system indices from the site indices.

Instantaneous voltages can be obtained from either measurement devices or time-domain simulation. Voltage sag measurements are time consuming and the results can vary considerably from year to year. This variation is due to the randomness of faults in the power system. The number of voltage sags is strongly linked to the number of faults in the power grid; this number however varies considerably from year to year.

Short-circuit calculation provides an approximation of event indices. The retained voltage can be estimated from the symmetrical component network model, and the event duration can be assessed considering the fault-clearing time. Once the event indices are estimated, a statistical approach can be used to estimate the site and system indices.

The main index to evaluate the system performance is the SARFI (IEEE P1564, 2004). This is an acronym for System Average rms Variation Frequency Index, in other words, it provides the number of voltage sags

within a certain retained voltage and duration for a location during a certain period of time (one year).

There are two types of SARFI indices. The SARFI-x refers to a certain sag threshold (x = 90 %, 70 %, 50 %, etc). This index indicates the number of voltage sags with a retained voltage below x %. The SARFI-curve indicates the number of events below a certain reference curve of sensitivity (CBEMA, ITIC, SEMI), the curves are shown in Figure 22.

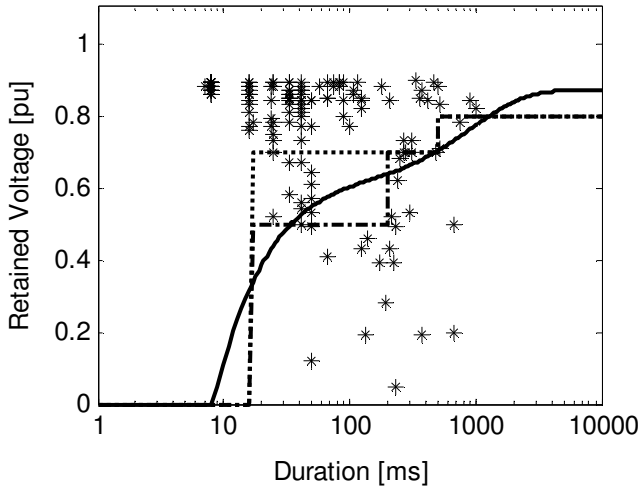

Figure 22 - Voltage sags representation and three standard sensitivity curves, CBEMA (solid line), ITIC (dotted line), and SEMI (dash-dotted line)

In order to illustrate how these indices are estimated, the results of a voltage sag survey are presented in Table 17. This survey was carried out in a distribution grid that supplied an industrial customer having sensitive processes. Voltage sag measurements were taken at 138 kV, 13.8 kV and 440 V during a period of approximately one year. Here, only a few events are shown. The complete table is presented in Appendix 2.

Figure 22 shows voltage sags and the tolerance curves (CBEMA, ITIC and SEMI) in a sag magnitude vs. duration chart. As can be expected most of the events are shallow sags, sags that are above the sensitivity curves. The severe sags are the ones below the tolerance curves.

The SARFI values calculated after one year of measurements are presented in Table 18. The SARFI-90 is the total number of events registered during the period; although this number is statistically interesting when comparing different sites it is not related to load sensitivity.

A more complete view of site and system performance is obtained by the cumulative frequency distribution of the voltage sag retained voltages, as shown in Figure 23. This curve allows comparing different sites and deriving conclusions about their strength. Weak busbars experience more

severe voltage sags while strong busbars suffer more shallow events (Olguin and Bollen, 2003).

Table 17 - Voltage sag monitoring on a 13.8 kV busbar, more in Appendix 2

Date@time	**Retained voltage (%)**	**Duration (ms)**
30/04/2002@17:47:05,133	88	8
03/05/2002@19:59:07,797	87	108
03/05/2002@19:59:10,922	89	467
13/03/2003@15:32:47.552	86	16
17/03/2003@11:03:35.727	84	49
22/03/2003@17:42:12.185	70	25
15/04/2003@11:24:52.627	89	8
16/04/2003@09:17:15.708	67	33
16/04/2003@09:17:17.924	89	8
02/05/2003@15:41:34.690	87	8
05/05/2003@06:12:23.031	77	16

Table 18 - SARFI estimation

$SARFI_{90\,\%}$	$SARFI_{70\,\%}$	$SARFI_{CBEMA}$	$SARFI_{ITIC}$	$SARFI_{SEMI}$
150	30	20	32	21

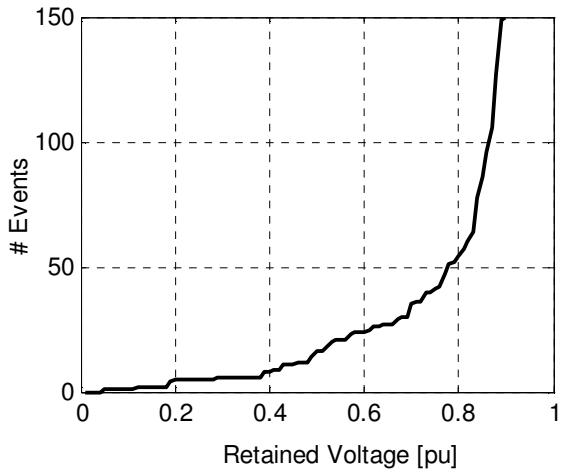

Figure 23 - Cumulative frequency distribution of event retained voltages

As can be seen in Figure 23, most of the voltage sags are shallow; they are risk-free even for sensitive equipment. Half of the events have a retained voltage higher than 0.84 pu.

The main limitation a monitoring program has in order to estimate the site indices is the time needed to obtain accurate results. The minimum required time of monitoring for a given level of accuracy can be estimated considering that the time between events can be favourably modelled as exponentially distributed. This means that the probability of an event to happen in the next minute is independent of the time elapsed since the last event. Under this condition the number of events within a certain period of time is a random variable that follows the Poisson distribution. For an expected number of n voltage sags per year the minimum monitoring time to limit the uncertainty ε is approximately given by

$$time > 4/n\varepsilon^2 \tag{4.1}$$

This implies that, in order to obtain an accurate result (uncertainty less than 10 %) for an expected number of 150 sags per year, the minimum monitoring period should be around 3 years. This result is extended for other scenarios of expected number of sags and required accuracy in Table 19.

Table 19 - Minimum monitoring period to obtain a given accuracy (Bollen, 2000)

	Uncertainty		
Sag frequency	**50 %**	**10 %**	**2 %**
1 per day	2 weeks	1 year	25 years
1 per week	4 months	7 years	200 years
1 per month	1 year	30 years	800 years

A study done by Leborgne *et al*. (2003) shows that an industry having many sensitive processes was affected by 42 voltage sags during one year but only 5 of the sags were severe (retained voltage below 0.70 pu). Considering these results, it can be concluded that sag measurements gives a rough approximation of the performance of a site for shallow sags with an accuracy of about 30 %. On the other hand, to predict the number of severe sags whose retained voltage is below 0.70 pu (less than 10 events per year), one year monitoring term is not enough and the results are affected by great uncertainty, in this case the error is about 90 %. This means that the results of a one-year monitoring period should not be used to forecast the number of equipment malfunction due to voltage sags.

4.2 Simulating voltage sags

This section is extracted from Paper VI.

Simulation methods provide an inexpensive choice to obtain voltage sags characteristics, thus avoiding long and expensive periods of measurements. The tools used to calculate voltage sags can be classified in three types: waveform simulation, fault calculation, and complex voltage estimation as a function of time (time-dependent phasors) (Xu, 2001).

During waveform simulations voltage sags are considered as transients and the waveform distortion in the time domain is calculated. This method can provide complete information about the characteristic of the disturbance; but a long time is required for the computing process due to the complexity of the system and component modelling (Bollen *et al*., 1998), (Martinez and Martin-Arnedo, 2004).

Built-in capabilities are available in most electromagnetic transient programs. They can be used to accurately reproduce most transients in power systems. However, the detailed representation of some components is not straightforward. For example, transformer models require the representation of the non-linear and frequency-dependent behaviour. The detailed model of power electronic devices like the DVR - dynamic voltage restorer or the VSC - voltage source converter requires a small time step size in time-domain simulation (Du and Bollen, 2006), (Bongiorno, *et al*. 2003). Therefore, the user is forced to choose between an accurate model and a feasible one (Cigre, 2005).

The components included in a voltage sag simulation are: conventional and distributed generators, power components, protective devices, mitigation devices, and loads. The model of the large generators includes the effect of the voltage regulation; whereas the small generators are modelled by a voltage source behind the machines' sub-synchronous reactance. The long transmission lines are modelled by distributed parameters considering the series resistance and reactance and the shunt capacitance. The short lines are modelled using lumped parameters, considering the resistance and the reactance. The model of the transformers considers the short-circuit impedance, the saturation, and the phase shift between the primary and the secondary voltages. Shunt reactors and capacitors are modelled by their reactance and susceptance. The circuit breakers, reclosers and any type of disconnectors are represented as ideal switches.

The load model influences the during fault voltage at low and medium voltage buses (Bollen *et al*., 2003). Usually the loads are modelled as constant impedances. However, in order to analyse the performance of a sensitive equipment connected in a grid with a high penetration of induction

machines a more detailed load modelling is needed. For stochastic assessment of voltage sags the load model should incorporate both daily and random variations.

The short-circuit calculation is more popular for voltage sag assessment due to its easy application and simple network modelling. The voltage magnitude is obtained in a straightforward manner from the bus impedance matrix, the sag duration can be estimated using the fault-clearing time, and the sag frequency is associated to the fault rate of the nearby network called region of vulnerability (Olguin, 2005), (Carvalho *et al*., 2000).

The short-circuit programs use the sequence representation of the network and sparse matrix properties to estimate the state of the network for a given event. Events are characterised by the fault location, fault type, and fault impedance. The generators are modelled as ideal voltage sources behind the synchronous or sub-synchronous reactance of the machines. The model adopted for the transmission lines considers the resistance and the reactance, neglecting the shunt capacitance. The transformer model includes the short-circuit impedance and the phase shift due to the winding configuration. The line and bus reactors and capacitors are modelled by a constant reactance and capacitance. Usually, the loads are neglected when performing short-circuit calculations, with the exception of large motor loads.

There is a third simulation method based on the estimation of the complex voltages as a function of time. This approach is also known as "time-dependent phasors". The fault current calculation obtained from the short-circuit analysis is repeated every time step. The generator and load are represented through a complex voltage and impedance, which are updated every time step. To obtain the sag duration the protective devices are included into the model either with a pre-defined fault-clearing time or by modelling the fault detection and clearing process in more detail. The calculation of the sag magnitude and duration requires some additional steps. It is reasonable to consider the magnitude and the angle of the complex voltage to be equal to the rms voltage and the phase angle (Cigre, 2005).

4.3 Time domain simulation vs. short-circuit calculation

This section is included in Papers VI and VII.

The power system shown in Figure 24 is used to evaluate time domain simulations and short-circuit calculations for the assessment of voltage sag indices.

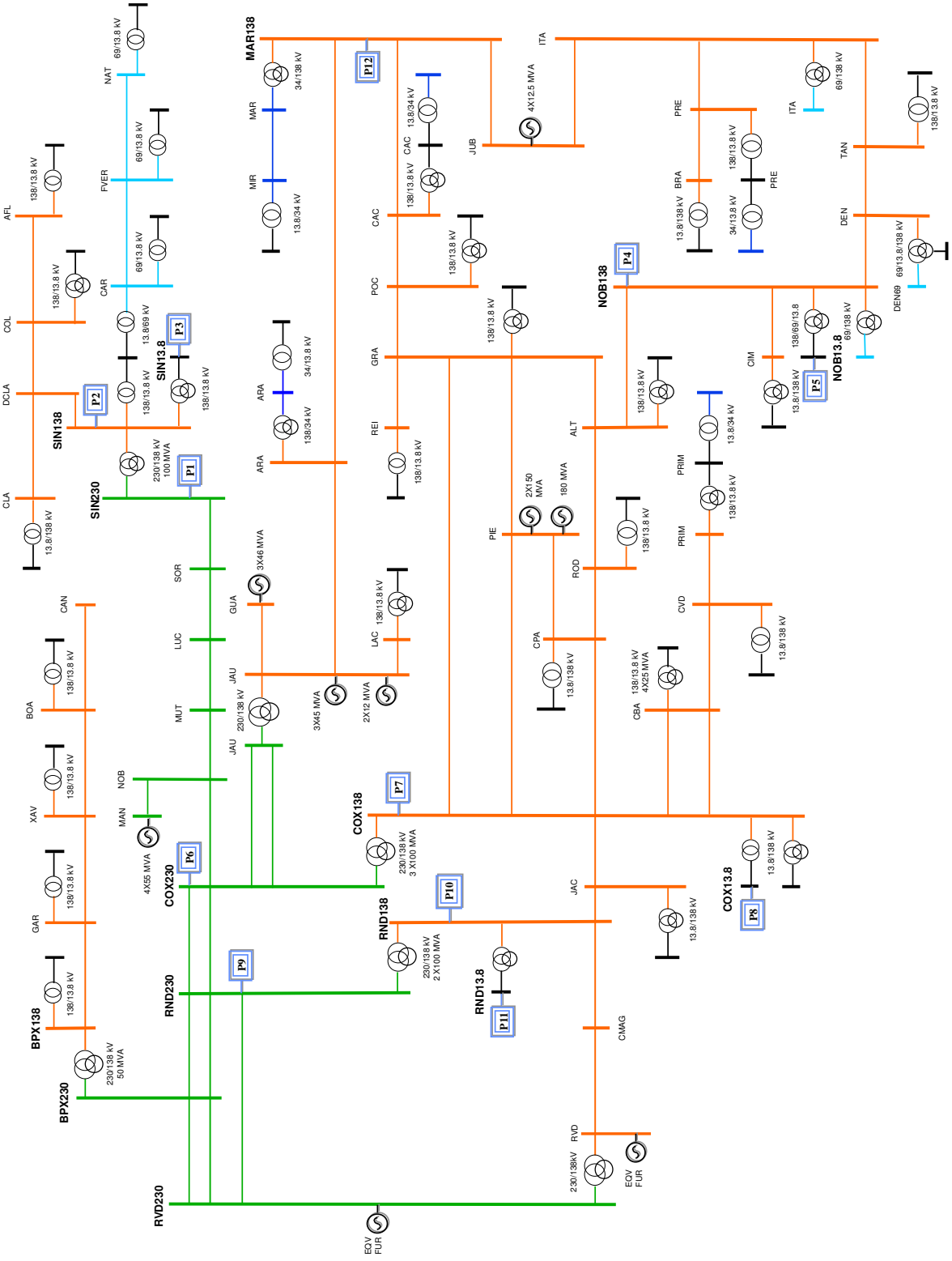

Figure 24 - Diagram of the monitored power system

A total of 12 buses (P1…P12) located at 5 substations were selected for voltage sag monitoring. The criteria for the bus choice included: network

topology, load concentration, sensitive-loads location, main generation plants, and transformer connections.

The monitoring system includes synchronised PQ-monitors. The synchronisation was needed to do a correct cause/effect correlation and to investigate the sag propagation. The information is uploaded to a centralised server located at the utility control room using the mobile telephone network.

The measurements included: sag magnitude, duration, and voltage phasors. The measurements are based on phase-to-neutral voltages. The selected sag threshold was 0.85 pu to avoid overloading the PQ-monitor system with shallow sags.

The electromagnetic transient program used is the well-known ATP-Alternative Transient Program (Caue, 2001). The short-circuit calculation program used is a widely employed program in Brazil (Cepel, 1998). Table 20 summarises the system modelling used for ATP and the short-circuit calculation program.

The pre-fault voltage adopted by ATP was the result of the steady-state solution of the network. The pre-fault voltage used by the short-circuit calculation program was 1.0 pu. Therefore, in order to be able to compare the results obtained from both programs, the loads simulated by ATP have been slightly adjusted to obtain pre-fault voltages close to 1.0 pu. This adjustment has been done in agreement with the utility load data.

Table 20 - System modelling

Equipment	**ATP**	**Short-circuit program**
Generators	Dynamic / ideal source	Ideal source
Short lines	Lumped parameters	Lumped parameters
Long lines	Distributed parameters	Lumped parameters
Transformers	R, X, saturation and phase shift	R, X and phase shift
Reactors/capacitors	Reactance	Reactance
Loads	Constant Impedance	Neglected

During the 6-month monitoring period a total of 30 events had the fault characterised by the location and the fault type, according to Table 46 in Appendix 3.

Using ATP and the short-circuit calculation program each fault is simulated to obtain the sag indices at 12 monitored buses. Then the simulated sag

indices are compared with the measured ones to evaluate the accuracy of the simulation approach.

It is important to remark that here the sag assessment is deterministic; it is done using a set of registered faults and therefore the simulated system performance does not include the characteristic likelihood of voltage sags.

4.3.1 Sag magnitude analysis

The magnitude of the three-phase sags is characterised by the sag magnitude of the critical phase. The error of the simulated sag magnitude is estimated for the results obtained at each monitored bus when the measured magnitude was lower than or equal to the sag threshold ($V \leq 0.85$ pu)

$$\varepsilon_1 = V_{Measured} - V_{Simulated} \tag{4.2}$$

where $V_{Measured}$ and $V_{Simulated}$ are the measured and simulated voltage sag magnitudes in pu.

The histograms of the sag magnitude error obtained using ATP and the short-circuit calculation program are shown in Figure 25. The error distribution for ATP is more symmetrical around zero; there is a similar probability of over- and under-estimation of the sag magnitude when using ATP. On the other hand, the fault calculation program estimates sag magnitudes larger than the measured ones in 73 % of the cases. In most of the cases (91 % and 93 % for ATP and the short-circuit calculation program, respectively) the error is less than 0.10 pu. However, some of the results deviate considerably.

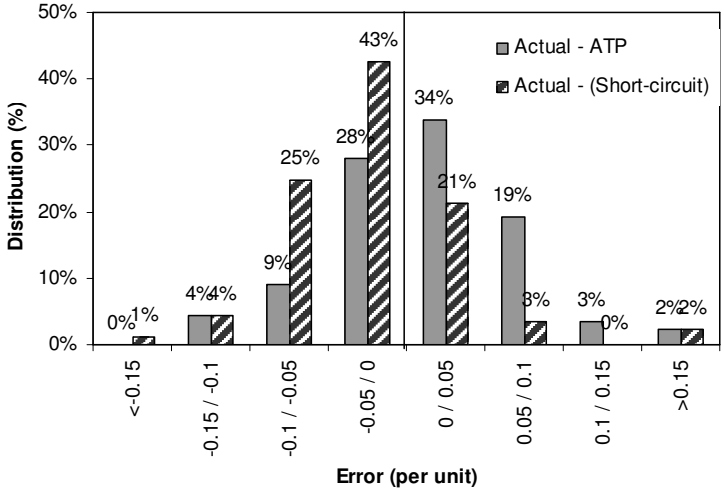

Figure 25 - Histogram of errors of simulated voltage sag magnitude

The errors are summarised in Table 21, where the average values, the standard deviation, the minimum, and the maximum values are given. The

largest errors are 0.57 and 0.64 pu for the ATP and the fault calculation program, respectively. These errors on the magnitude estimation are found for the same event registered at P6. This event is caused by a SLG fault in a 230 kV line close to P6, and it is Event 2 presented in Appendix 3.

Table 21 - Sag magnitude error for ATP and short-circuit calculation program

	ATP	**Short-circuit program**
Maximum	0.57	0.64
Minimum	-0.13	-0.21
Average	0.050	0.050
Std. deviation	0.066	0.073

Note: the average error and standard deviation is calculated considering the absolute value of the errors.

The accuracy of the results is affected by some uncertainties such as the pre-fault voltage, the precise location of the fault, and the fault impedance.

In some cases the measured pre-fault voltage reached values below 0.92 pu, whereas the ATP simulated pre-fault voltages were about 0.98 pu and those adopted for the short-circuit calculation program were 1.0 pu. Hence, these variations were recorded and the largest absolute variation at each monitor location is presented in Table 22.

Table 22 - Pre-fault voltage variations [pu]

Bus	**|Actual-ATP|**	**|Actual-(Short-Circuit program)|**
P1	0.09	0.08
P2	0.03	0.01
P3	0.04	0.01
P4	0.04	0.03
P5	0.08	0.04
P6	0.04	0.04
P7	0.05	0.05
P8	0.03	0.02
P9	0.06	0.04
P10	0.02	0.02
P11	0.05	0.02
P12	0.04	0.02
Max.	**0.09**	**0.08**

The deviations are lower than 0.10 pu as expected considering normal system operation and the voltage regulation at transmission level.

Due to a symmetrical fault at bus *f* the voltage sag magnitude at bus *k* is given by

$$V_{SAG} = V_{pref(k)} - V_{pref(f)} \frac{z_{kf}}{z_{ff}} \tag{4.3}$$

where $V_{pref(k)}$ and $V_{pref(f)}$ are the pre-fault voltages at the buses *k* and *f*, respectively. Z_{kf} is the transfer impedance between bus *f* and *k*, and Z_{ff} is the driving point impedance at bus *f*.

Therefore, in order to avoid the error due to the use of different pre-fault voltages at the monitored bus, the errors are recalculated normalised by the pre-fault voltages

$$\varepsilon_2 = \frac{V_{Measured}}{V_{pre-Measured}} - \frac{V_{Simulated}}{V_{pre-Simulated}} \tag{4.4}$$

where $V_{Measured}$ and $V_{Simulated}$ are the measured and simulated voltage sag magnitudes, and $V_{pre\text{-}Measured}$ and $V_{pre\text{-}simulated}$ are the pre-fault voltages obtained from the measurements and simulations at the monitored bus.

The new average errors are shown in Table 23. The average magnitude error for the ATP results decreased from 0.050 to 0.044 pu. However, the average error for the short-circuit calculation program is still 0.050 pu.

Table 23 - Magnitude error for ATP and short-circuit calculation program after pre-fault voltage normalisation

	ATP	**Short-circuit program**
Maximum	0.57	0.64
Minimum	-0.14	-0.22
Average	0.044	0.050
Std deviation	0.065	0.072

Note: the average error and standard deviation are calculated considering the absolute value of the errors.

The actual fault location is estimated with an uncertainty of 5 % of the power line length, as informed by the utility. Therefore, it was decided to repeat the simulation considering two new fault locations at the boundaries of the uncertainty interval.

The sag magnitude errors obtained for the new fault locations are presented in Table 24 and Table 25 for the ATP and the short-circuit program respectively. The variations are related to the average error obtained at each bus, estimated using (4.4). Therefore, the single event large variations are hidden in the averaging process.

Event 2 is the one with the largest error and also the one having the largest error variation when the fault location is adjusted. The initial error was 0.64 pu and for the new fault location the error reduced to 0.32 pu. This large variation is a consequence of the close location of Event 2 from bus P6. After adjusting the fault location the error obtained in the calculated sag magnitude is still significant. Therefore, another variable such as the fault impedance is suspected to influence this result.

The assumption of zero fault impedance affects the sag magnitude, especially for systems where large fault impedances are common. Therefore, the sag magnitude estimation must be re-done considering other values of fault impedances. According to the utility experience three other values are simulated (5, 25, and 40 Ω).

In order to quantify the influence of the fault impedance, the sag assessment is repeated for the 17 faults to ground considering the above-mentioned fault impedances. The error of the sag magnitude is summarised in Table 24 and Table 25 for each one of the analysed cases - the ATP simulation and the short-circuit calculation, respectively.

The sag magnitude error for the base case was presented before in Table 21 and the sag magnitude error after the adjustment of the pre-fault voltage was presented in Table 23. The results for the diverse fault locations and fault impedances are obtained after pre-fault voltage adjustment.

The results show that both programs are sensitive to variations of the fault location and the fault impedance. In addition, both of them presented better performance for magnitude estimation when the fault location is shifted by -5 %.

The fault impedance greatly influenced the estimated sag magnitude as well. ATP and short-circuit program show the same trend. When the fault impedance is increased the maximum magnitude error becomes lower. However, the average absolute error increases. Therefore, it is not possible to improve all the results by changing the fault impedance.

Table 24 - Sag magnitude error for ATP

	Fault loc. -5 %	**Fault loc. +5 %**	**5 Ω**	**25 Ω**	**40 Ω**
Maximum	0.37	0.74	0.52	0.17	0.08
Minimum	-0.13	-0.14	-0.22	-0.23	-0.35
Average	0.042	0.054	0.047	0.055	0.065
Std. dev.	0.048	0.082	0.062	0.044	0.059

Note: the average error and standard deviation is calculated considering the absolute value of the errors.

Table 25 - Sag magnitude error for the short-circuit calculation program

	Fault loc. -5 %	**Fault loc. +5 %**	**5 Ω**	**25 Ω**	**40 Ω**
Maximum	0.33	0.71	0.48	0.13	0.06
Minimum	-0.20	-0.20	-0.22	-0.25	-0.37
Average	0.050	0.060	0.052	0.064	0.074
Std dev.	0.049	0.078	0.061	0.052	0.070

Note: the average error and standard deviation is calculated considering the absolute value of the errors.

4.3.2 Sag frequency analysis

The sag frequency index is deterministically calculated for each of the monitored buses. Three different sag thresholds are chosen (0.85, 0.70, and 0.50 pu). The system indices for the three sag thresholds are shown in Table 26. The results indicate that ATP overestimates the number of sags for the three analysed thresholds, whereas the fault calculation program estimates a number of sags closer to the actual values.

Table 26 - Voltage sag frequency for diverse thresholds

# sags	**SARFI-85 %**	**SARFI-70 %**	**SARFI-50 %**
Actual	89	43	21
ATP	120	67	25
Short-circuit program	102	59	18

The sag frequency as a function of the sag magnitude obtained by the two simulation approaches and by the measurements is shown in Figure 26. The frequency error is rather small for sags with a magnitude below 0.45 pu. After that the frequency deviation is somewhat proportional to the number of sags. It seems that the frequency deviation is due mainly to single line-to-ground faults that give more shallow sags. The deviation may be due to an inaccurate representation of the zero sequence impedance.

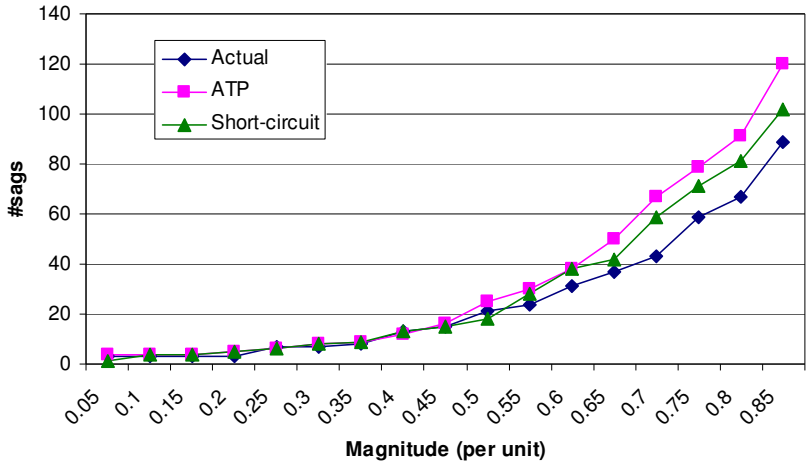

Figure 26 - Cumulative frequency of sags

The SARFI-85 % obtained for each bus is presented in Figure 27. In some buses, the simulated sag frequency diverges considerably from the measured one. One of the reasons of the high divergence is that the selected threshold (0.85 pu) is in the region where most of the sags are located. Consequently, for this threshold the largest variations are expected.

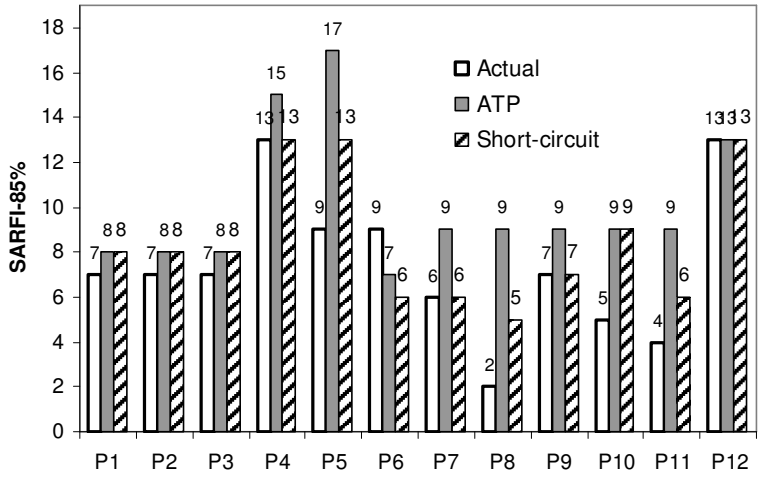

Figure 27 - SARFI-85 % for each monitored bus

Now, when the sag frequency obtained for the base case has been presented, the influence of the pre-fault voltage, the fault location, and the fault impedance will be analysed.

After the sag magnitudes have been adjusted by the pre-fault voltage, the sag frequency is again estimated and presented in Table 27. The adjustment of the pre-fault voltage keeps the tendency of the base case: the simulated sag frequency is larger than the measured one.

As shown in Table 27 the variation of the fault location within +/-5 % has only a small influence on the calculated sag frequency. The number of sags obtained by the simulation reduces when the fault impedance increases, as expected. A fault impedance of 45 Ω considerably improves the system sag frequency index obtained by ATP, whereas a fault impedance of 25 Ω is the best choice for the short-circuit calculation program.

The system frequency index estimated by simulations overestimates the actual value for most of the simulated scenarios. Only two cases obtained by the short-circuit calculation program with a fault impedance of 25 Ω and 45 Ω give a sag frequency lower than the measured one. Moreover, the best result for the system index is obtained by the short-circuit program for a fault impedance of 25 Ω.

The fault impedance is a random variable. However, it would be better to choose an impedance value to perform the voltage sag calculations. The analysis performed permits the calibration of the simulation programs to obtain the minimum errors. Nevertheless, the adjusting is not unique. The values of fault impedance that minimise the error for a given bus can be different from the values that minimise the error for other buses.

Table 27 - SARFI-85 % for the several simulated cases

SARFI-85%	**Pre-fault voltage adjusted**	**Fault loc. -5%**	**Fault loc. +5%**	**5 Ω**	**25 Ω**	**45 Ω**
Actual	85	85	85	85	85	85
ATP	111	120	115	113	103	92
Short-circuit program	102	115	101	99	89	78

4.4 Stochastic assessment

This section is included in Paper VIII.

One of the first papers proposing a stochastic assessment based on fault simulation for voltage sags was written by Conrad *et al.* (1991). Later Qader *et al.* (1999) published an investigation were this method, applied to the England and Wales transmission grid, was called the "method of fault positions". Then this method was largely extended by Bollen (2000) to include the effect of motor reacceleration and generator outages.

The method of fault positions for voltage sag assessment consists of simulating faults at numerous points of the system, estimating the retained voltage at selected busbars. Each fault location is associated with a fault frequency and so is each estimated retained voltage, permitting the statistical analysis of the retained voltages in the analysed busbar. The algorithm for this method can be summarised as follows:

- Select the region of the network where the faults will be simulated, as shown in Figure 28;
- Divide this region into small segments so that a fault at any point within a segment should result in a similar retained voltage;
- The fault frequency (number of faults per year) of each segment is estimated. Normally the line fault rate is divided by the number of segments, so that all segments within a transmission line have the same fault rate;
- Using a suitable network model, the sag characteristics at the busbar analysed are estimated for each simulated fault.

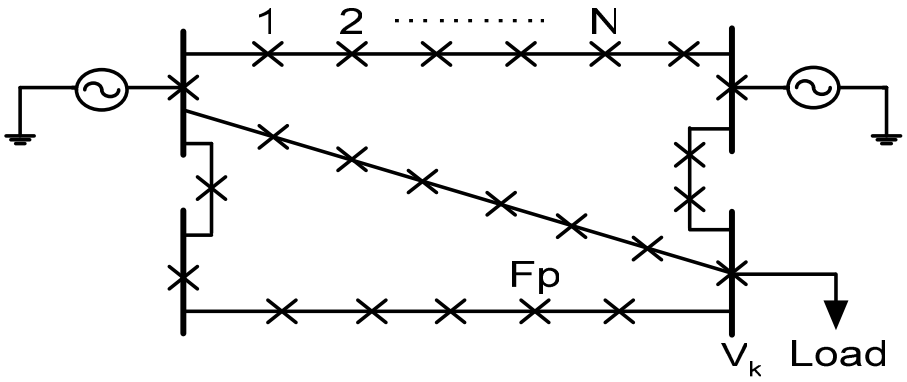

Figure 28 - Schematic network indicating all fault positions used for the estimation of voltage sags

For voltage sag assessment based on the retained voltage, the sequence impedance model of the network gives sufficiently accurate results. These results include retained voltage and the expected number of sags per year as shown in Table 28. For instance, when a fault is simulated at position *N*, the retained voltage at busbar *k* is V_{kN} and this sag is expected to happen λ_N times per year. When a more complete sag characterisation is needed, a time domain simulation tool should be implemented in order to obtain the instantaneous voltages during the event.

Table 28 - Retained voltages at busbar *k* for a simulated fault at location *f* and the frequency (λ) (events per year) of each event

Retained voltage (V_{kf}) at busbar *k*	**Frequency (λ)**
V_{k1}	λ_1
V_{k2}	λ_2
⋮	⋮
V_{kN}	λ_N
⋮	⋮
V_{kFp}	λ_{Fp}

In order to investigate the performance of the method of fault positions for voltage sag assessment in a large transmission system, a model of the Brazilian transmission grid is used. The main characteristics of this system are presented in Table 29. The selection of this system was made considering:

- Size of the system;
- Availability of the system symmetrical-components model;
- Availability of monitoring results for further comparisons.

Table 29 - Brazilian transmission network characteristics

	230 kV	**345 kV**	**440 kV**	**500 kV**	**Total**
Lines #	518	113	33	129	793
Length [km]	30976	10296	5408	17554	64234
Busbars #	409	74	20	153	656

The symmetrical components model of the Brazilian transmission system is available on the web site of the Brazilian System Operator (ONS, 2003). The transmission model available is continuously updated. This study was done considering the model available in December 2003.

The Brazilian transmission network is a continental network, having a geographical extension of 6000 km from north to south. The peak load demand is about 60 GW, while the generation capacity is 90 GW. The main

generation comes from hydroelectric plants (68 GW), followed by thermoelectric plants (20 GW), and nuclear generation plants (2 GW). Therefore, during dry years the hydroelectric power available is not enough to meet the peak load.

The method of fault positions was applied to the model of the Brazilian transmission grid. For the reference case a total of 793 fault positions considering symmetrical and unsymmetrical faults were simulated and, for this simulation, the fault position was at the mid point of each transmission line. Four types of faults were simulated at each fault position: LLL, LLG, LL, SLG faults. The minimum retained voltage was used to characterise the unbalanced sags.

The fault-rate and the fault-type distribution simulated at different voltage levels corresponding to the reference case are shown in Table 30. The values are typical values for a transmission grid (Carvalho Filho *et al*., 2002).

Table 30 - Fault rates and fault distribution for the reference case

Transmission Voltage [kV]	Faults/ 100km·year	LLL	LLG	LL	SLG
500	2.09	1 %	4 %	1 %	94 %
440	1.1	1 %	5 %	2 %	92 %
345	1.1	1 %	5 %	2 %	92 %
230	1.9	2 %	15 %	3 %	80 %

The simulation results were statistically analysed in order to obtain the site indices for a selected number of busbars. The estimated sag indices are SARFI-90 % and sag magnitude, as shown in Table 31. The system SARFI-90 % index was estimated averaging the sites SARFI-90 %. The system sag magnitude index was estimated by the weighted average of the sites sag magnitudes. The weight factor of each site is its own SARFI-90 % index.

The Brazilian Independent System Operator ran a voltage sag survey during 2001 and 2002. A total of 55 busbars were monitored during a period of time within these two years. The monitored locations are distributed as follows: 22 busbars at <34 kV, 16 busbars at 69-88 kV, 9 busbars at 138-161 kV, 6 busbars at 230 kV, and 2 busbars at 440 kV. Unfortunately, the monitoring period of many locations were just a few months, affecting the results due to the seasonal characteristic of the faults in that transmission network. The frequency of faults is highly dependent on the weather conditions. The results are shown in Table 32.

Table 31 - Sag indices estimated by the method of fault positions

Voltage level	Busbar	SARFI-90 % (sags per year)	Average sag magnitude (pu)
<34 kV	B5420	13	0.78
<34 kV	B1944	16	0.83
<34 kV	B7360	70	0.78
<34 kV	**System index**	**33**	**0.79**
69 kV	B2519	56	0.83
69 kV	B1103	12	0.88
69 kV	B6247	13	0.77
69 kV	B2671	69	0.75
69 kV	B5284	9	0.78
69 kV	**System index**	**32**	**0.79**
138 kV	B2515	56	0.83
138 kV	B1250	29	0.84
138 kV	B5463	14	0.77
138 kV	B1405	27	0.81
138 kV	B1385	37	0.85
138 kV	B1941	17	0.83
138 kV	B2620	55	0.74
138 kV	B5924	19	0.74
138 kV	**System index**	**32**	**0.80**
230 kV	B1563	28	0.79
230 kV	B5962	19	0.71
230 kV	B5994	26	0.77
230 kV	B5283	12	0.76
230 kV	B7350	70	0.78
230 kV	**System index**	**31**	**0.77**
440 kV	B1404	28	0.78
440 kV	B1383	39	0.82
440 kV	**System index**	**34**	**0.80**

Table 32 - Sag indices obtained by monitoring

Voltage level	SARFI-90 % (sags per month)	Average sag magnitude (pu)
<34 kV	11.2	0.77
69-88 kV	5.8	0.78
138-161 kV	5.8	0.77
230 kV	3.6	0.69
440-500 kV	1.2	0.23

Results from the use of the method of fault positions and monitoring are shown in Table 33 for comparison. The monitoring results from Table 32 are extrapolated for a one-year monitoring period. Average values of the simulated system indices are extracted from Table 31.

Table 33 - Comparison of results from simulation and monitoring

Voltage level	Monitored SARFI-90 % (sags per year) (2001-02)	Simulated SARFI-90 % (sags per year)	Monitored Sag magnitude (pu) (2001-02)	Simulated Sag magnitude (pu)
<34 kV	134	33	0.77	0.79
69-88 kV	66	32	0.78	0.79
138-161 kV	66	32	0.77	0.80
230 kV	43	31	0.69	0.77
440-500 kV	14	34	0.23	0.80

As shown in the table, monitored and simulated results strongly diverge. The main reasons for the divergence are:

- The monitoring period was too short and failed to include the effect of the seasonal variation of the fault frequency;
- Long-term average fault rates are used for the application of the method of fault positions, but the actual number of faults varies considerably from year to year. This is one of the key factors to explain the large difference in the number of sags obtained by simulation and by monitoring;
- Faults at distribution level were not simulated, resulting in an underestimation of the number of events at distribution and subtransmission voltages (34–161 kV).

The method of fault positions is suitable for the assessment of voltage sags in a long term approach, but fails to describe the short term performance. Nevertheless, it can be used to obtain an indication of the expected number of events and their average retained voltage. Long term analysis using this method will match better with the actual performance than short term analysis. When some adjustments are done in the fault rate to better describe the monitored period, the difference between measured and simulated SARFI-90 % index may be reduced down to 10 % (Carvalho Filho *et al.*, 2002).

4.5 Sensitivity analysis of the method of fault positions

This section is included in the Paper VIII.

The accuracy of the assessment of voltage sags using the method of fault positions depends on the quality of the data used for the simulations. The expected number of voltage sags at a given busbar is directly related to the number of faults occurring within the electrical nearness. This electrical nearness is known as the exposed area and it usually includes different voltage levels. Many surveys have been published pertaining to transmission line outages over a period of time (McGranaghan and Roettger, 2001), (IEEE Std. 497, 1997). It has been pointed out that faults are strongly correlated to severe weather conditions or poor maintenance. The number of faults or the fault rates used for the sag assessment must be as close as possible to the statistical fault rate of the simulated system.

In order to analyse the variation of voltage sag indices (SARFI-90 % and sag magnitude) various cases are simulated and the results are compared to the reference case, introduced in the previous section. The first case considers a 50 % increased fault rate for all transmission lines. Then, four different cases show the effect of a 50 % increased fault rate for each voltage level, one at the time. The variation of the system index SARFI-90 %, with respect to the reference case, is presented in Table 34.

As shown in Table 34 the index variation depends on which fault rate is changed. For instance, when the 440 kV transmission lines fault rate is increased by 50 %, the most affected system index is the 440 kV system (35 %). On the other extreme, the 34 kV system index does not change (0 %); meaning that there are no 440 kV transmission lines within the 34 kV sites exposed area for a sag threshold of 90 %. In other words, whatever fault rate is adopted for the 440 kV lines, the SARFI-90 % for the 34 kV system will not change.

Table 34 - System SARFI-90 % variation for different fault rate scenarios

Fault rate is increased 50 % in:	System SARFI-90 % variation				
	<34 kV	**69 kV**	**138 kV**	**230 kV**	**440 kV**
Case 1 – All kV	50 %	50 %	50 %	50 %	50 %
Case 2 – 500 kV	15 %	16 %	8 %	9 %	0.3 %
Case 3 – 440 kV	0 %	2 %	12 %	39 %	35 %
Case 4 – 345 kV	0 %	7 %	8 %	3 %	13 %
Case 5 – 230 kV	35 %	26 %	22 %	34 %	2 %

The assessment of voltage sags can be performed based exclusively on symmetrical faults but accurate results require a reasonable combination of symmetrical and unsymmetrical faults. Two new additional scenarios are simulated to analyse the variation of the sag indices. A first scenario considers only symmetrical faults (LLL), a second one takes exclusively unsymmetrical SLG faults. The estimated SARFI-90 % for both scenarios is plotted in Figure 29.

The expected number of sags (SARFI-90 %) is much higher when only three-phase faults are simulated. For example, for busbar B1103 the SARFI-90 % is three times larger than for the reference case, when only three-phase faults are simulated. Nevertheless, for a rough and conservative assessment, simulating just three-phase faults can be an option. Instead, if only SLG faults are considered, the SARFI-90 % will be slightly underestimated.

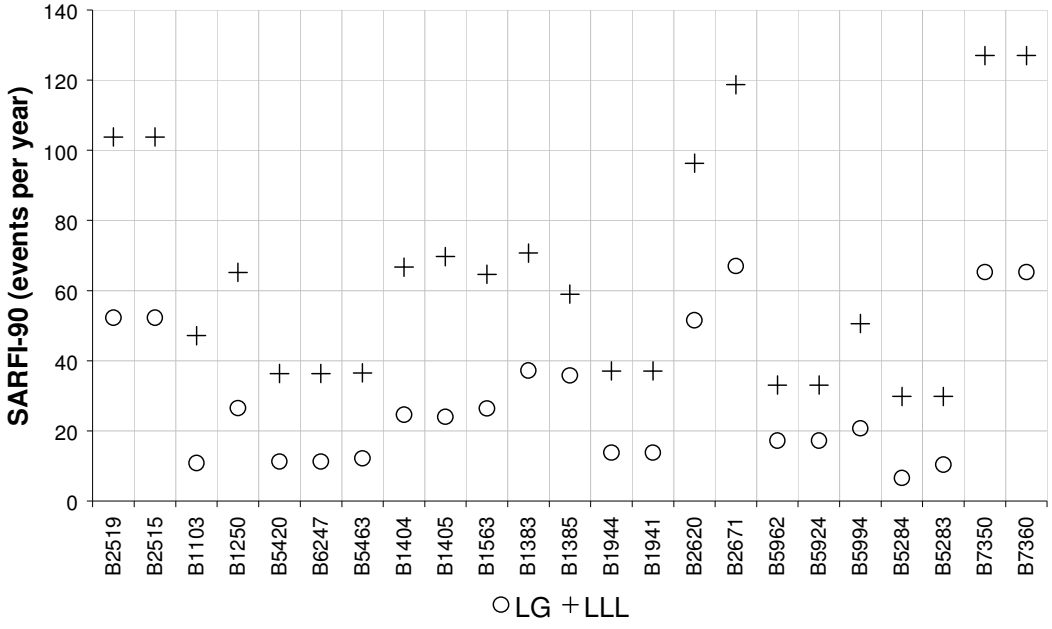

Figure 29 - SARFI-90 % estimated for SLG and LLL faults

The method of fault positions can be performed considering faults only at busbars. The main advantage of this approach is the simplicity. Applying all the faults at busbars makes the computation process easy, but the results are less accurate. Simulating faults at busbars gives a large SARFI-90 % and a lower expected sag magnitude, as can be derived from Figure 30 and Figure 31.

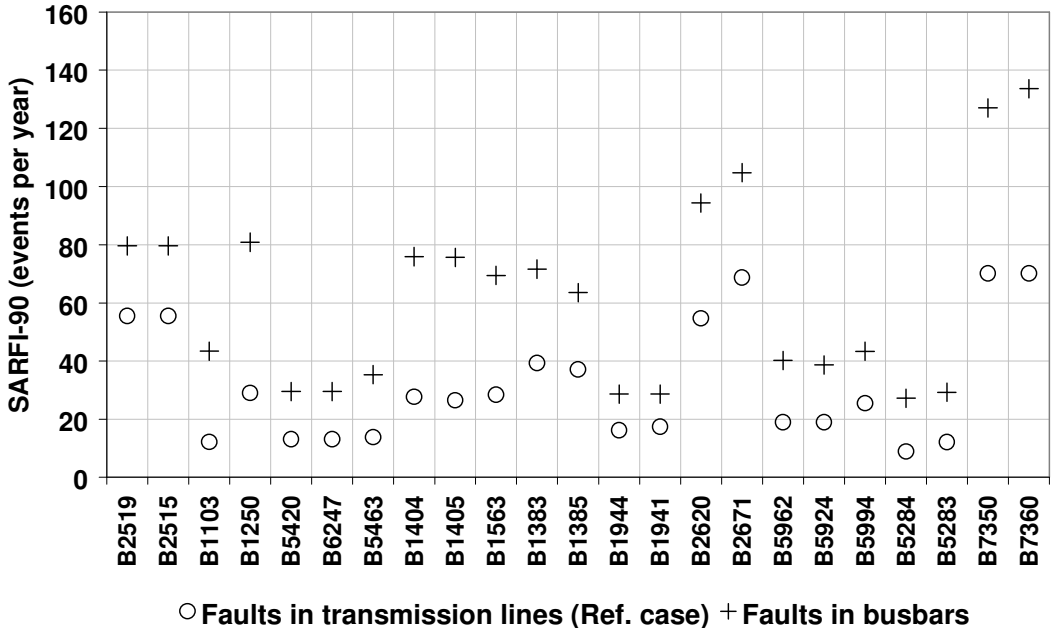

Figure 30 - SARFI-90 % for faults at busbars (+) and for faults at transmission lines (o)

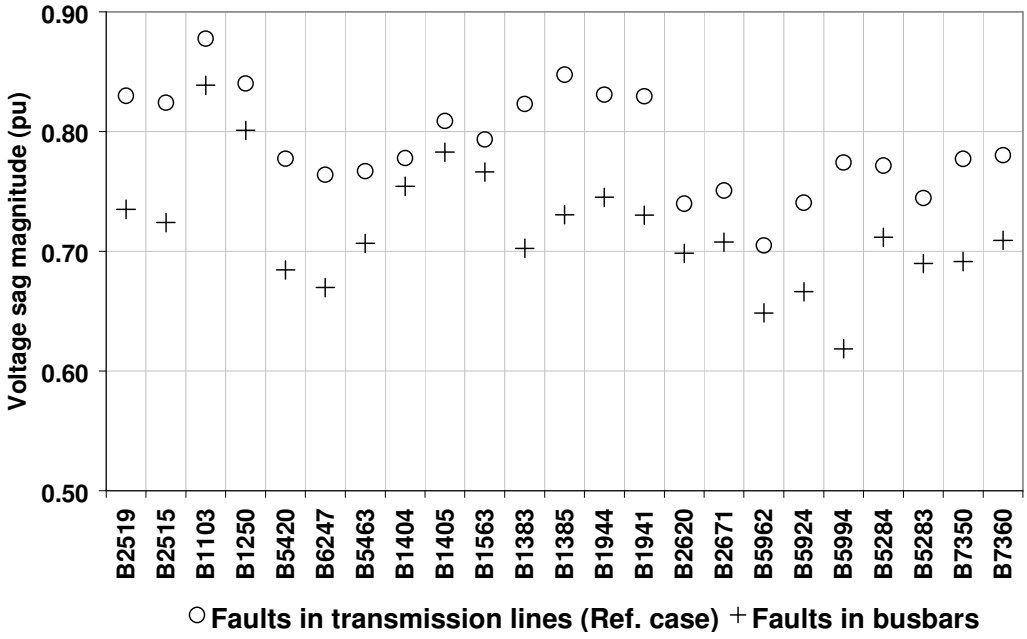

Figure 31 - Voltage sag magnitude for faults at busbars (+) and for faults at transmission lines (o)

It is clear that simulating faults only at busbars leads to an overestimation of the voltage sag indices. This simulation approach results in both the overestimation of the SARFI-90 % and the underestimation of the expected sag magnitude. Nevertheless, simulating faults at busbars can be a first approach, taking into account that we are dealing with a pessimistic scenario.

4.6 Phase-to-neutral vs. phase-to-phase voltage sags

This section is included in Papers IX and X.

In order to investigate the influence of the choice between PN - phase-to-neutral and PP - phase-to-phase voltages on the sag assessment, a new set of simulations, using the method of fault positions, is performed. The same Brazilian network as described in Section 4.5 is used. A new fault statistic is considered, as shown in Table 35. Faults are located at busbars and transmission lines.

Table 35 - Fault statistics used in this section

Transmission Voltage	Fault/ 100 km·year	LLL	LLG	LL	SLG
500 kV	1.14	1.5 %	6 %	5.5 %	87 %
440 kV	1.14	1.5 %	6 %	5.5 %	87 %
345 kV	1.98	3.5 %	1.5 %	5.5 %	90 %
230 kV	1.57	4 %	6 %	14 %	76 %

In order to describe the performance of the analysed sites, the SARFI-90 % and the sag magnitude are estimated for both PN and PP voltages. The estimated values of SARFI-90 % are presented in Figure 32 and the obtained values of sag magnitude are shown in Figure 33.

Most of the 23 busbars show the same tendency, PN voltage sags are more frequent and severe than PP voltage sags. For instance, 70 PN sags per year with an average sag magnitude of 0.74 pu, are expected at busbar B1383 (440 kV). However, only 53 PP sags with an average sag magnitude of 0.82 pu are expected at the same busbar.

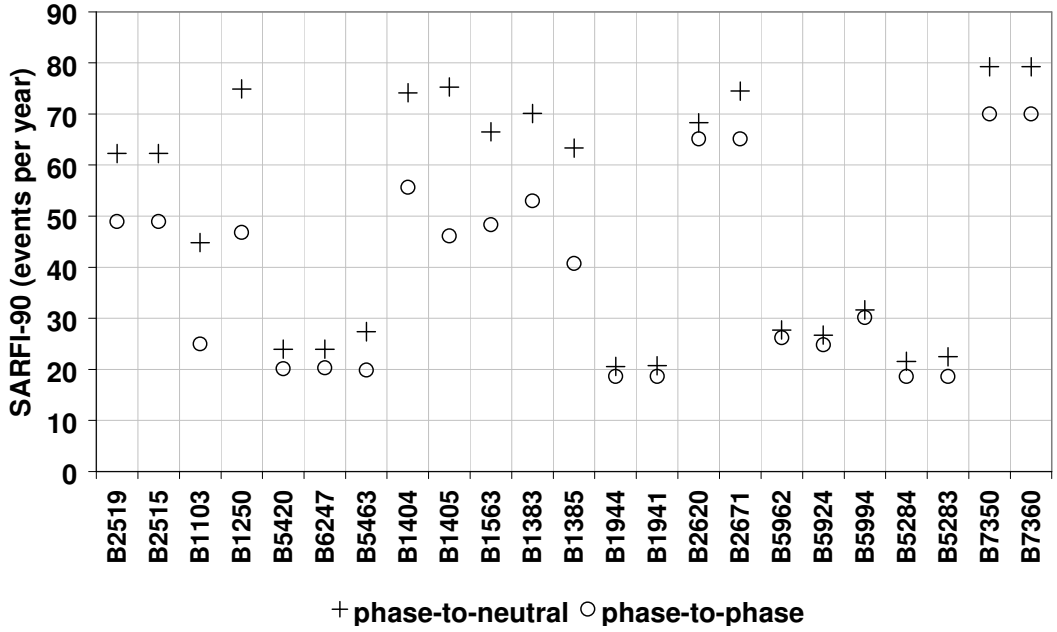

Figure 32 - SARFI-90 for PN and PP voltage sags

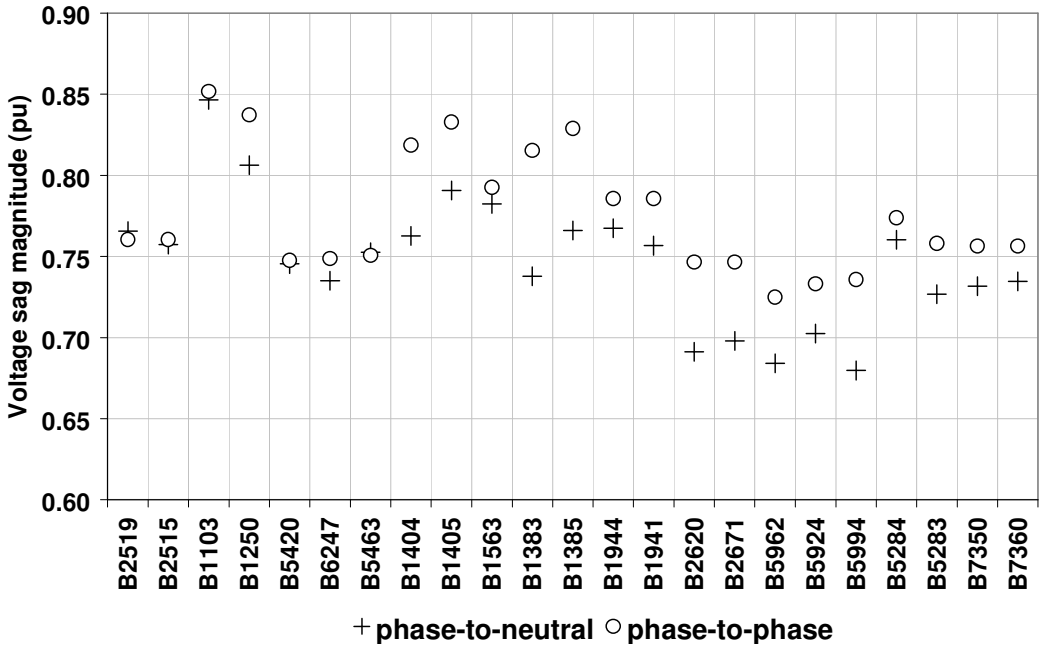

Figure 33 - Sag magnitude for PN and PP voltage sags

Generally, at distribution busbars the difference in voltage sag indices for PN and PP voltages is rather small. For instance, the distribution busbar B5420 expects 24 sags per year having an average retained voltage of 0.75 pu for PN voltages, whereas for PP voltages the expected number of events is 20 having an average retained voltage of 0.75 pu.

5 Voltage Sag Source Location

Fault location is not a new issue in power system research. Until now, however, the approach has been mainly from the protection and maintenance point of view. Here, the location of faults is done considering them as the main source of severe voltage sags. The location of the sag source is the first step towards mitigation actions and liability assignment. An extensive analysis on existing methods using voltage and current information is presented and a novel method based on voltage information only is introduced. The performance of the methods is assessed through sag simulation and actual sag measurements.

5.1 Methods based on voltage and current information

This section is covered by Paper XI.

5.1.1 Disturbance power and energy

The location of the sag source as observed from a monitored bus is defined as upstream and downstream, using the pre-fault power flow direction as indicator. Upstream is the region against the flow of power and downstream is the region following the flow of power, as shown in Figure 34.

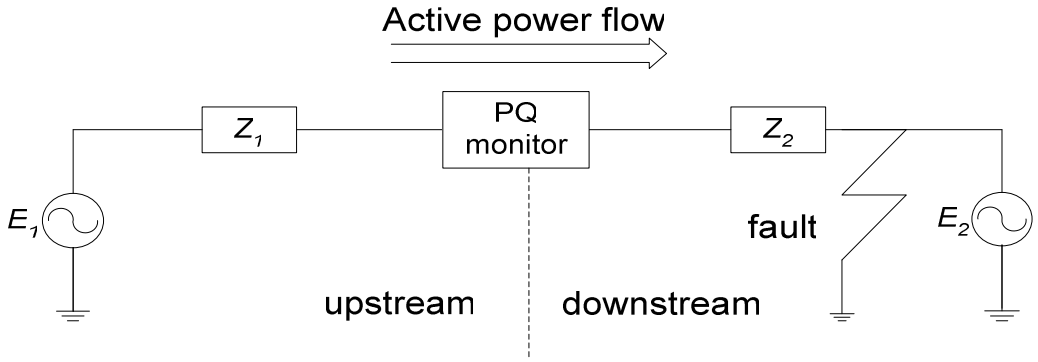

Figure 34 - Basic circuit to describe the localisation of the sag source

The first published method aiming to locate the source of the disturbances is based on the DP - disturbance power and the DE - disturbance energy (Parsons *et al.*, 2000). The disturbance power is defined as the difference between the power delivered during the event and the steady-state delivered power. The disturbance energy results from the time integral of the disturbance power.

$$DP = P_f - P_{ss} \tag{5.1}$$

$$DE(t) = \int_0^t DP(u)du \tag{5.2}$$

where P_f and P_{ss} are the power delivered during the fault and during the pre-fault steady-state condition.

This method prescribes that the final sign of the disturbance energy defines the location of the sag source. If the final value of the disturbance energy is greater than 80 % of the peak value this test is conclusive. Then, if the final disturbance energy is positive the sag source is located downstream. If the final disturbance energy is negative the source of the sag is located upstream. If the sign of the initial peak of the disturbance power coincides with the sign of the final disturbance energy a high degree of confidence is expected.

5.1.2 Slope of system trajectory

The method of the slope of the system trajectory (Li *et al.*, 2003) is based on the relation between the voltage and the current shown in Figure 34. For instance, for a fault located downstream of the monitored point, the active power measured at the PQ-monitor is

$$VI\cos\theta = -R_1 I^2 + E_1 I\cos\theta_1 \tag{5.3}$$

where E_1 is the voltage at the source 1, R_1 is the real part of Z_1, V and I are the rms voltage and current measured by the PQ-monitor, θ is the angle between voltage and current at the monitored location and θ_1 is the angle at the source E_1.

Considering that $V{\cdot}cos(\theta)>0$, this expression can be substituted by $|V{\cdot}cos(\theta)|$. Both parts of the equation 5.3 can be divided by I to obtain the equation 5.4. This is the equation of a line with slope $-R$

$$\left|V\cos\theta\right| = -R_1 I + E_1\cos\theta_1 \tag{5.4}$$

On the other hand, the authors claim that if the fault is upstream, a similar linear equation is obtained but the slope is $+R$

$$\left|V\cos\theta\right| = +R_1 I + E_1\cos\theta_1 \tag{5.5}$$

Applying linear fitting by the least-square method on a set of values of I and $|Vcos(\theta)|$ during a voltage sag, a straight-line equation is obtained. The sign of the slope of this line indicates the position of the fault: positive slope indicates upstream fault and negative slope means downstream fault. This method also considers a possible inversion of the power flow during the sag.

An inversion of the power flow indicates an upstream fault. This method is clear for symmetrical faults, here positive sequence voltage and positive sequence current are used. The method has not been extensively tested for asymmetrical faults. It is possible that the slopes have different signs for each phase and this method may not be conclusive.

5.1.3 Resistance sign

An extended method, developed later, proposes to use the sign of a calculated resistance to classify the source location of the sag (Tayjasanant *et al.*, 2005). This method uses the positive-sequence voltage and current. The resistance is estimated using equations (5.6) and (5.7), taking a set of n measured currents and voltages including pre-event and during-event values. If the two estimated resistances have the same sign the test is conclusive. A positive sign means an upstream fault whereas a negative sign indicates a downstream fault.

$$\begin{bmatrix} R \\ X \\ E_{RE} \end{bmatrix} = \begin{bmatrix} I_{RE}(1) & I_{IM}(1) & 1 \\ \vdots & \vdots & \vdots \\ I_{RE}(n) & I_{IM}(n) & 1 \end{bmatrix}^{-1} \begin{bmatrix} V_{RE}(1) \\ \vdots \\ V_{RE}(n) \end{bmatrix} \tag{5.6}$$

$$\begin{bmatrix} R \\ X \\ E_{IM} \end{bmatrix} = \begin{bmatrix} I_{IM}(1) & I_{RE}(1) & 1 \\ \vdots & \vdots & \vdots \\ I_{IM}(n) & I_{RE}(n) & 1 \end{bmatrix}^{-1} \begin{bmatrix} V_{IM}(1) \\ \vdots \\ V_{IM}(n) \end{bmatrix} \tag{5.7}$$

The subscripts $_{RE}$ and $_{IM}$ denote the real and imaginary parts. The matrix exponent (-1) represents the pseudo-inverse of the matrix when the matrix is not square.

In order to apply this method, the power flow must be observed. If the power flow is reversed during the sag, the voltages and currents used in (5.6) and (5.7) must only include values before the reversion of the power flow.

5.1.4 Real current component

The method of real current component (Hamzah *et al.*, 2004) is based on the analysis of the variation of the real part of the current ($I \cdot \cos(\theta)$). The authors claim that if, at the beginning of the fault, $I \cdot \cos(\theta) > 0$ then the fault is located downstream, and if $I \cdot \cos(\theta) < 0$ then the fault is upstream. The paper does not mention, but the analysis must be done on the current variation, otherwise the inversion of polarity could not happen. The analysis is done

using phase values and it is expected to obtain the same indication in each of the faulted phases.

5.1.5 Distance relay

The approach of using a distance relay algorithm was proposed by Pradhan and Routray (2005). The impedance seen before and during the event indicates the relative location of the fault. The impedance is estimated using the voltage and current phasors at the monitored location

$$Z_{seen} = \frac{\overline{V}}{\overline{I}} = Z_2 + \Delta Z \tag{5.8}$$

where $\overline{V}$ and $\overline{I}$ are the measured voltage and current phasors, ΔZ is a function of the fault resistance and the load characteristics.

Therefore, this method proposes the following rule for the sag source detection: if $|Z_{SAG}|<|Z_{PRE\text{-}SAG}|$ and $angle(Z_{SAG})>0$ then the sag source is located downstream, otherwise the sag source is located upstream.

5.2 Case study

This section is included in Paper XI.

In order to test the performance of the methods to locate the sag source, faults are simulated in a power grid. The simulations are realised using the PSCAD/EMTDC program. Several fault location cases are simulated and 2 substations are monitored, as shown in Figure 35.

The monitors M2 and M3 are located at the boundary of two radial 138 kV sub-transmission grids. The 230 kV transmission and the 138 kV sub-transmission grids are owned by two different utilities, therefore it is relevant to locate the source of the sag taking into account the borders between the two utilities.

The simulated faults are located at both the 138 kV and the 230 kV networks, upstream and downstream with respect to the monitored buses. It is necessary to recall that upstream/downstream is related to the active power flow. The active power always flows from the 230 kV to the 138 kV bus at the monitored substations.

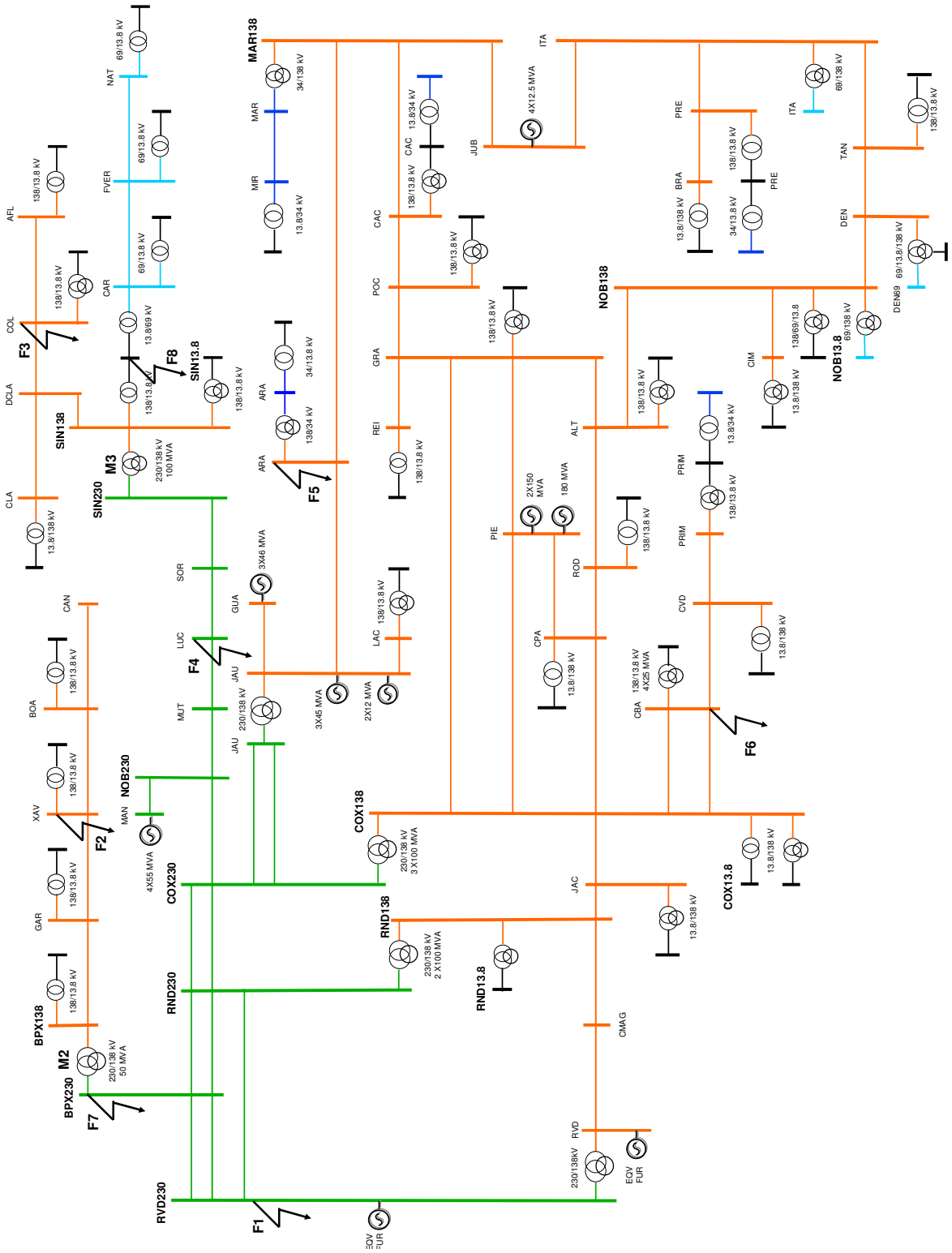

Figure 35 - Single-line diagram of simulated power system, fault locations (F1,…,F8) and monitored buses (M2, M3) are indicated

The power network includes transmission, sub-transmission and distribution levels, as well as meshed and radial system configurations. The network contains 67 power lines (69, 138, and 230 kV) with a total length of

6619 km. There are 93 substations with an installed transformer capacity of 2076 MVA. The generation capacity is larger than the present demand. The excess of power is exported to other regional grids through the RVD substation.

At each fault location three-phase-to-ground and single-line-to-ground faults are simulated. The sag source location algorithms are implemented at each monitored bus. The results are discussed for symmetrical faults and asymmetrical faults independently.

5.2.1 Symmetrical faults

Symmetrical faults are simulated at 6 locations (F1…F6) as shown in Figure 35. **Fault at F1.** First a fault located at F1 is simulated. This fault is located upstream the monitored buses, M2 and M3.

Disturbance power and energy. The results, applying the method of disturbance power and energy, are presented in Figure 36. The fault is classified as upstream at both M2 and M3, as indicated by the negative disturbance energy at both the monitored buses. The disturbance power transient seen at the beginning and ending of the events is a consequence of the Fourier transform applied to a non-stationary signal.

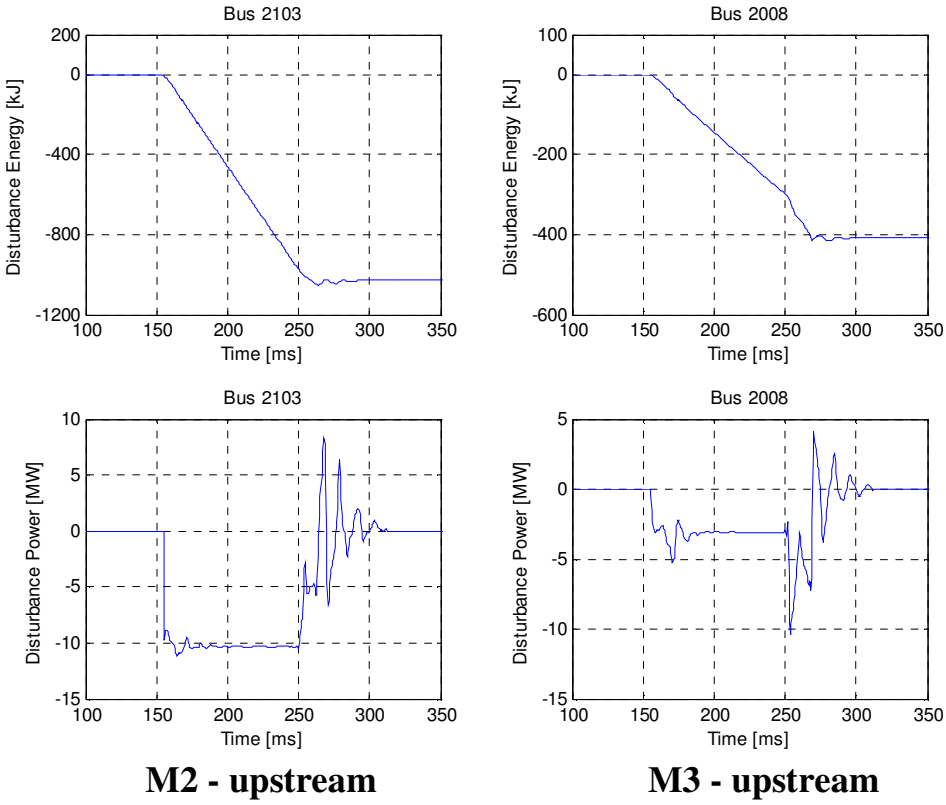

Figure 36 - Disturbance energy and disturbance power at M2 and M3 for a LLLG fault at F1

Slope of system trajectory. The method of the slope of the system trajectory is applied and the result is shown in Figure 37. The slope of the system trajectory is positive at M2 for the 3 phases meaning that the fault is located upstream. However, phase A has a negative slope at M3, whereas phase B and phase C have a positive slope. Therefore the method is not conclusive at M3.

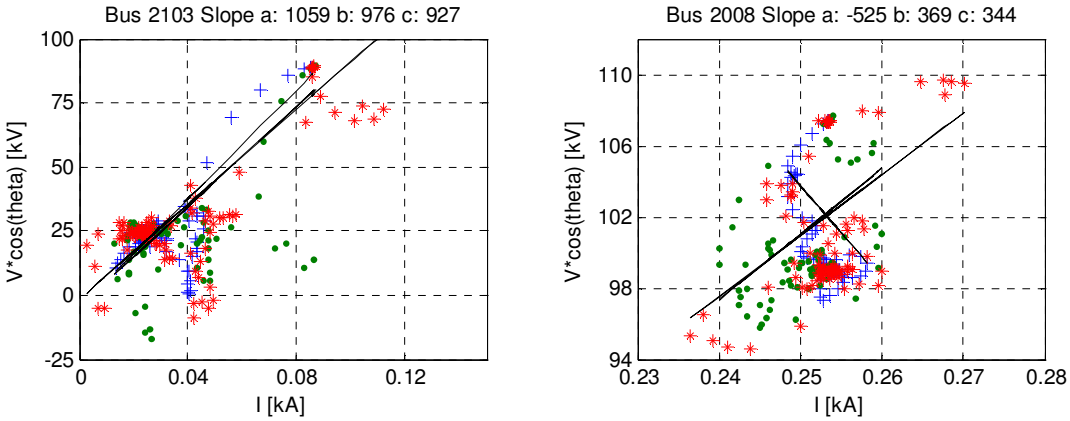

M2 - upstream **M3 - Not conclusive**

Figure 37 - Slope of system trajectory at M2 and M3 for a LLLG fault at F1

Real current component. Applying the real current component method, negative values are obtained at M2 and M3, indicating that the sag source is upstream at both buses. The initial transient could lead to the wrong result, as shown in Figure 38 for the bus M3. The real current component transient seen at the beginning and ending of the events is a consequence of the Fourier transform applied to a non-stationary signal.

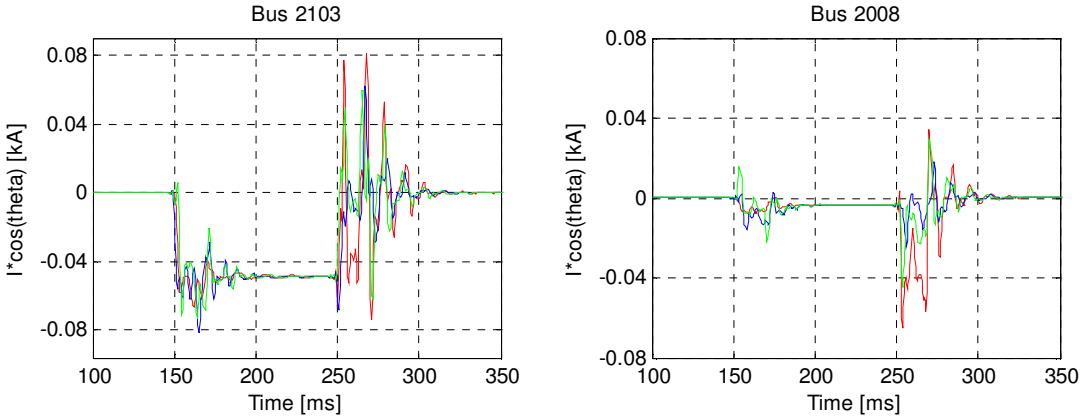

M2 - upstream **M3 - upstream**

Figure 38 - Real current component at M2 and M3 for a LLLG fault at F1

Resistance sign and distance relay. The results of the method of resistance sign and distance relay are shown in Table 36. The method of the resistance sign applied at the monitored bus M2 classifies the source correctly, but

when applied at the bus M3 the result is not conclusive because there is not sign agreement on the resistance calculated by using equations (5.6) and (5.7). The methods of real current component and distance relay locate correctly the sag source as upstream at the two buses.

Table 36 - Results for resistance sign and distance relay methods for a LLLG fault at F1

Methods	**M2**	**M3**
R (eq. 5.6) [Ω]	706	-524
R (eq. 5.7) [Ω]	313	60
RS result	**upstream**	**Not conclusive**
$Z_{pre\text{-}sag}$ [Ω]	1320	445
Z_{sag} [Ω]	1320	415
$arg(Z_{sag})$ [deg]	-40	-21
DR result	**upstream**	**upstream**

Note: RS: resistance sign, DR: distance relay.

Fault at F3. A second fault located at F3 is analysed. Now the fault location is upstream with respect to M2 and downstream to M3.

Disturbance power and energy. The location obtained using the method of disturbance power and energy is shown Figure 39. The disturbance energy is negative for both buses indicating an upstream fault location. Nevertheless, the disturbance power at M3 shows a positive peak reducing the confidence of the result for this bus. In fact the correct result is that the location is downstream at M3. Therefore, the method fails to correctly indicate the location of the fault at M3. However, the confidence of the result was low, indicating that the test was not truly conclusive at M3.

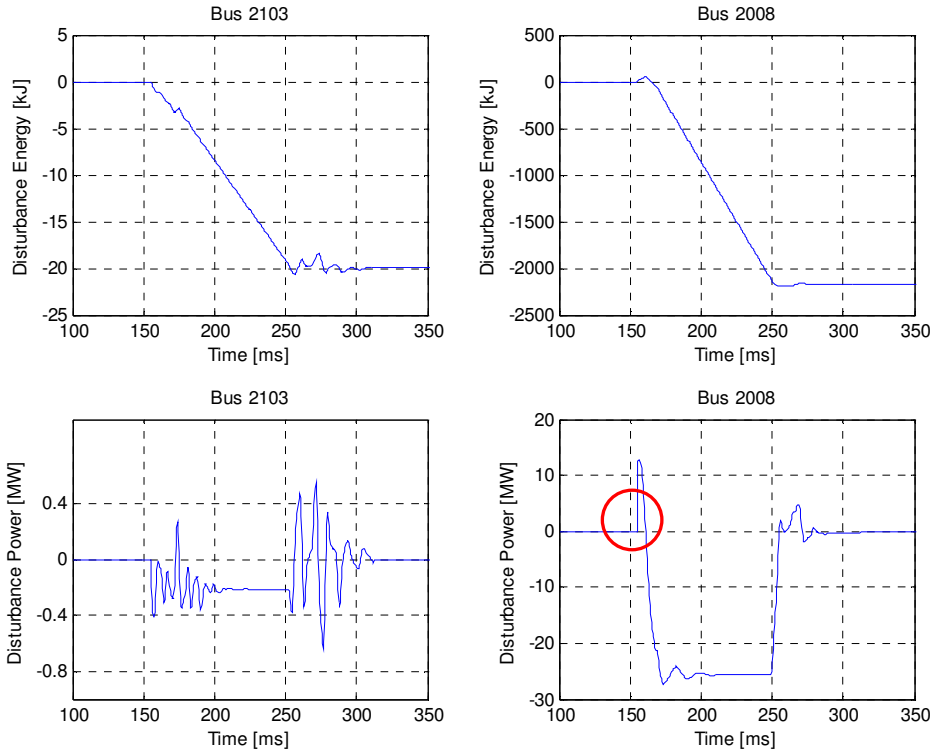

M2 – upstream **M3 – upstream, low confidence**

Figure 39 - Disturbance power and disturbance energy at M2 and M3 for a LLLG fault at F3

Slope of system trajectory. The method of the slope of the system trajectory is applied as shown in Figure 40. The result shows positive slopes at M2 and negative slopes at M3, indicating that the fault is located upstream at M2 and downstream at M3. In this case, the method of the slope of the system trajectory locates correctly the fault at the two monitored buses.

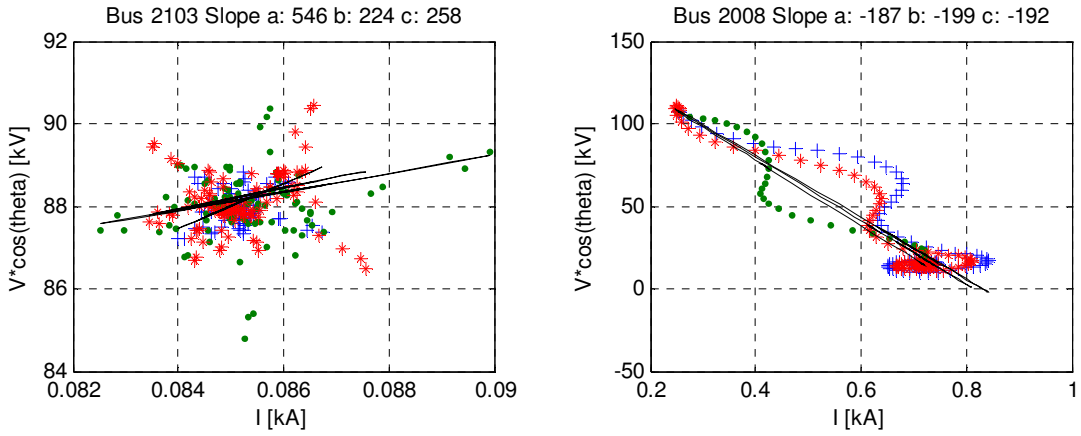

M2 - upstream **M3 - downstream**

Figure 40 - Slope of system trajectory at M2 and M3 for a LLLG fault at F3

Real current component. The result of the real current component method is shown in Figure 41. The fault is well located at the monitored buses M2 and M3. However, the initial transient observed at M2 and M3 makes the location decision weak. Only when the fault reaches the steady state the correct results are given.

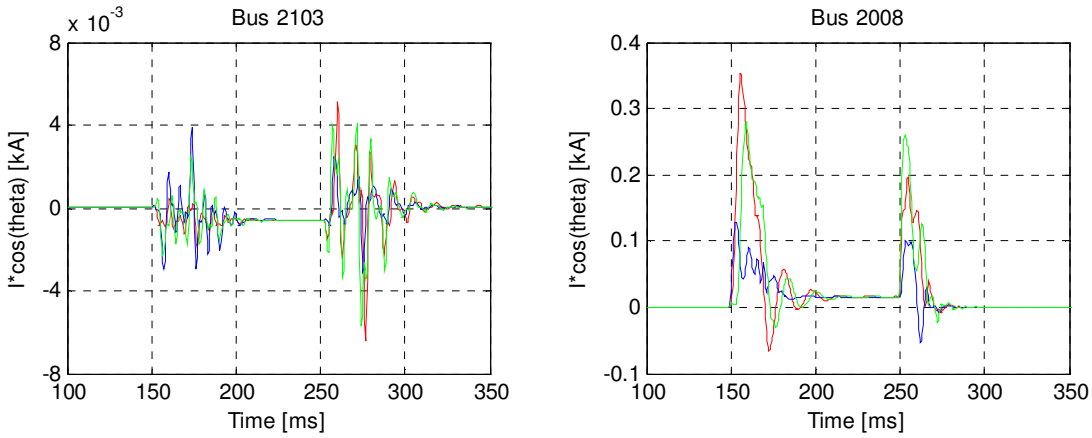

M2 - upstream **M3 - downstream**

Figure 41 - Real current component at M2 and M3 for a LLLG fault at F3

Resistance sign and distance relay. The results of the resistance sign and distance relay for a symmetrical fault at F3 are presented in Table 37. The method of resistance sign is not conclusive at M3 because two different signs are obtained. The method of distance relay correctly classifies the location of the fault at M2 and M3.

Table 37 - Results for resistance sign and distance relay methods for a LLLG fault at F3

Methods	**M2**	**M3**
R (eq. 5.6) [Ω]	866	41
R (eq. 5.7) [Ω]	273	-38
RS result	upstream	Not conclusive
$Z_{pre\text{-}sag}$ [Ω]	1324	450
Z_{sag} [Ω]	1324	60
$arg(Z_{sag})$ [deg]	-39	70
DR result	upstream	downstream

Note: RS: resistance sign, DR: distance relay.

Faults at F2, F4, F5, and F6. In order to test the methods more extensively symmetrical faults are simulated at the locations F2, F4, F5, and F6. The result of this analysis is presented in Table 38. The first column shows the real location of the faults and the next columns show the results for each of

the applied methods. It can be seen that most of the methods accurately classify symmetrical faults. However, the method of resistance sign is not conclusive in 4 of the 8 cases and it gives incorrect result in one case.

Table 38 - Symmetrical faults at locations F2, F4, F5, and F6

Monitor M2					
Location	**DPE**	**SST**	**RCC**	**RS**	**DR**
F2 / DS	DS	DS	DS	NC	DS
F4 / US	US	US	US	US	US
F5 / US	US	US	US	US	US
F6 / US	US	US	US	NC	US
Monitor M3					
Location	**DPE**	**SST**	**RCC**	**RS**	**DR**
F2 / US	US	US	US	DS	US
F4 / US	US	US	US	US	US
F5 / US	US	US	US	NC	US
F6 / US	US	US	US	NC	US

Note: US: Upstream, DS: Downstream, NC: Not conclusive, DPE: disturbance power & energy, SST: slope of system trajectory, RCC: real current component, RS: resistance sign, DR: distance relay.

In general we can conclude that most of the methods give accurate results for symmetrical faults. Summarizing, the number of accurate results is 51 out of 60 cases.

5.2.2 Asymmetrical faults

Here the methods are tested for a single-line-to-ground fault in phase A at the same 6 fault locations (F1…F6). Asymmetrical faults are more difficult to locate because each phase shows a particular behaviour. Figure 42 shows the result of the method of the slope of the system trajectory for a fault located at F1. The slope sign is different for different phases at M2. Therefore, no conclusive results are obtained at this bus. The estimated slope is positive for the three phases at M3, so the fault could be classified as upstream, agreeing with the real location.

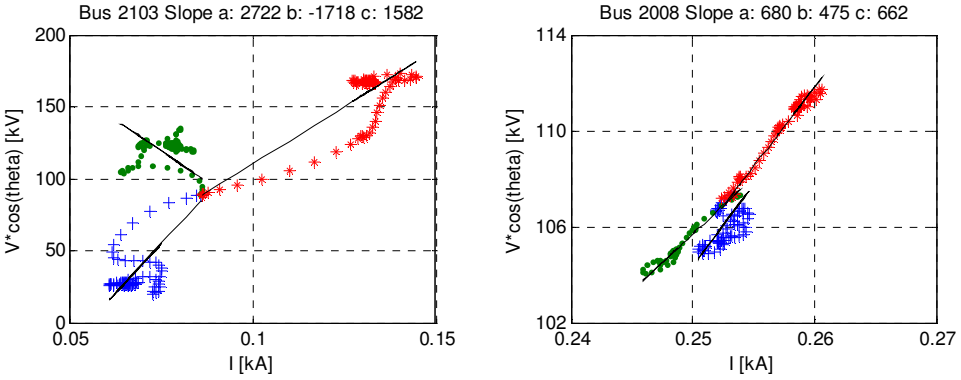

M2 - Not conclusive **M3 - upstream**

Figure 42 - Slope of system trajectory at M2 and M3 for a SLG fault at F1

The results for the 6 fault locations are summarised in Table 39. The method of distance relay presented the best performance, and obtained the correct location for the sag source for 11 of the 12 cases. The other methods obtained accurate results in 8 cases (disturbance power & energy and slope of the system trajectory), 7 cases (resistance sign), and 5 cases (real current component).

Table 39 - Results for SLG faults

Monitor M2					
Location	**DPE**	**SST**	**RCC**	**RS**	**DR**
F1 / US	DS	NC	NC	US	US
F2 / DS	DS	NC	DS	NC	DS
F3 / US	US	US	US	NC	US
F4 / US	US	US	US	US	US
F5 / US	DS	US	NC	NC	US
F6 / US	DS	US	NC	US	DS
Monitor M3					
Location	**DPE**	**SST**	**RCC**	**RS**	**DR**
F1 / US	US	US	NC	US	US
F2 / DS	US	NC	US	US	US
F3 / DS	NC	NC	DS	NC	DS
F4 / US	US	US	NC	NC	US
F5 / US	US	US	NC	US	US
F6 / US	US	US	NC	US	US

Note: US: Upstream, DS: Downstream, NC: Not conclusive, DPE: disturbance power & energy, SST: slope of system trajectory, RCC: real current component, RS: resistance sign, DR: distance relay.

It is possible to differentiate two kinds of methods: the ones that use phase values and the ones that use positive sequence values. The ones that use positive sequence values avoid the conflicting results that may be obtained at different phases.

5.3 Methods based on voltage sag magnitude only

This section is included in paper XII.

A method based on the analysis of the voltage sag magnitude and phase-angle jump was proposed to classify the sag source at the connection point of sensitive customers (Gomez *et al.*, 2005). It is stated that for a typical industrial installation the phase-angle jump vs. sag magnitude plot will have different patterns for sags caused by faults at the transmission network and for sags caused by faults within the industrial grid. This particular behaviour of the phase-angle jump vs. sag magnitude is not expected to be observed for voltage sags between transmission utilities.

An alternative simple approach to locate the sag source, based on the voltage sag magnitudes at both sides of the transformer that interconnects two grids, as shown in Figure 43, is now proposed.

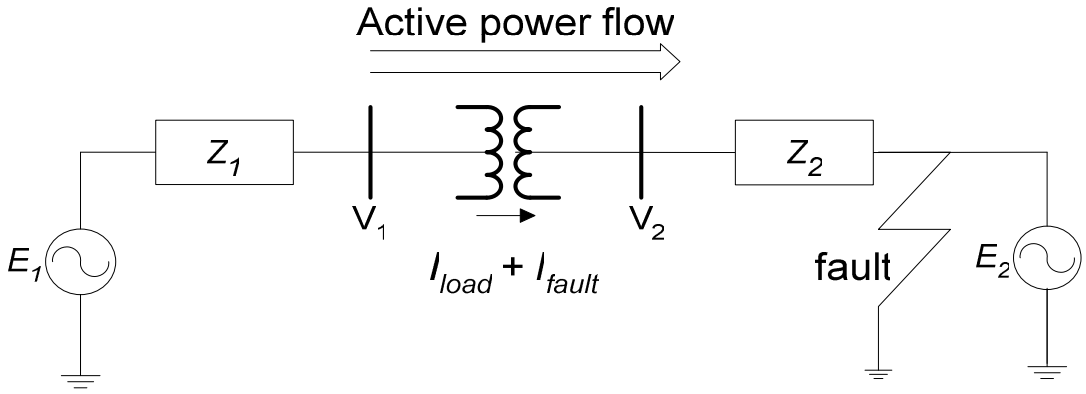

Figure 43 - Basic circuit to illustrate the sag magnitude method for sag source location

The idea is to compare the voltage sag magnitudes in pu with respect to pre-fault voltages at both sides of the transformer

$$V_1 = \frac{V_{1-sag}}{V_{1-prefault}} \tag{5.9}$$

$$V_2 = \frac{V_{2-sag}}{V_{2-prefault}} \tag{5.10}$$

where $V_{i\text{-}sag}$ is the during sag voltage and $V_{i\text{-}prefault}$ is the pre-fault voltage.

The voltage drop at each side of the transformer is given by

$$\Delta V_1 = Z_1 \left(I_{fault} + I_{load} \right) \tag{5.11}$$

$$\Delta V_2 = \left(Z_1 + Z_{TRAFO} \right) \left(I_{fault} + I_{load} \right) \tag{5.12}$$

where Z_{TRAFO} is the transformer impedance and I_{fault} is the fault current.

The voltage drop is higher on the side where the fault is located. Therefore, if $\Delta V_2 > \Delta V_1$ i.e. ($V_1 > V_2$) the fault is downstream, otherwise the fault is upstream. If there are no generation units downstream, V_1 and V_2 are expected to be almost equal during upstream faults.

This method is intended to locate the sag source at the interconnection point of transmission utilities. At this level the influence of loads is not so evident and the effect of constant power loads may not affect the performance of the method. This last phenomenon is due to the fact that loads such as induction machines may supply the extra current demanded by the constant power loads during short sags.

Another concern is when unbalanced voltage sags propagate through a delta/wye transformer. The relation between the voltage sag magnitudes for line-to-line (delta) and line-to-ground (wye) monitor connections depend on the sag type as described in Paper II in Appendix 4.

The method to locate the sag source is tested using a model of the regional network shown in Figure 35. The simulation is performed using the PSCAD/EMTDC program. The instantaneous phase-to-ground voltages obtained from the simulation are processed using MatLab in order to get the rms voltages. As a result the rms voltage as a function of time is obtained, as shown in Figure 44. The voltage sag magnitude is defined as the lowest steady state rms voltage during the fault. When each phase experiences different sag magnitudes the lowest magnitude of the three phases is used to characterise the three-phase sag.

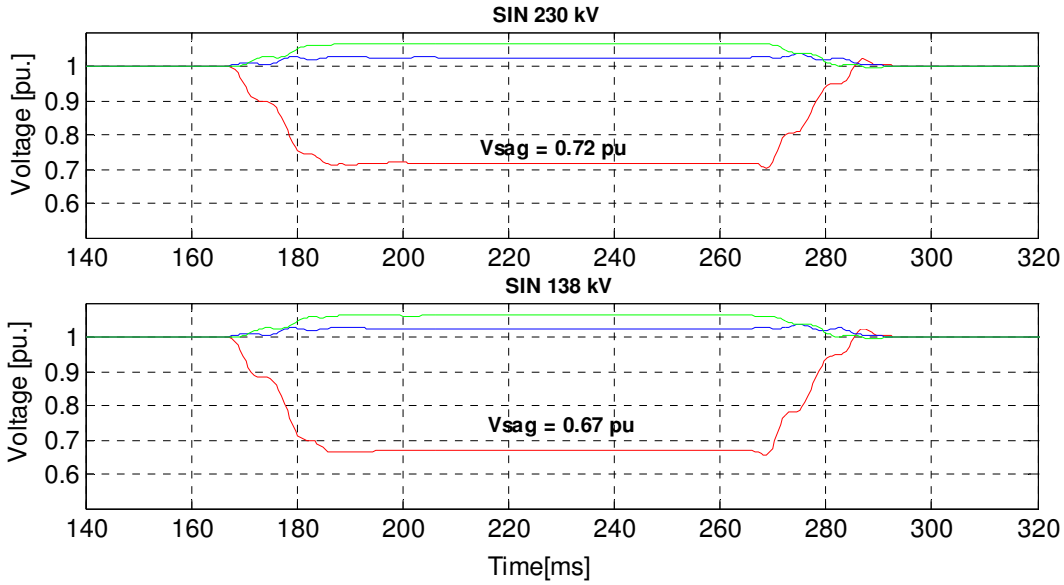

Figure 44 - Rms voltage vs. time at the 230 and 138 kV buses measured at M3 substation for a SLG fault at F8 (downstream location)

At each fault location (F1, F2, F3, F4, and F8) 4 types of faults are simulated (LLLG, LL, LLG, and SLG). The results for the simulations are organised in Table 40 to Table 43, one table for each type of fault. The first row of the tables indicates the fault position; the second and the third rows show the sag magnitude at the 230 kV and 138 kV buses; and the fourth row shows the location assessed by the test.

The location decision is based on the sag magnitude at 230 kV and 138 kV buses. Considering that the power flows from the 230 kV bus to the 138 kV bus, when the sag magnitude is lower at the 138 kV bus than at the 230 kV bus the source of the sag is located downstream, otherwise the source is located upstream.

There are two fault positions (F3 and F8) that are located downstream. The results obtained for each type of fault confirm the fault location. For instance, for a LLLG fault at F8 the sag magnitude at the 230 kV bus is 0.78 pu, whereas the sag magnitude at the 138 kV bus is 0.73 pu, as shown in Table 40. The difference in the sag magnitude is due to the additional voltage drop over the power transformer impedance caused by the fault current.

On the other hand, for the faults at F1, F2, and F4, that are located upstream, the sag magnitude at each side of the transformer is the same. However, for upstream faults it may occur that the sag magnitude is lower at the 230 kV bus than at the 138 kV bus, when there is a contribution to the fault current from some loads or co-generation units installed at a downstream location.

Table 40 - Source location for LLLG faults

Fault	Vsag 230 kV	Vsag 138kV	Location
F1/US	0.93	0.93	**US**
F2/US	0.92	0.92	**US**
F4/US	0.01	0.01	**US**
F3/DS	0.66	0.57	**DS**
F8/DS	0.78	0.73	**DS**

Table 41 - Source location for LL faults

Fault	Vsag 230 kV	Vsag 138kV	Location
F1/US	0.93	0.93	**US**
F2/US	0.92	0.92	**US**
F4/US	0.50	0.50	**US**
F3/DS	0.74	0.69	**DS**
F8/DS	0.81	0.77	**DS**

Table 42 - Source location for LLG faults

Fault	Vsag 230 kV	Vsag 138kV	Location
F1/US	0.94	0.94	**US**
F2/US	0.93	0.93	**US**
F4/US	0.07	0.07	**US**
F3/DS	0.67	0.60	**DS**
F8/DS	0.74	0.69	**DS**

Table 43 - Source location for SLG faults

Fault	Vsag 230 kV	Vsag 138kV	Location
F1/US	0.98	0.98	**US**
F2/US	0.97	0.97	**US**
F4/US	0.11	0.11	**US**
F3/DS	0.72	0.67	**DS**
F8/DS	0.72	0.67	**DS**

Voltage sags have been measured during a one year period in several buses of the system shown in Figure 35. The two buses used during the simulations are among the monitored buses. During this sag survey only voltage information was recorded. The fault location has been obtained for faults at 230 kV and 138 kV lines. Therefore, it is possible to evaluate the proposed method to locate the sag source.

Table 44 shows the voltage sag magnitude obtained at both buses in the substation M3 during the identified faults. Not all the measured sags are used to test the method because the fault location must be previously

known. Therefore, only faults that happened in the 230 kV and 138 kV networks are identified and used for the method validation.

Table 44 - Voltage sags measured at the substation M3

Fault type	Fault location	Relative Location	Vsag 230 kV	Vsag 138 kV
LL	COL/ALF	DS	0.67	0.60
SLG	COX/JAU	US	0.65	0.66
SLG	NOB/DEN	US	0.97	0.97
SLG	COL/ALF	DS	0.71	0.63
SLG	COX/JAU	US	0.90	0.89
SLG	BPX/RND	US	0.92	0.92
SLG	JAC/COX	US	0.90	0.90
SLG	COX/JAU	US	0.88	0.88
SLG	COL/ALF	DS	0.68	0.63
LL	CBA/CVD	US	0.87	0.86
LLL	CMAG/RND	US	0.94	0.93
LLL	JUB/MAR	US	0.96	0.95
LLL	DEN/TAN	US	0.96	0.96
LLG	JAC/COX	US	0.90	0.89
SLG	GRA/POC	US	0.93	0.93
SLG	JUB/MAR	US	0.97	0.97
SLG	DCLA/COL	DS	0.58	0.46
SLG	JUB/MAR	US	0.97	0.97
SLG	NOB/DEN	US	0.97	0.97
SLG	RVD/RND	US	0.93	0.92
LLG	DCLA/COL	DS	0.50	0.37
LLL	PRE/ITA	US	0.92	0.92
LL	ITA/JUB	US	0.93	0.93
LLL	NOB/MUT	US	0.00	0.00
LL	JUB/MAR	US	0.93	0.93
LLL	DCLA/COL	DS	0.38	0.23
LL	DEN/TAN	US	0.96	0.96
LL	DEN/TAN	US	0.96	0.96
LLG	MAR/CAC	US	0.97	0.96
LL	JAC/COX	US	0.89	0.90

The downstream events are highlighted with grey. In all the downstream cases the sag magnitude is lower at the 138 kV bus. There are some events, where the sag magnitude is slightly lower (0.01 pu) at the 138 kV bus, but the faults that caused these sags were located upstream. To ensure the reliability of the test the difference between the sag magnitudes must exceed a certain threshold.

The voltage sag magnitudes obtained from the measurements are shown in a way, where the location decision is seen graphically. Figure 45 shows the plot of the 138 kV sag magnitudes vs. the 230 kV sag magnitudes. The straight-line divides the plot into two zones. The events represented above or on the line correspond to the ones whose source is located upstream. The events represented below the line are the sags whose source is located downstream.

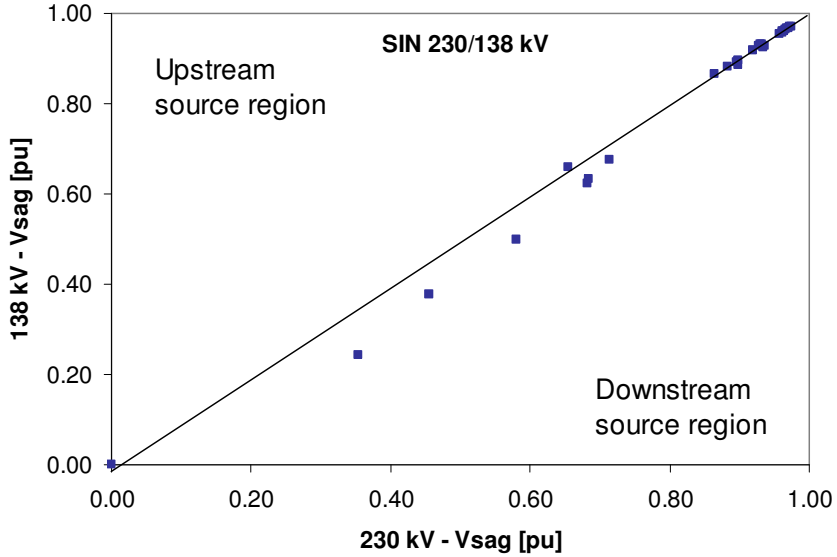

Figure 45 - Voltage sag magnitudes measured at 230 and 138 kV buses

Whenever there are generation units or a great penetration of induction machines at the downstream location, it is expected to find events above the boundary line, but that is not the case of the measured network.

The proposed method for source location can be straightforwardly applied when the transformer at the substation has a wye/wye winding connection. This is a typical transformer at the interconnection of two transmission utilities in the Brazilian network, where the measurements have been taken.

However, a more general approach includes other types of transformer connections. The sag propagation through a delta/wye transformer is analysed. This type of transformer swaps the sag type. Considering the characterisation of unbalanced three-phase voltage sags (Bollen, 2000), a set of equations describing the relation between sag magnitudes for delta and wye connected PQ-monitors was proposed (Paper II, Appendix 4). The relation between these sag magnitudes is plotted in Figure 46.

The generalisation of the proposed method includes an additional step. In order to locate the sag source it is necessary to classify the sag according to the ABC classification (Bollen, 2000). Then, if the event is under the reference curve, the source location is at the delta side of the transformer, otherwise it is at the wye side.

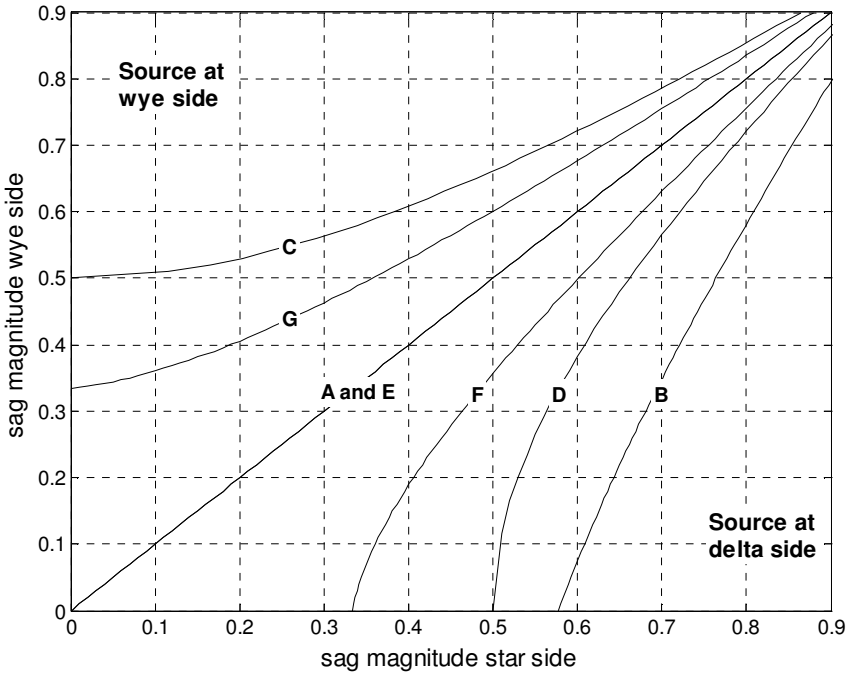

Figure 46 - Sag magnitude relation at both sides of a transformer with delta/wye windings connection

The load behaviour during the voltage sag may affect the performance of the method. The initial hypothesis, that only a downstream fault produces an increase of the current flowing through the transformer, may fail when the load is mainly constant power and the time response of the load is in the order of milliseconds. In such a situation the reduction of the voltage during a voltage sag increases the load current.

The proposed method for sag source location is intended to be used at the connection substation of two transmission utilities, where the load cannot be considered as constant power but as composite load (Karlsson, 1992)

$$S = P_0\left(\frac{V}{V_0}\right)^{\alpha} + Q_0\left(\frac{V}{V_0}\right)^{\beta} \tag{5.13}$$

where P_0 and Q_0 are the active and reactive power at nominal voltage and V_0 is the nominal voltage; α and β are empiric coefficients that express the voltage dependency of the load.

It has been shown that during a voltage sag the behaviour of such a composite load is close to a constant impedance model. Considering different periods of the year (winter, summer) and bus characteristics (residential loads, industrial loads) the values of α varies from 1.5 (industrial area during summer) to 2.5 (residential area during winter). The β values are greater than 4.0 for all scenarios (Karlsson, 1992). Therefore the proposed

method should not fail as a consequence of load behaviour when it is applied at transmission and subtransmission levels.

6 Conclusions and Future Work

This chapter presents a summary of the findings of this research. A discussion about the generalization of the results is included. The main conclusions are highlighted and several ideas for future work are proposed.

6.1 Summary and conclusions

The summary and conclusions are split into different sections to facilitate the understanding and to highlight the links to the main topics of this thesis. The different sections are: Single event characterisation, Sag propagation, Power system performance and Voltage sag source location.

6.1.1 Single event characterisation

Time-domain simulation tools such as electromagnetic transient programs are a powerful approach to obtain voltage sag characteristics such as magnitude, duration, phase-angle jump, and voltage sag type. Raw data (instantaneous voltage samples) obtained from PQ-monitoring and time domain simulations were used to test signal-processing algorithms that estimate rms voltage and fundamental voltage (50/60 Hz signal). Results show that rms voltage and the fundamental voltage present similar behaviour. Hence, voltage sag magnitude and duration can be accurately estimated from either rms voltage or fundamental voltage.

During three-phase sags the characteristic voltage can be used to estimate the sag magnitude and the phase-angle jump. However, for some unbalanced voltage sags the magnitude and phase-angle jump of the characteristic voltage differs from the magnitude and phase-angle jump of the phase voltages.

The effect of induction machines is seen in the behaviour of the during-sag voltage. The sag magnitude is affected by the induction machine if the sag duration is short. For longer sags the event magnitude is similar to the one obtained when there is no induction machine loads. The induction machine also affects the post-fault voltage, delaying the voltage raise and in some cases extending the sag duration.

The phasor measurement unit is a promising device for voltage sag detection and characterisation. Today the main limitations are related to the availability of the phase voltages and the time resolution of the measurements.

When instantaneous phase-to-neutral voltages are available it is possible to obtain the voltage sag type comparing the phase-to-neutral and the phase-to-

phase sag magnitudes. The phase-to-phase and phase-to-neutral sag magnitudes follow theoretical relations ($V_{PP} = f(V_{PN})$) derived from the ABC classification of three-phase sags.

The parameters used for voltage sag characterisation undergo important variations during the event. The single values chosen to characterise the sag are useful for statistical assessment of site performance. However, the variation of the rms voltage and phase-angle is relevant to quantify the single sag event. The variation of these values were analysed individually as a function of time and in a combined way. The independent analysis covers the study of the rms voltage and phase-angle versus time. The phase-angle, estimated from instantaneous voltage values using the Discrete Fourier Transform, faces high variations during the starting and ending of the sag. This behaviour is due to the lack of periodicity of the voltage signal during these periods.

A novel sag representation was presented in terms of the phasor locus, extreme phasor, and as a multi-chart representation. The phasor locus shows the path that phasors follow during the event. Combined with the phasor locus two extreme phasors are also presented; the minimum retained voltage and the maximum phase-angle jump. These two phasors are suitable to represent the voltage sag, however the choice of the most appropriate one depends on the purpose of the study.

6.1.2 Sag propagation

The study was based on system measurements carried out during a 6 month period. A detailed analysis of voltage sag propagation in the power system was described. The 30 analysed events generated 89 voltage sags on the 12 monitored buses. It was noticed that 48 % of the sags were deep enough to cause malfunction on critical sensitive loads. The duration of the sags agreed with the typical fault clearing time of the distance protection in the analysed system. About 50 % of the sags had a duration shorter than 100 ms.

The average sag propagation index (SPI) indicates that in average each fault generated sags at 3 of the 12 monitored buses. However, some faults were more severe. These faults that affected a large part of the grid were located near the main generation bus.

It was concluded that LLL faults propagate twice as much as the SLG faults. However, the number of SLG faults was about double compared to the number of LLL faults. Consequently, LLL and SLG faults contributed similarly to the number of measured sags.

The generation dispatch affects the average SPI. When the system was dispatching the thermal units that are located near the monitored buses the SPI was considerably lower than when the power came from the hydro plants that are located far from the monitored buses.

The vertical sag propagation through transformers affects the voltage sag type as a consequence of the transformer winding connections confirming the previous theoretical analysis. However, the changes in the sag type are also influenced by the proximity of active loads and the pre-fault unbalance level of the system.

6.1.3 System performance

Voltage sag indices have been calculated using two types of programs: an electromagnetic transient program, ATP, and a short-circuit calculation program. The ATP simulation includes the loads and the pre-fault system condition, whereas the short-circuit calculation program neglects the load and simplifies all pre-fault voltages to 1.0 pu. As a result, the voltage sag assessment using ATP is more conservative than the one using the short-circuit program. The ATP simulation leads to a larger number of sags and lower average magnitude. However, the divergence of the estimated sag indices is not significant.

In order to estimate the accuracy of the voltage sag magnitude and frequency obtained by the electromagnetic transient program and the short-circuit calculation, the result of a 6 month sag survey was compared with the simulations of the faults detected during this period.

Voltage sag magnitudes obtained from simulations are in general very close to the measured ones. In more than 90 % of the simulated cases the error of the sag magnitude is lower than 10 %. The few cases that presented large error are due to faults located near the monitored bus where the exact fault location and fault impedance considerably affect the calculated sag magnitude.

The sensitivity of the method of fault positions to estimate voltage sag indices was analysed with respect to three uncertainties: fault rate, fault type and fault location. With respect to fault rate, it has been found that the sag frequency highly depends on the fault rate of lines and busbars. In particular, the frequency is proportional to the fault rate of lines and buses contained within the exposed area of the analysed bus. It has also been found that the average sag magnitude is less sensitive than the frequency index to fault rate variations.

Regarding fault type, the results have shown that fault type distribution do affect the frequency index. In general considering only three-phase faults

leads to an overestimation of the sag frequency. The average sag magnitude is less sensitive to the fault type distribution than the frequency index.

The fault position has an important influence on the indices. The simulations have shown that when only faults at busbars are considered, the sag frequency is much larger than when faults are applied along the lines.

The sag indices for phase-to-phase and phase-to-neutral voltage sags are different at a high voltage level. The results obtained from the method of fault positions show that phase-to-neutral sags are more frequent and more severe than phase-to-phase ones. A set of measurements obtained from a one-year sag survey at three buses (138 kV, 13.8 kV, and 440 V) confirms the results obtained from the simulations. However, at the low voltage level phase-to-neutral and phase-to-phase voltages presented similar performance. Therefore, for the monitored system, the way the PQ-monitor is connected at the low voltage level will not significantly affect the results.

The similar results obtained for the SARFI-70 % and SARFI-ITIC indices encourage the adoption of the former one for the assessment of the busbar performance. The SARFI-70 % is easier to estimate than the SARFI-ITIC because only the dip amplitude is needed, disregarding the duration of the event.

6.1.4 Sag source location

Several methods using voltage and current values have been applied to locate the voltage sag source in a transmission network. In general the performance of the methods is much more accurate for symmetrical faults, where correct results were obtained in 87 % of the cases. On the other hand, for asymmetrical faults correct results were obtained in 65 % of the cases.

The voltage sag magnitude, estimated in terms of the pre-fault voltage, at both sides of a power transformer was proposed to find the relative location of the sag source. The method was successfully implemented, and the excellent performance was confirmed by simulated and measured events.

The method was applied at a substation where the transformer winding connections is wye/wye grounded at both sides. The generalisation of the method for other types of transformers was explained as well. The applicability of the method considering different load behaviour was also analysed.

The analysis for meshed grids needs a broader idea of system boundaries. Hence, the concepts of upstream and downstream cannot be applied. More investigations are needed to develop a method to locate the sag source as

inside or outside the system boundaries using wide area measurements techniques.

6.2 Generalisation and discussion of the contributions

It is important to mention that the influence of the voltage and current waveform on the behaviour of loads has been investigated for several years. In the literature review of Chapter 2, several publications are written in other languages than English. The English translation of the abstracts of these papers is available in the Inspec database. This is necessary to make international scientific exchange possible, especially because other languages are becoming popular for technical publication. Therefore, this research is mainly based on English language publications and orienting on the translated abstracts found in Inspec.

The proposed method for the classification of unbalanced sags in the ABC types shows a great performance for simulated sags, where the pre-fault voltages are considered balanced and the loads are neglected. The performance of the method has to be tested with measured sags. The relation between the type of fault and the measured sag depends in system characteristics such as the transformer winding connections. Therefore, the correlation of the fault type and the obtained sag shown in Figure 12 cannot be transferred directly to other systems.

The analysis of the voltage sag propagation based on measurements depends on the localisation of the PQ-monitors. The only way to have independent results is to install monitors at all the buses. Considering the usual limitation of resources this scenario is in general not feasible.

The propagation of the faults caused by each type of fault depends on system characteristics such as the transformer winding connections and grounding. Therefore the SPI shown in Table 12 cannot be used as reference for other systems.

The comparison of the simulation of voltage sags using an electromagnetic transient program and a short-circuit calculation program illustrates the minor differences obtained in the sag magnitude and frequency for a deterministic assessment. The analysis has been made for two typical programs. However, with the advance of the computing capability of modern computers the calculation programs include more detailed models also for short-circuit calculation. Moreover, it is common that programs calculate instantaneous currents and voltages as well as rms quantities. Therefore, the differentiation between electromagnetic transient programs and short-circuit calculation programs may not be relevant in the future.

The performance obtained for phase-to-phase measurements is better than for phase-to-neutral measurements, which is a consequence of the fault type distribution and the transformer winding connections. Most of the transformers at transmission level are wye/wye grounded at both sides in the analysed system. Therefore, systems that have other types of transformer winding connections may experience the same performance for phase-to-phase and phase-to-neutral measurements.

The voltage sag source location method based only on voltage measurements proposed here has been reliable in systems with transformers connected wye/wye grounded at both sides. Theoretically, the method should work in systems with other characteristics. However, it has to be applied using concrete measurements to test its performance in other systems.

6.3 Future work

The fault location methods have to be extended for cases where there are several interconnections between the utilities. This is a crucial point to establish responsibilities for the lack of power quality in de-regulated power systems. The methods that originally used phase values have to be tested using positive sequence values in order to check their accuracy.

Power quality standards lack a well defined voltage sag performance standard. The recently updated standards recommend several ways to estimate sag indices and to obtain the system performance. However, there are no reference values and in most countries the regulations miss the maximum allowed indices. It is believed that this is a major work and has to be done in agreement between the independent regulator bodies, the utilities, and the end-users associations. Therefore, we are now running our first attempt to obtain reference values at a country level. This research will be developed in Uruguay.

7 References

Bollen, M.H.J., 2000. *Understanding Power Quality Problems, Voltage Sags and Interruptions*. New York: IEEE Press.

Bollen, M.H.J., Hager, M., Roxenius, C., 2003. Voltage dips in distribution systems: load effects, measurements and theory. *In Proc. Congrès International des Réseaux Electriques de Distribution CIRED 2003, Barcelona*.

Bollen, M.H.J., Yalcinkaya, G., Hazza, G., 1998. The use of electromagnetic transient programs for voltage sags analysis. *In Proc. IEEE 8th International Conference on Harmonics and Quality of Power, Oct.1998, Athens.*

Bollen, M.H.J., and Zhang, L.D., 2003. Different methods for classification of three-phase unbalanced voltage dips due to faults. *Electric Power Systems Research*, 66 (1), 59-69.

Bongiorno, M., Sannino, A., Dusonchet, L., 2003. Cost-effective power quality improvement for industrial plants. *In Proc. IEEE Bologna PowerTech, 23-26 June 2003, Bologna, Italy.*

Carvalho Filho, J.M., Abreu, J.P.G., Leborgne, R.C., Oliveira, T.C., Correia, D.M., de Oliveira, J.F., 2002. Comparative analysis between measurements and simulations of voltage sags. *In Proc. IEEE 10th International Conference on Harmonics and Quality of Power*, *6-9 Oct.2002, Rio de Janeiro*.

Carvalho Filho, J.M., Abreu, J.P.G., Caminha Noronha, J.C., Arango, H., 2000. Analysis of power system performance under voltage sags. *Electric Power Systems Research*, 55 (3), 211-218.

CAUE – Comite Argentino de Usuarios de EMTP - ATP, 2001. ATP - Rule Book, Dec.2001, Buenos Aires.

Cepel – Centro de Pesquisas de Energia Elétrica, 1998. Programa de análise de faltas simultâneas – ANAFAS, versão 3.0, Manual do Usuário, Dec.1998, Rio de Janeiro. (*in Portuguese*)

Cigre Task Force C4.1.02, 2005. Voltage Dip Evaluation and Prediction Tools. Draft Nov.2005.

Colding, S., 1982. What quality can be demanded from the electricity supply. *Elteknik med Aktuell Elektronik*, 25 (2), 20-22. (*in Swedish*)

Conrad, L., Little, K., and Grigg, C., 1991. Predicting and preventing problems associated with remote fault-clearing voltage dips. *IEEE Transactions on Industry Applications*, 27 (1), 167-72.

Correia, D.M., and D. Brasil, D.O.C., 2003. Pilot project for the evaluation of the sag performance of some Brazilian network busbars. *In Proc. CIGRE/IEEE PES International Symposium. Quality and Security of Electric Power Delivery Systems, 8-10 Oct.2003, Montreal.*

Degeneff, R.C., Barss, R., Carnovale, D., Raedy, S., 2000. Reducing the effect of sags and momentary interruptions: a total owning cost prospective. *In Proc. IEEE 9th International Conference on Harmonics and Quality of Power, 1-4 Oct.2000, Orlando FL, USA*.

Deloux, G., 1974. International standardization and electric power supply network disturbances. *In Proc. IEE International Conference on Sources and Effects of Power System Disturbances, 22-24 Apr.1974, London.*

Dettloff, A., 2000. Power quality performance component of the special manufacturing contracts between energy provider and customer. *In Proc. IEEE Power Engineering Society Summer Meeting, 16-20 Jul.2000, Seattle, WA, USA.*

Djokic, S.Z., Stockman, K., Milanovic, J.V., Desmet, J.J.M., Belmans, R., 2005. Sensitivity of AC adjustable speed drives to voltage sags and short interruptions. *IEEE Transactions on Power Delivery,* 20 (1), 494-505.

Du, C., Bollen, M.H.J., 2006. Power-frequency control of VSC-HVDC during island operation, *In Proc. IEE 8th International Conference on AC and DC Power Transmission, Mar.2006, London.*

Ermakov, V.F., and Cherepov, V.I., 1983. A statistical analysis of voltage surges and dips. Izvestiya Vysshikh Uchebnykh Zavedenii, *Elektromekhanika,* (3), 97-100. (*in Russian*)

ERGEG, 2006. European Energy Regulators' hard hitting Final Report to the European Commission on the November 2006 Blackout criticises transmission system operators. www.ergeg.org/portal/page/portal/ERGEG_HOME/ERGEG

FERC, 2003. Interim Report: Causes of the August 14th Blackout in the United States and Canada. www.ferc.gov/industries/electric/indus-act/blackout.asp

Frichtel, J.S., and Dougherty, J.W., 1970. Specific avionic system benefits through improved electric power quality. *In Proc. IEEE National Aerospace Electronics Conference, 18-20 May 1970, Dayton OH, USA*.

Giorgi, E., 1975. High quality electric power. *Naval Research Reviews*, 28 (4), 23-34.

Gnativ, R., and Milanovic, J.V., 2001. Voltage sag propagation in systems with embedded generation and induction motors. *In Proc. IEEE Power Engineering Society Summer Meeting, 15-19 July 2001, Vancouver.*

Gomez, J.C., and Campetelli, G.N., 2000. Voltage sag mitigation by current limiting fuses. *In Proc. World Congress on Industrial Applications of Electrical Energy and 35th IEEE-IAS Annual Meeting, 8-12 Oct.2000, Rome, Italy.*

Gomez, J., Morcos, M., Tourn, D., and Felici, M., 2005. A novel methodology to locate originating points of voltage sags in electric power systems. *International Conference on Electricity Distribution, Jun.2005, Turin*.

Hamzah, N., Mohamed, A., and Hussain, A., 2004. A new approach to locate the voltage sag source using real current component. *Electric Power Systems Research*, 72 (2), 113-123.

Heikkila, H., 1976. Harmonics in a power system. *Saehkoe*, 49 (1), 27-30. (*in Finnish*)

Heine, P., Pohjanheimo, P., Lehtonen, M., and Lakervi, E., 2002. A method for estimating the frequency and cost of voltage sags. *IEEE Transactions on Power Systems,* 17 (2), 290-6.

Hilger, C.H., 1972. What is the quality of electric power? *Elektroteknikeren*, 68 (19), 418-22. (*in Danish*)

Hucker, D. J., 1970. Aircraft a.c. electric system power quality. *In Proc. National Aerospace Electronics Conference, 18-20 May1970, Dayton OH, USA.*

IEC 61000, 1990. *Electromagnetic compatibility (EMC).*

IEEE Std C57.18.10, 1998. *Standard practices and requirements for semiconductor power rectifier transformers.*

IEEE Std C62.48, 1995. *Guide on interactions between power system disturbances and surge-protective devices.*

IEEE Std 493, 1997. *Recommended practice for the design of reliable industrial and commercial power systems.*

IEEE Std 519, 1992. *Recommended practices and requirements for harmonic control in electrical power systems.*

IEEE Std 1100, 1999. *IEEE recommended practice for powering and grounding electronic equipment.*

IEEE Std 1124, 2003. *Guide for the analysis and definition of DC-side harmonic performance of HVDC transmission systems.*

IEEE Std 1159, 1995. *Recommended practice for monitoring electric power quality.*

IEEE Std 1159.3, 2003. *Recommended practice for the transfer of power quality data.*

IEEE Std 1250, 1995. *Guide for service to equipment sensitive to momentary voltage disturbances.*

IEEE Std 1346, 1998. R*ecommended practice for evaluating electric power system compatibility with electronic process equipment.*

IEEE Std 1531, 2003. *Guide for application and specification of harmonic filters.*

IEEE Std 1564 draft 6, 2004. *Recommended practice for the establishment of voltage sags indices.*

Johns, M., and Morgan, L., 1994. Voltage sag mitigation through ridethrough coordination. *In Proc. IEEE/IAS Annual Textile, Fiber and Film Industry Technical Conference, 4-5 May 1994, Greenville SC, USA.*

Kagan, N., Ferrari, E.L., Matsuo, N.M., Duarte, S.X., Sanommiya, A., Cavaretti, J.L., Castellano, U.F., Tenorio, A., 2000. Influence of RMS variation measurement protocols on electrical system performance indices for voltage sags and swells. *In Proc. of 9th International Conference on Harmonics and Quality of Power, 1-4 Oct.2000, Orlando FL, USA.*

Kajihara, H.H., 1968. Quality Power for Electronics. *Electro-Technology*, 82 (2), 46-50.

Karlsson, D., 1992. *Voltage stability simulations using detailed models based on field measurements*. Thesis (PhD), School of Electrical and Computer Eng., Chalmers University of Technology, Sweden.

Key, T. S., 1979. Diagnosing power quality related computer problems. *IEEE Transactions on Industry Applications*, 25(4), 381-393.

Konstantinov, B.A., Zhezhelenko, I.V., Nikiforova, V.N., Lipskii, A.M., Slepov, A.M., Yu, V., 1978. A system of indices and standardising the quality of electric energy. *Elektrichestvo*, (9), 11-19. (*in Russian*)

Leborgne, R.C., Carvalho Filho, J.M., de Abreu, J.P.G., Oliveira, T.C., Postal, A.A., Zaparoli, L.H., 2003. Alternative methodology for characterization of industrial process sensitivity to voltage sags. *In Proc. IEEE Bologna PowerTech, 23-26 June 2003, Bologna, Italy.*

Li, C., Tayjasanant, T., Xu, W., and Liu, X., 2003. Method for voltage-sag-source detection by investigating slope of the system trajectory. *IEE Proceedings - Generation, Transmission and Distribution*, 150 (3), 367-372.

Lonngren, K., 1974. Quality of electricity supply. *Saehkoe,* 47 (3), 118-23. (*in Finnish*)

Macken, K.J.P., Bollen, M.H.J., and Belmans, R.J.M., 2004. Mitigation of voltage dips through distributed generation systems. *IEEE Transactions on Industry Applications*, 40 (6), 1686-1693.

Marquet, J., 1993. CREUTENSI: software for determination of depth, duration and number of voltage dips (sags) on medium voltage networks. *Materiel electrique, transport et distribution d'energie*. (*in French*)

Martinez, J.A., and Martin-Arnedo, J., 2004. Voltage sag stochastic prediction using an electromagnetic transients program. *IEEE Transactions on Power Delivery*, 19 (4), 1975-82.

McEachern, A., 1993. Power quality: how bad is bad? *Electrical Construction and Maintenance*, 92 (2), 26, 30, 32.

McFadden, R.H. 1969. How does plant power distribution design affect today's machine tools? *Electrical Construction Design*, 21-28.

McFadden, R.H., 1970. Power system analysis-what it can do for industrial plants. *In Proc. 5th Annual Meeting of the IEEE Industry and General Applications Group, 5-8 Oct.1970, Chicago.*

McGranaghan, M., 1995. Effects of voltage sags in process industry applications. *In Proc. Stockholm PowerTech International Symposium on Electric Power Engineering, 18-22 June 1995, Stockholm.*

McGranaghan, M., and Roettger, B., 2001. Benchmarking International Transmission System Fault Performance. *In Proc. Power Quality Applications,* EPRI.

Mestres, C., 1972. Computer power supply, analysis of service quality in voltage dips field. *Revue Générale de l'Electricité,* 81 (9), 531-536. (*in French*)

Meynaud, P., 1983. The quality of the voltage in the supply of electrical energy. *2 Colloque National et Exposition sur la Compatibilité Electromagnetique (2nd National Colloquium and Exposition on Electromagnetic Compatibility)*, 1-3 June 1983, Tregastel, France, CNET. (*in French*)

Olguin, G., 2005. *Voltage Dip (Sag) Estimation in Power Systems based on Stochastic Assessment and Optimal Monitoring*. Thesis (PhD). Division of Electric Power Engineering, Chalmers University of Technology.

Olguin, G., and. Bollen, M.H.J., 2003. Stochastic assessment of unbalanced voltage dips in large transmission systems. *In Proc. IEEE Bologna PowerTech, 23-26 June 2003, Bologna, Italy*.

ONS - Operador Nacional do Sistema Interligado, 2003, Brasil. www.ons.org.br. (*in Portugues*)

Ohrstrom, M., and Soder, L., 2003. A comparison of two methods used for voltage dip characterization. *In Proc. IEEE Bologna PowerTech, 23-26 June 2003, Bologna, Italy*.

Outhred, H., and Schweppe, F.C., 1980. Quality of supply pricing for electric power systems. *In Proc. IEEE Power Engineering Society Winter Meeting, 3-8 Feb.1980, New York.*

Parsons, A.C., Grady, W.M., Powers, E.J., and Soward, J.C., 2000. A direction finder for power quality disturbances based upon disturbance power and energy. *IEEE Transactions on Power Delivery*, 15 (3), 1081-1086.

Plette, D.L., 1969. The effects of improved power quality on utilization equipment. *In Proc. IEEE National Aerospace Electronics Conference, 19-21 May 1969, Dayton OH, USA.*

Poeata, A., Ivas, D., Alexandrescu, Gh.V., Ilinca, M., 1978. Possibilities of calculating the effects of voltage dips on the industrial consumer on using digital simulation. *Buletinul Institutului de Studii si Proiectari Energetice,* 21 (1-2), 53-61. (*in French*)

Pradhan, A.K., and Routray, A., 2005. Applying distance relay for voltage sag source detection. *IEEE Transactions on Power Delivery*, 20 (1), 529-531.

Qader, M.R., Bollen, M.H.J., Allan, R.N., 1999. Stochastic prediction of voltage sags in a large transmission system. *IEEE Transactions on Industry Applications*, 35 (1), 152-162.

Reason, J., 1988. End-use power quality: new demand on utilities. *Electrical World*, 202 (11), 43-46.

Ribeiro, T.N., 1999. Power quality issues relating of IEEE and IEC standards. *In Proc. Conference on Electrical Machines, Converters and Systems*, 14-16 Sept. 1999, Lisbon.

Sabin, D.D., Grebe, T.E., and Sundaram, A., 1999. RMS voltage variation statistical analysis for a survey of distribution system power quality performance. *In Proc. IEEE PES Winter Meeting, 31 Jan.-4 Feb. 1999, New York*.

Sang-Yun, Y., Jung-Hwan O., Seong-Jeong R., Jae-Chul K., 2000. Mitigation of voltage sag using feeder transfer in power distribution system. *In Proc. IEEE PES Summer Meeting, 16-20 July 2000, Seattle WA, USA*.

Sannino, A., and Svensson, J., 2000. A series-connected voltage source converter for voltage sag mitigation using vector control and a filter compensation algorithm. *In Proc. World Congress on Industrial Applications of Electrical Energy and 35th IEEE - IAS Annual Meeting, 8-12 Oct. 2000, Rome*.

Stockman, K., Didden, M., D'hulster, F., and Belmans, R., 2004. Bag the sags. *IEEE Industry Applications Magazine*, 10 (5), 59-65.

Tayjasanant, T., Li, C., and Xu, W., 2005. A resistance sign-based method for voltage sag source detection. *IEEE Transactions on Power Delivery*, 20 (4), 2544-51.

Thallam, R.S., and Heydt G. T., 2000. Power acceptability and voltage sag indices in the three phase sense. *In Proc. PES Summer Meeting, 16-20 July 2000, Seattle WA, USA*.

Tosato, F., 2001. Voltage sags mitigation on distribution utilities. *European Transactions on Electrical Power,* 11 (1), 17-21.

Tosato, F., and Quaia, S., 2000. Equipment fault-clearing time reduction: an approach to utility voltage sag mitigation. *Elektrotehniski Vestnik,* 67 (5), 294-299.

Wagner, V.E., Andreshak, A.A., Staniak, J.P., 1990. Power quality and factory automation. *IEEE Transactions on Industry Applications*, 26 (4), 620-6.

Woodley, N.H., and Sezi, T., 2000. Voltage sag and swell mitigation using a static series compensation device. *In Proc. 6th European Power Quality Conference, 6-8 June 2000, Germany*.

Xu, W., 2001. Component Modeling Issues for Power Quality Assessment, *IEEE Power Engineering Review*, 21 (11), 12-17.

Appendix 1: List of Acronyms

ABC:	Types of asymmetrical voltage sags
ANSI:	American National Standard Institute
ATP:	Alternative transient program
CBEMA:	Computer and Business Equipment Manufacturers Association
CENELEC:	European Committee for Electrotechnical Standardisation
DE:	Disturbance energy
DFT:	Discrete Fourier Transform
DP:	Disturbance power
DPE:	Disturbance power & energy method
DR:	Distance relay method
DS:	Downstream
DVR:	Dynamic voltage restorer
EPRI:	Electric Power Research Institute
FFT:	Fast Fourier Transform
GPS:	Global position system
IEEE:	Institute of Electric and Electronic Engineers
IEC:	International Electrotechnical Commission
IET:	Institution of Engineering and Technology (ex-IEE)
ITIC:	Information Technology Industry Council
LLLG:	Three phase to ground fault
LLL:	Three phase fault
LLG:	Line-to-line-to-ground fault
LL:	Line-to-line fault
LG and SLG:	Line-to-ground fault
ONS:	Brazilian Independent System Operator
PC:	Personal computer
PMU:	Phasor measurement unit
PN:	Phase-to-neutral
PP:	Phase-to-phase
PQ:	power quality
RS:	Resistance sign method
RCC:	Real current component method
SARFI:	System average rms variation frequency index
SEMI:	Semiconductor Equipment and Materials International
SLG and LG:	Line-to-ground fault
SPI:	Voltage sag propagation index
SST:	Slope of system trajectory method
UNIPEDE:	International Union of Producers and Distributors of Electrical Energy
US:	Upstream
VSC:	Voltage source converter

Appendix 2: Sag survey I

Table 45 - Voltage sag survey on a distribution feeder 13.8 kV.

Date	Retained voltage (%)	Duration (ms)
30/04/2002@17:47:05,133	88	8
03/05/2002@19:59:07,797	87	108
03/05/2002@19:59:10,922	89	467
03/05/2002@19:59:11,297	84	892
03/05/2002@20:00:01,938	83	517
03/05/2002@20:00:36,130	89	8
03/05/2002@20:03:15,318	89	25
07/05/2002@15:00:49,921	88	58
13/05/2002@11:44:36,516	83	33
19/05/2002@10:14:47,201	73	25
19/05/2002@10:24:48,236	89	41
21/05/2002@03:55:51,739	88	8
12/06/2002@05:11:02,615	85	358
12/06/2002@06:04:21,416	88	500
17/07/2002@07:35:26,046	89	33
17/07/2002@07:35:26,054	81	41
27/07/2002@07:58:41.924	84	41
29/07/2002@14:50:23,319	39	175
01/08/2002@23:10:43,611	70	266
01/08/2002@23:32:34,540	88	16
02/08/2002@12:56:06,179	70	307
02/08/2002@23:18:06,356	70	283
03/08/2002@10:59:49,981	81	16
04/08/2002@06:40:37,418	86	108
04/08/2002@13:26:50,374	68	250
06/08/2002@10:41:28.942	90	341
09/08/2002@15:03:15.261	80	41
09/08/2002@15:03:17.760	71	526
09/08/2002@15:03:20.217	70	491
09/08/2002@19:10:44.346	82	125
26/08/2002@18:17:26.380	89	33
26/08/2002@18:17:28.564	86	42
26/08/2002@18:38:10.649	87	33
30/08/2002@02:17:46.953	87	41
06/09/2002@13:45:07.255	89	83
06/09/2002@19:28:40.893	77	100
06/09/2002@19:28:45.116	88	8
07/09/2002@03:22:40.736	82	41
07/09/2002@03:47:08.028	73	274
07/09/2002@03:56:16.495	58	33
07/09/2002@03:56:23.045	53	50
07/09/2002@03:56:37.217	39	225
07/09/2002@03:58:04.859	88	8

07/09/2002@03:59:36.364	88	8
07/09/2002@05:27:31.638	88	83
07/09/2002@05:58:59.848	89	16
07/09/2002@10:29:52.366	89	83
10/09/2002@14:25:06.805	88	8
14/09/2002@10:55:33.598	89	16
22/09/2002@11:52:16.395	88	8
29/09/2002@23:16:52.778	84	208
29/09/2002@23:29:37.507	84	41
01/10/2002@11:34:14.952	87	33
01/10/2002@11:34:21.304	78	25
01/10/2002@11:34:34.873	89	25
02/10/2002@16:07:46.578	28	191
02/10/2002@16:08:47.421	52	25
09/10/2002@09:02:17.733	78	17
13/10/2002@06:42:39.683	67	41
13/10/2002@06:42:41.866	62	242
13/10/2002@06:42:43.882	43	124
13/10/2002@06:42:43.890	19	133
13/10/2002@06:46:07.354	54	41
13/10/2002@06:46:25.175	78	751
14/10/2002@14:11:15.955	86	33
15/10/2002@11:43:48.323	73	41
22/10/2002@00:35:10.786	86	8
25/10/2002@20:54:41.023	88	16
27/10/2002@23:38:49.016	84	124
27/10/2002@23:38:51.107	84	33
27/10/2002@23:38:53.356	85	66
28/10/2002@14:20:10.026	84	16
28/10/2002@14:32:21.382	88	8
28/10/2002@14:37:59.658	86	8
28/10/2002@14:38:55.146	84	24
28/10/2002@15:45:13.101	88	74
28/10/2002@17:17:24.554	83	16
28/10/2002@19:10:36.002	89	8
29/10/2002@08:47:47.527	19	374
29/10/2002@23:28:58.172	12	50
10/11/2002@07:01:33.826	41	66
10/11/2002@08:31:20.532	50	683
15/11/2002@08:44:22.260	84	41
19/11/2002@07:58:29.741	89	8
21/11/2002@12:11:03.534	88	41
28/11/2002@09:51:22.499	20	676
02/12/2002@15:01:31.271	89	66
03/12/2002@14:13:14.876	85	33
03/12/2002@14:13:20.900	85	33
03/12/2002@14:13:33.416	85	125
03/12/2002@20:16:23.202	88	25
03/12/2002@20:38:01.465	77	41
03/12/2002@20:39:16.766	85	33

04/12/2002@16:47:19.630	86	16
04/12/2002@16:51:15.519	89	8
05/12/2002@16:54:46.196	85	33
09/12/2002@10:04:30.876	5	233
10/12/2002@00:58:14.887	85	66
13/12/2002@17:19:49.705	87	375
13/12/2002@19:28:50.180	89	116
16/12/2002@16:33:48.405	88	183
16/12/2002@16:33:48.921	84	416
20/12/2002@13:08:04.212	75	25
24/12/2002@09:49:44.187	81	33
29/12/2002@16:52:59.156	57	50
29/12/2002@16:53:01.371	52	216
29/12/2002@16:53:03.420	46	141
17/01/2003@19:26:08.085	78	33
18/01/2003@11:02:56.733	77	50
18/01/2003@11:03:14.740	84	49
21/01/2003@01:14:03.341	80	91
22/01/2003@13:08:37.338	87	8
27/01/2003@17:29:42.013	86	16
30/01/2003@18:36:15.122	84	91
30/01/2003@18:36:15.130	82	1007
30/01/2003@20:54:11.114	89	91
01/02/2003@18:49:39.081	89	8
02/02/2003@17:06:14.839	86	33
02/02/2003@17:29:15.444	84	33
06/02/2003@17:21:24.394	88	7
06/02/2003@17:57:44.323	61	50
16/02/2003@15:25:10.936	87	8
16/02/2003@15:25:13.153	88	16
16/02/2003@15:25:15.346	89	8
17/02/2003@16:04:54.384	83	41
19/02/2003@01:14:29.651	88	24
22/02/2003@13:06:09.463	64	50
22/02/2003@13:06:12.037	73	308
22/02/2003@13:36:05.849	56	41
22/02/2003@13:36:08.109	53	300
22/02/2003@13:36:10.251	43	208
22/02/2003@13:37:44.386	79	24
26/02/2003@11:41:04.220	88	8
04/03/2003@15:54:26.801	50	41
04/03/2003@15:54:28.727	49	49
04/03/2003@15:54:30.902	49	233
05/03/2003@00:59:44.399	77	24
05/03/2003@02:12:19.687	76	16
13/03/2003@15:32:42.863	89	74
13/03/2003@15:32:47.552	86	16
17/03/2003@11:03:35.727	84	49
22/03/2003@17:42:12.185	70	25
29/03/2003@17:34:16.539	87	16

30/03/2003@08:52:25.672	86	33
04/04/2003@10:05:15.096	87	41
15/04/2003@11:24:52.627	89	8
16/04/2003@09:17:15.708	67	33
16/04/2003@09:17:17.924	89	8
02/05/2003@15:41:34.690	87	8
05/05/2003@06:12:23.031	77	16

Appendix 3: Sag survey II

Table 46 – Fault events registered at 230 kV and 138 kV networks.

Event #	Fault type	Fault location	Thermal Generation
1	LL	COL/ALF	ON
2	SLG	COX/JAU	ON
3	SLG	NOB/DEN	ON
4	SLG	COL/ALF	ON
5	SLG	COX/JAU	ON
6	SLG	BPX/RND	ON
7	SLG	JAC/COX	ON
8	SLG	COX/JAU	ON
9	SLG	COL/ALF	ON
10	LL	CBA/CVD	ON
11	LLL	CMAG/RND	ON
12	LLL	JUB/MAR	ON
13	LLL	DEN/TAN	ON
14	LLG	JAC/COX	ON
15	SLG	GRA/POC	ON
16	SLG	JUB/MAR	ON
17	SLG	DCLA/COL	ON
18	SLG	JUB/MAR	ON
19	SLG	NOB/DEN	ON
20	SLG	RVD/RND	OFF
21	LLG	DCLA/COL	ON
22	LLL	PRE/ITA	OFF
23	LL	ITA/JUB	OFF
24	LLL	NOB/MUT	OFF
25	LL	JUB/MAR	OFF
26	LLL	DCLA/COL	ON
27	LL	DEN/TAN	ON
28	LL	DEN/TAN	ON
29	LLG	MAR/CAC	ON
30	LL	JAC/COX	ON

Table 47 - Voltage sag magnitudes measured during the sag survey.

Event	P1	P2	P3	P4	P5	P6	P7	P8	P9	P10	P11	P12
1	0.62	0.59	0.58									
2						0.83						
3				0.54	0.59							0.83
4	0.66	0.63	0.63									
5						0.81						
6									0.64			
7						0.83	0.79					
8						0.83						
9		0.73	0.69									
10				0.80	0.83	0.77	0.71	0.74	0.85	0.84		
11									0.77	0.69	0.73	
12				0.72	0.75							0.20
13				0.44	0.47							0.71
14						0.85	0.81	0.80	0.82	0.74	0.72	
15				0.83			0.81					0.72
16												0.35
17	0.54	0.45	0.46									
18				0.81								0.39
19				0.45	0.50							0.84
20						0.83			0.64			
21	0.49	0.36	0.39									
22				0.58	0.61							
23				0.66	0.69							0.49
24	0.00	0.00	0.00	0.66	0.70	0.55	0.58		0.73	0.72	0.73	0.79
25				0.75	0.77							0.30
26	0.38	0.22	0.21									
27				0.57								0.78
28				0.58								0.76
29												0.22
30	0.85					0.82	0.81		0.82	0.77	0.73	

Appendix 4: Selected Publications

PAPER I

Chouhy Leborgne, R., and Chen, P., 2006. Using PQ-monitor and PMU for voltage sag extended-characterization. *In Proc. IEEE PES Transmission and distribution Conference and Exposition Latin America, Aug.2006, Caracas*.

PAPER II

Leborgne, R.C., Olguin, G., and Bollen, M.H.J., 2004. The influence of PQ-monitor connection on voltage dip measurements. *In Proc. IEE MedPower, Nov.2004, Cyprus.*

PAPER III

Leborgne, R.C., and Karlsson, D., 2005. Phasor Based Voltage Sag Monitoring and Characterisation. *In Proc. CIRED International Conference on Electricity Distribution, Jun.2005, Turin*.

PAPER IV

Chouhy Leborgne, R., Karlsson, D., and Olguin, G., 2005. Analysis of Voltage Sag Phasor Dynamics. *In Proc. IEEE-PES Power Tech, Jun.2005, St Petersburg*.

PAPER V

Chouhy Leborgne, R., Carvalho Filho, J.M., Novaes, E.G.C., and Abreu, J.P.G., 2006. Voltage sag propagation: Case study based on measurements. *In Proc. IEEE 12th International Conference on Harmonics and Quality of Power, Oct.2006, Cascais Portugal.*

PAPER VI

Carvalho Filho, J.M., Chouhy Leborgne, R., Silveira, P.M., and Bollen, M.H.J., 2007. Voltage sag index calculation: Comparison between time-domain simulation and short-circuit calculation. *Electric Power System Research, in print.*

PAPER VII

Carvalho Filho, J.M., Chouhy Leborgne, R., Abreu, J.P.G., Novaes, E.G.C., and Bollen, M.H.J., 2007. Validation of voltage sag simulation tools: ATP and short-circuit calculation vs. field measurements. Submitted to *IEEE Trans. Power Delivery, TPWRD-00032-2007.*

PAPER VIII

Chouhy Leborgne, R., Olguin, G., and Bollen, M.H.J., 2004. Sensitivity Analysis of Stochastic Assessment of Voltage Dips. *In Proc. IEEE PowerCon, Nov.2004, Singapore.*

PAPER IX

Chouhy Leborgne, R., Olguin, G., Carvalho Filho, J.M., and Bollen, M.H.J., 2006. Effect of PQ-monitor connection on voltage dip indices: PN vs PP voltages. *Electric Power Quality and Utilisation Magazine*, 2(1), 19-26.

PAPER X

Chouhy Leborgne, R., Olguin, G., Carvalho Filho, J.M., and Bollen, M.H.J., 2007. Differences in voltage dip exposure depending upon phase-to-phase and phase-to-neutral monitoring connections. *IEEE Trans. Power Delivery,* 22 (2), 1153-59.

PAPER XI

Chouhy Leborgne, R., Karlsson, D., and Daalder, J., 2006. Voltage sag source location methods performance under symmetrical and asymmetrical fault conditions. *In Proc. IEEE PES Transmission and distribution Conference and Exposition Latin America, Aug.2006, Caracas*.

PAPER XII

Chouhy Leborgne, R., Karlsson, D., 2006. Voltage sag source location based on voltage measurements only. Submitted to *IEEE Trans. Power Delivery, TPWRD-00715-2006.*